

# University of Cincinnati

Date: 7/7/2022

I, Paul L Deford, hereby submit this original work as part of the requirements for the degree of Doctor of Philosophy in Toxicology (Environmental Health).

It is entitled:

**HGF/Met-mediated Phosphorylation of Stathmin1 Serine 16 Regulates Cell Proliferation and not Metastasis**

Student's name: Paul L Deford

This work and its defense approved by:

Committee chair: Susan Kasper, Ph.D.

Committee member: Katherine Burns, Ph.D.

Committee member: Saulius Sumanas, Ph.D.

Committee member: Susan Waltz, Ph.D.



43030

# **HGF/Met-mediated Phosphorylation of Stathmin1 Serine 16 Regulates Cell Proliferation and not Metastasis**

A dissertation submitted to the  
Graduate School of the University of Cincinnati  
in partial fulfillment of the  
requirements for the degree of  
**Doctor of Philosophy (Ph.D.)**  
in the Department of Environmental and Public Health Sciences  
of the College of Medicine  
July 7<sup>th</sup>, 2022

By

**Paul Lawrence Deford**

B.S., University of Michigan, 2016

Committee Chair: Susan Kasper, PhD  
Committee Members: Katherine Burns, PhD  
Susan Waltz, PhD  
Saulius Sumanas, PhD

# Abstract

The focus of this dissertation is Hepatocyte Growth Factor (HGF)/MET-mediated phosphorylation of STMN1 on Serine 16 and the impact on cell cycle progression and cell proliferation. While the treatment of low-grade prostate cancers (PCa) with androgen deprivation therapy (ADT) often eliminates androgen receptor (AR)<sup>+</sup> bulk tumor cells, 20-30% of the men treated will eventually develop castration resistant prostate cancer (CRPC). Of note is that AR normally represses the transcription of the HGF receptor MET, and that prolonged therapy can downregulate AR expression, resulting in a corresponding increase in MET expression, reported to be an indicator of late stage PCa and poor overall survival. Progression to late stage PCa is also characterized by an increased production and secretion of HGF from cells within the tumor microenvironment (TME) to upregulate metastatic and proliferative cellular processes.

In this dissertation, Chapter 1 provides context regarding the role of the TME in cancer development, progression, and therapeutic resistance; and a brief summary of the current understanding of HGF/MET signaling in cancer and its role in STMN1 phosphorylation. Chapter 2 presents novel findings regarding HGF/MET-mediated phosphorylation of STMN1 S16 and how this modulates cell cycle progression, proliferation and metastatic potential in both PCa cells and normal mouse mammary gland cells. Chapter 3 investigates how calcium/calmodulin-dependent protein kinase II (CAMKII) regulates PCa cell proliferation without triggering metastasis, and the role that the other three regulatory serines in STMN1 play in regulating PCa cell proliferation. Chapter 4 reports the role of constant degradation of AR by Mouse Double Minute 2 (MDM2) to maintain prostate cancer stem cell integrity. Chapter 5 provides an in-depth analysis of the advantages and challenges faced in our attempt to use CRISPR/Cas9 technology to generate stable

mutant DU-145 cell lines expressing STMN1 substitution mutations. Finally, Chapter 6 discusses the overall conclusions of the dissertation and provides future directions for further study.

For the first time, we demonstrate HGF/MET signaling phosphorylates STMN1 on S16 to promote cell cycle progression through the shortening of cell-doubling time, resulting in an increase in cellular proliferation. We also demonstrate that differential phosphorylation of the other three regulatory serines of STMN1 do not play a significant role in the regulation of cell cycle progression and cell proliferation. The Kasper Laboratory previously published that downregulation of total STMN1 resulted in an inhibition of proliferation and an induction of metastasis. Herein, we show, for the first time, that HGF/MET-mediated phosphorylation of STMN1 S16 does not induce metastasis. Finally, we provide evidence in support of a novel therapeutic strategy of utilizing the potent c-MET inhibitor AMG337 in combination with ADT to decrease or eliminate the development of late-stage PCa and metastasis.



# Acknowledgements

First, I would like to thank my mentor, Dr. Susan Kasper, for her guidance, financial and academic support, and critique throughout the entirety of this project. I would also like to thank my dissertation committee members Dr. Katherine Burns, Dr. Susan Waltz, Dr. Saulius Sumanas, and the late Dr. Peter Stambrook. The advice and contributions I received from each of my committee members helped to shape this project and drove me to improve and challenge myself throughout the progression of my degree. It was a true pleasure to work alongside my lab colleagues Dr. Alison Pecquet, Dr. Austin McDermott, and MJ See and I thank them for their camaraderie and their technical support.

I would like to thank my friends, especially Andrew Waugh and Michael Newhall, who patiently and graciously listened to my countless frustrations throughout my project and offered nothing less than complete support. Thanks to Dr. Bitá Minaravesh, a close friend and fellow recent graduate, for her professional reassurances and for being a compassionate ear who understood the challenges I faced and encouraged me to keep going. Thank you to my family, especially my parents Larry and Connie Deford for being the most loving, supportive, and generous parents anyone could ask for. Thank you to my sisters Ashley Deford and Sarah Moser, and my brother-in-law Nathan Moser for checking in on me and doing whatever they could to help me. Most of all, thank you to my incredible wife Dr. Amanda Deford, without whom this may never have been possible. I'm forever indebted to you for the love, support, and patience you've shown me each day. Words cannot explain my gratitude towards you.

# Table of Contents

<b>Abstract.....</b>	<b>i</b>
<b>Acknowledgements.....</b>	<b>iv</b>
<b>List of Figures.....</b>	<b>xiv</b>
<b>List of Tables.....</b>	<b>xvii</b>
<b>Abbreviation List.....</b>	<b>xviii</b>
<b>Chapter 1: Introduction.....</b>	<b>1</b>
<b>1.1. The Tumor Microenvironment in Cancer Development, Progression and Therapeutic Resistance.....</b>	<b>2</b>
<b>1.1.a. The androgen receptor in stroma regulates normal prostate and prostate cancer growth and progression.....</b>	<b>2</b>
<b>1.1.b. Impact of the tumor microenvironment on prostate cancer progression.....</b>	<b>4</b>
<b>1.2. The HGF/MET signaling axis in prostate cancer and other solid tumors.....</b>	<b>6</b>
<b>1.3 HGF/MET as a target for PCa therapy.....</b>	<b>7</b>
<b>1.4 HGF/MET regulation of Stathmin phosphorylation.....</b>	<b>8</b>
<b>1.5 Hypothesis.....</b>	<b>9</b>

<b>Chapter 2: HGF/MET-mediated Phosphorylation of Stathmin S16 Regulates Cell Cycle Progression and Cell Proliferation.....</b>	<b>11</b>
<b>2.1. Abstract.....</b>	<b>12</b>
<b>2.2. Introduction.....</b>	<b>13</b>
<b>2.2.a. Role of the Tumor Microenvironment in Modulating Cancer Progression...13</b>	
<b>2.2.b. Role of HGF/MET signaling in regulating STMN1 phosphorylation and tumor growth.....</b>	<b>13</b>
<b>2.2.c. Therapeutics that could target HGF/MET and the phosphorylation of STMN1.....</b>	<b>14</b>
<b>2.2.d. Hypothesis .....</b>	<b>15</b>
<b>2.3. Materials and Methods.....</b>	<b>16</b>
<b>2.3.a. Materials.....</b>	<b>16</b>
<b>2.3.b. Methods.....</b>	<b>16</b>
<b>2.3.b.i. Analysis of HGF, MET and STMN1 expression in tumors from men with metastatic castration resistant prostate cancer (mCPRC).....</b>	<b>17</b>
<b>2.3.b.ii Cell culture.....</b>	<b>17</b>
<b>2.3.b.iii. Proliferation assay.....</b>	<b>17</b>
<b>2.3.b.iii. Doubling time assay.....</b>	<b>18</b>
<b>2.3.b.iv. Migration and invasion assay.....</b>	<b>18</b>

2.3.b.v. Conditioned Media Evaluation.....	18
2.3.b.vi. Western blot analysis.....	19
2.3.b.vii Total RNA extraction, purification, and cDNA synthesis.....	19
2.3.b.viii. Flow Cytometry.....	20
2.3.b.x. Quantification and statistical analysis.....	20
2.4 Results.....	22
2.4.a. Increased MET expression correlates with an increase in STMN1 expression in mCRPC.....	22
2.4.b. HGF/MET signaling regulates cell proliferation.....	24
2.4.c. HGF-mediated MET signaling phosphorylates Stathmin S16 and shortens cell cycle progression.....	30
2.4.d. HGF/MET signaling regulates cyclin expression during cell cycle progression.....	34
2.4.e. HGF/MET mediates a decrease in p21 levels in G2/M.....	37
2.4.f. STMN1 S16 phosphorylation selectively regulates cell cycle progression.....	38
2.4.g. Phosphorylation of STMN1 S16 shortens the time of progression through the cell cycle.....	44
2.4.h. STMN1 S16 phosphorylation regulates the expression of factors during cell cycle progression.....	45
2.4.i. STMN1 S16 phosphorylation does not regulate metastatic potential.....	49
2.5. Discussion.....	53

<b>Chapter 3: The Role of CAMKII in Regulating Stathmin S16 Phosphorylation, Proliferation, and Metastatic Potential.....</b>	<b>57</b>
<b>3.1. Abstract.....</b>	<b>58</b>
<b>3.2. Introduction.....</b>	<b>59</b>
<b>3.2.a. CAMKII-mediated phosphorylation of STMN1 S16 in breast cancer.....</b>	<b>59</b>
<b>3.2.b. CAMKII phosphorylation of STMN1 S16 in dendrites.....</b>	<b>60</b>
<b>3.2.c. CAMKII phosphorylation of STMN1 S16 in hepatoma cells (HepG2).....</b>	<b>60</b>
<b>3.3. Materials and Methods.....</b>	<b>62</b>
<b>3.3.a. Materials.....</b>	<b>62</b>
<b>3.3.b. Methods.....</b>	<b>62</b>
<b>3.3.b.i. Proliferation Assays.....</b>	<b>62</b>
<b>3.3.b.ii. Migration and invasion Assays.....</b>	<b>62</b>
<b>3.4. Results.....</b>	<b>63</b>
<b>3.4.a. CAMKII promotes cell proliferation but does not induce EMT.....</b>	<b>63</b>
<b>3.4.b. CaMKII does not promote cell migration or invasion.....</b>	<b>66</b>
<b>3.4.c. PP2A inhibits DU-145 cell proliferation.....</b>	<b>68</b>
<b>3.4.d. CaMKII does not phosphorylate STMN1 S16.....</b>	<b>69</b>
<b>3.4.e. The effect of small molecules targeting STMN1 S25, 38, 63 on cell proliferation.....</b>	<b>71</b>
<b>3.5. Discussion.....</b>	<b>76</b>

<b>Chapter 4: Constant Degradation of the AR by MDM2 Conserves Prostate Cancer Stem Cell Integrity.....</b>	<b>78</b>
<b>4.1. Abstract.....</b>	<b>79</b>
<b>4.2. Introduction.....</b>	<b>80</b>
<b>4.3. Materials and Methods.....</b>	<b>81</b>
<b>4.3.1. Materials.....</b>	<b>83</b>
<b>4.3.2. Methods.....</b>	<b>83</b>
<b>4.3.2.a. Cell Culture.....</b>	<b>83</b>
<b>4.3.2.b. Sphere formation assay.....</b>	<b>84</b>
<b>4.3.2.c. Proliferation Assay.....</b>	<b>85</b>
<b>4.3.2.d. Western Blot Analysis.....</b>	<b>85</b>
<b>4.3.2.e. Immunoprecipitation.....</b>	<b>85</b>
<b>4.3.2.f. Luciferase Assay.....</b>	<b>86</b>
<b>4.3.2.g. Total RNA Extraction, Purification, and cDNA Synthesis.....</b>	<b>86</b>
<b>4.3.2.h. Quantitative Polymerase Chain Reaction and Data Analysis.....</b>	<b>87</b>
<b>4.3.2.i. Quantification and Statistical Analysis.....</b>	<b>87</b>
<b>4.4. Results.....</b>	<b>88</b>
<b>4.4.a. Inhibition of the proteasome induces AR expression in CSC-like PCa cells.....</b>	<b>88</b>

4.4.b. HPET and HuSLCs express full-length AR but not AR-Vs.....	91
4.4.c. An AR(-) phenotype is essential for prostate CSC self-renewal and proliferation...	93
4.4.d. Induction of AR down-regulates stem/progenitor characteristics and promotes luminal epithelial cell fate.....	95
4.4.e. Poly-ubiquitination regulates the dynamic turnover of AR protein.....	99
4.4.f. MDM2 E3 ligase selectively degrades AR in prostate CSCs.....	102
4.4.g. MDM2 knockdown inhibits CSC self-renewal and cell proliferation and promotes luminal epithelial cell differentiation.....	103
4.5. Discussion.....	106
Chapter 5: CRISPR/Cas9 - Advantages and Challenges.....	122
5.1. Abstract.....	123
5.2. Introduction.....	124
5.3. Materials and Methods.....	126
5.3.a Sequencing the STMN1 gene.....	126
5.3.b. Design of the CRISPR gRNA and dsDNA templates.....	128
5.3.c. Introduction of CRISPR/Cas9 components to the cells.....	130
5.4. Results.....	132
5.5. Discussion.....	133
Chapter 6: Conclusions and Future Directions.....	137

<b>6.1. Conclusions.....</b>	<b>138</b>
<b>6.1.a. The role of HGF in the phosphorylation of Stathmin on S16 in prostate cancer progression.....</b>	<b>138</b>
<b>6.1.a.1. Therapeutic relevance of HGF/MET signaling inhibitor in combination with ADT.....</b>	<b>138</b>
<b>6.1.a.2. Utilization of AMG337 to target HGF/MET signaling.....</b>	<b>138</b>
<b>6.1.b. Implications on the tumor microenvironment.....</b>	<b>139</b>
<b>6.1.c. Summary of the effect of HGF on cancer cell proliferation.....</b>	<b>139</b>
<b>6.1.d. HGF phosphorylation results in increases in cell cycle progression and overall PCa cell proliferation without induction of metastasis.....</b>	<b>140</b>
<b>6.1.e CAMKII phosphorylation of STMN1 on S16 seems to be cell type specific.....</b>	<b>141</b>
<b>6.1.f. Discussion of the impact that MDM2 has on maintaining PCa stem cell integrity through the degradation of the androgen receptor and the potential therapeutic implications of that process.....</b>	<b>141</b>
<b>6.2 Future Directions.....</b>	<b>143</b>
<b>6.2.1.a. Determine the relationship between increased concentration of HGF and varied cellular processes.....</b>	<b>143</b>
<b>6.2.1.b. Assess the impact of differential phosphorylation of STMN1 S16 <i>in vivo</i>.....</b>	<b>144</b>

<b>6.2.2. Investigate the efficacy of dual treatment of MDM2 inhibitor and ADT in vivo.....</b>	<b>145</b>
<b>Chapter 7 – References.....</b>	<b>146</b>

# Figure List

<b>1.1 Diagram summarizing the tumor microenvironment in PCa.....</b>	<b>3</b>
<b>1.2. Diagram summarizing transcriptional repression of MET receptor as well as the impact of ADT on MET expression per data from Verras et al.....</b>	<b>7</b>
<b>2.1. MET and STMN1 expression positively correlates with and are predictive of advanced PCa.....</b>	<b>23</b>
<b>2.2 HGF/MET signaling regulates DU-145 proliferation.....</b>	<b>25</b>
<b>S.2.1 Morphology Changes in DU-145 cells after HGF treatment.....</b>	<b>26</b>
<b>S.2.2. Investigating potential HGF expression by DU-145 cells.....</b>	<b>27</b>
<b>2.3 HGF treatment induces phosphorylation of MET and STMN1 S16, which is inhibited by MET inhibitor AMG337.....</b>	<b>28</b>
<b>2.4 Doubling time decreases with inhibition of MET signaling.....</b>	<b>30</b>
<b>2.5 HGF/MET activity shortens cell cycle and inhibition of HGF/MET-mediated signaling lengthens the S phase and cell cycle length.....</b>	<b>31</b>
<b>2.6 MET modulates Stathmin phosphorylation during cell cycle progression.....</b>	<b>33</b>
<b>2.7 HGF/MET mediates Cyclin protein levels.....</b>	<b>35</b>
<b>2.8 Modulating HGF/MET activity decreases p21 expression.....</b>	<b>38</b>
<b>2.9 Stathmin1 S16E increases, while S16A inhibits, DU-145 and NMuMG cell proliferation.....</b>	<b>39</b>
<b>2.10 Stathmin1 S16 is the primary serine that modulates cell proliferation.....</b>	<b>41</b>
<b>2.11 STMN1 S16 is the primary substitution mutation regulating DU-145 cell doubling time.....</b>	<b>42</b>

2.12	In NMuMG cells, the trend is that STMN1 S16 regulates cell doubling time.....	43
2.13	STMN1 S16 phosphorylation shortens progression through the cell cycle.....	45
2.14	STMN1 phosphorylation regulates total STMN1 and Cyclin expression.....	47
2.15	STMN1 S16 phosphorylation regulates p21 expression.....	49
2.16	STMN1 S16 phosphorylation does not regulate metastatic potential.....	50
2.17	STMN1 S16 phosphorylation does not regulate metastatic potential in NMuMG cells.....	51
2.18	Schematic representation of HGF/MET as a putative therapeutic target in combination with androgen/AR targeted therapy for the treatment of CRPC.....	55
3.1	CaMKII signaling promotes DU-145 prostate cancer cell proliferation.....	64
3.2	KN92 does not alter DU-145 prostate cancer cell proliferation or viability.....	66
3.3	CaMKII signaling does not promote cell migration.....	67
3.4	CaMKII signaling does not promote cell invasion.....	68
3.5	Okadaic acid inhibits DU-145 cell proliferation.....	69
3.6	CaMKII signaling does not phosphorylate STMN1 S16.....	70
3.7	Regulation of p38 MAPK does not affect DU-145 cell proliferation.....	72
3.8	Inhibition of CDK1 significantly inhibited DU-145 cell proliferation.....	73
3.9	Inhibition of PKA decreases DU-145 cell proliferation.....	74
4.1	AR expression in CSC-like PCa cells is modulated by the proteasome.....	89
4.2	CSC-like HPET cells and HuSLCs express full-length AR, but not AR-Vs.....	92
4.3	Induction of AR protein down-regulates sphere formation and cell proliferation.....	94

<b>4.4</b>	<b>MG132 treatment down-regulates expression of stem cell-associated markers and promotes luminal epithelial cell fate.....</b>	<b>96</b>
<b>4.5</b>	<b>Induction of exogenous AR down-regulates expression of stem cell-associated markers and promotes luminal epithelial cell fate.....</b>	<b>98</b>
<b>4.6</b>	<b>The E3 ligase MDM2 selectively degrades AR in prostate CSCs.....</b>	<b>101</b>
<b>4.7</b>	<b>MDM2 maintains stemness in human prostate CSC-like cells.....</b>	<b>104</b>
<b>4.S1</b>	<b>AR protein is induced following treatment with proteasomal inhibitors.....</b>	<b>116</b>
<b>4.S2</b>	<b>CSC-like HuSLC and HPET cells express higher levels of the E3 ligase, MDM2, as compared to standard PCa cell lines.....</b>	<b>117</b>
<b>4.S3</b>	<b>CSC-like HPET and HuSLCs express AR-fl, but not AR-Vs.....</b>	<b>118</b>
<b>4.S4</b>	<b>CSC-like HPET and HuSLCs express AR-fl, but not AR-Vs.....</b>	<b>119</b>
<b>4.S5</b>	<b>Induction of AR promotes expression of AR target genes <i>HES1</i> and <i>HEY1</i>.....</b>	<b>120</b>
<b>4.S6</b>	<b>Expression of p53 is heterogeneous in prostate CSCs.....</b>	<b>121</b>
<b>5.1</b>	<b>Diagram of CRISPR/Cas9 creates DNA damage, and the two primary processes of repair being NHEJ and HDR.....</b>	<b>125</b>

# List of Tables

<b>Table 2.S1. Primary antibody list.....</b>	<b>56</b>
<b>Table 4.S1. Primary antibody list (related to figures 1-5).....</b>	<b>110</b>
<b>Table 4.S2. Primer sets used to characterize AR-V expression.....</b>	<b>111</b>
<b>Table 4.S3. Primers to characterize epithelial and stem cell marker expression.....</b>	<b>112</b>
<b>Table 4.S4. Summary comparing CSC-like AR(-) HPET and HuSLCs with a standard PCa cell line, AR(+) LNCaP cells.....</b>	<b>113</b>
<b>Table 5.1. CRISPR gRNA design.....</b>	<b>128</b>
<b>Table 5.2. CRISPR/Cas9 double-stranded template DNA sequences.....</b>	<b>130</b>

# List of Abbreviations

- ADT – Androgen Deprivation Therapy
- AR – Androgen Receptor
- AR-Vs – Androgen Receptor Splice Variants
- ATCC – American Type Culture Collection
- BPH-1 – Benign Prostatic Hyperplasia -1 cell line
- BSA – Bovine Serum Albumin
- CAF – Cancer Associated Fibroblast
- CAMKII – calcium/calmodulin-dependent protein kinase II
- CARNs – Castration-Resistant NKX3.1-expressing cells
- CHIP – C-terminus of Hsp70-interacting protein
- CSC – Cancer Stem Cells
- CDK – cyclin dependent kinase
- CRISPR – Clustered Regularly Interspaced Short Palindromic Repeats
- CRPC – Castration Resistant Prostate Cancer
- CXCL12 – C-X-C Motif Chemokine Ligand 12
- CXCL2 – C-X-C Chemokine Ligand 2
- CXCR4 – C-X-C Motif Chemokine Receptor 4
- DBS – Double Strand Breaks
- DDR – DNA Damage Repair
- DHT – Dihydrotestosterone
- DMEM – Dulbecco's Modified Eagle Medium
- DNA-PK – DNA Dependent Protein Kinases
- dsDNA – double stranded DNA
- ECL – Enhanced Chemiluminescence
- EMT – Epithelial Mesenchymal Transition

ES – Embryonic Stem  
FBS – Fetal Bovine Serum  
FGF – Fibroblast Growth Factor  
gRNA – guide Ribonucleic Acid  
HA – Anti-Hemagglutinin  
HCC – Hepatocellular Carcinoma  
HDR – Homology Directed Repair  
HGF – Hepatocyte Growth Factor  
HPET – Human Prostate Epithelial cell expressing human telomerase reverse transcriptase (hTERT)  
HuSLC – Human Stem Like Cell  
HSC – Hepatic Stellate Cell  
IP – Immunoprecipitation  
lncRNA – long non-coding Ribonucleic Acid  
MEM/EBSS – Minimum Essential Medium / Eagle with Earl's Basic Salt Solution  
MEF – Murine Embryonic Fibroblasts  
MMP – Matrix Metalloproteinases  
NHEJ - Non-Homologous End Joining  
NMuMG – Normal Murine Mammary Gland  
NSCLC – Non-Small Cell Lung Cancer  
OA – Okadaic Acid  
OHF – Hydroxyflutamide  
PAM – Protospacer Adjacent Motif  
PBS – Phosphate Buffered Saline  
PCa – Prostate Cancer  
PI – Propidium Iodide  
PP2A – Protein Phosphatase 2A  
PVDF – Polyvinylidene Difluoride

RLIM – Ring Finger Protein, LIM Domain Interacting

RT-qPCR – Real Time - quantitative Polymerase Chain Reaction

SB – SB203580

SDF-1 – Stromal Cell Derived Factor-1

SKP2 – S-Phase Kinase-Associated Protein 2

STMN1 – Stathmin 1

TGFβ1 – Transforming Growth Factor beta 1

THR – Thyroid Hormone Receptor

TME – Tumor Microenvironment

VEGF – Vascular Endothelial Growth Factor

WT – Wild Type

# **Chapter 1 - INTRODUCTION**

## **1.1. The Tumor Microenvironment in Cancer Development, Progression and Therapeutic Resistance**

Charles B. Huggins discovered that hormone deprivation therapy caused regression of hormone-sensitive cancers, including breast and prostate cancer (PCa) [1]. These observations sparked the search for drugs that blocked the production of steroids and/or activity of steroid hormone receptors [2-4]. In addition to hormones, factors produced by the surrounding tumor microenvironment (TME) have gained considerable interest as they can also promote cancer growth, progression, metastatic spread and therapeutic resistance [5]. The following sections provide an overview of the role of androgens and androgen receptor (AR) in regulating normal prostate and PCa growth, and the impact of TME-derived factors in contributing to cancer progression, metastasis, and the development of therapeutic resistance.

### **1.1.a. The androgen receptor in stromal cells regulate normal prostate and prostate cancer growth and progression**

The microenvironment of the developing prostate is critical for organ development. The AR is first expressed in the embryonic urogenital mesenchyme, and mesenchymal androgen-dependent signals induce the formation of solid epithelial chords, followed by induction of epithelial cell AR expression, canalization, and arborization to form the prostate [6]. Prostatic glands consist of AR<sup>+</sup> luminal, AR<sup>low/no</sup> basal, and AR<sup>low/no</sup> neuroendocrine epithelial cells underpinned by a loose stroma consisting of fibroblasts, smooth muscle cells, blood vessels and immune cells [7]. Using a mouse xenograft model, Cunha and colleagues recombined prostate mesenchymal and/or epithelial cells from normal mice with prostate mesenchymal and/or epithelial cells from mice carrying the non-functional, testicular feminization (tfm/y) mutation in AR and demonstrated that: (a) mesenchymal

AR expression was essential for proliferation and differentiation into epithelial cells, and normal prostate formation, and (b) epithelial AR was required for expression of the secretory proteins produced by differentiated epithelial cells [8].

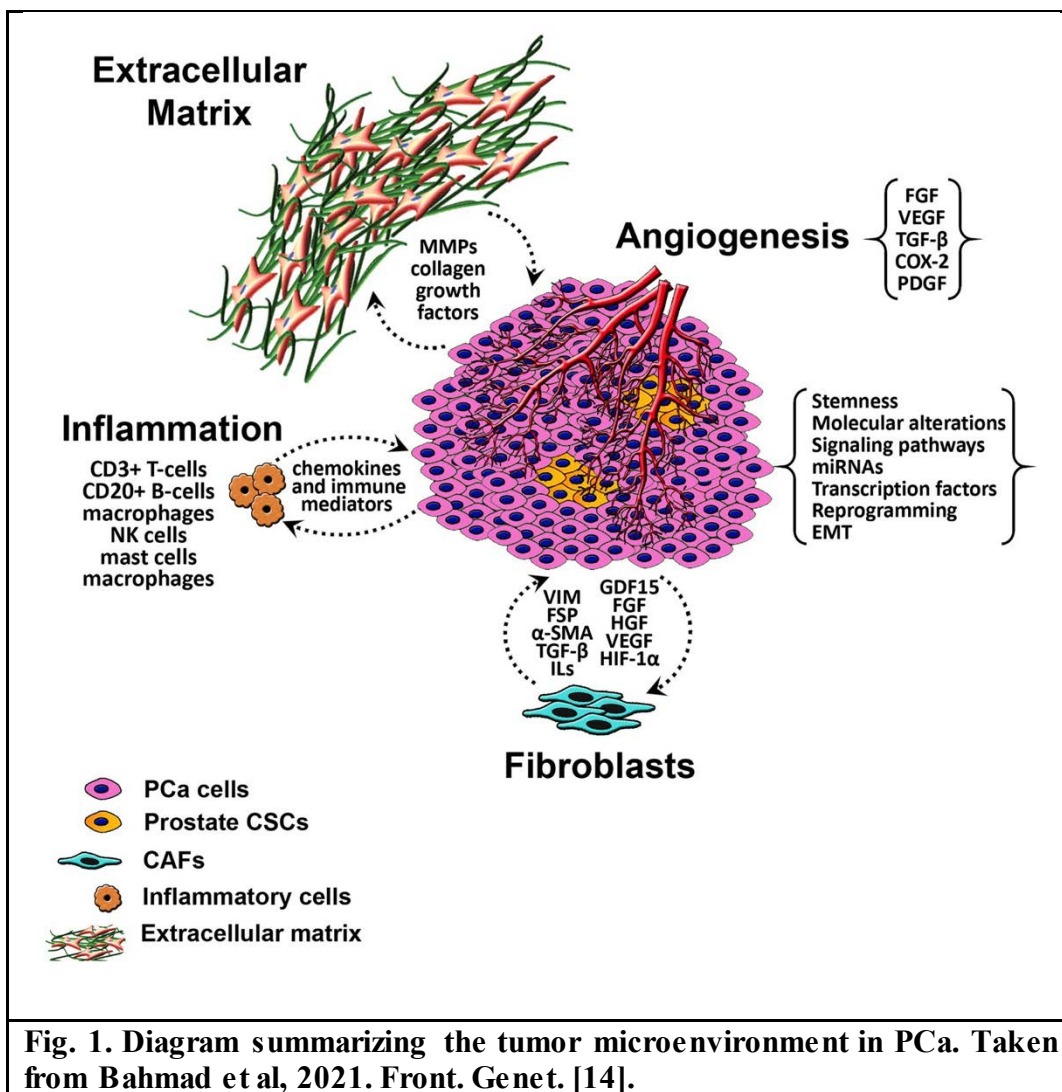
The expression levels of stromal and epithelial AR remain critical in PCa development. Prostate cancer is considered a multifocal cancer in that more than one cancer lesion (or focus) can be present in the same prostate, and that these foci can exhibit significant genomic differences. To provide a clinical diagnosis that represented the overall cancer in the same prostate specimen, the pathologist Dr. Donald Gleason determined that cancer foci fell into 5 distinct histopathological patterns; and based on this histopathology, he developed the Gleason scoring system where pattern 1 represented benign histology and pattern number increased through to pattern 5 representing undifferentiated adenocarcinoma [9]. Thus, the Gleason score typically ranges from 6-10 and is a composite score of the two grades of cancer that make up the largest areas of a biopsied tissue sample [9]. The lower the score, the less likelihood the cells will grow and spread [9].

Analysis of tissue sections obtained from prostatectomies determined that stromal AR expression was downregulated, and that this loss was 67% in well-differentiated PCa (Gleason score, 2 to 4), 91% in moderately differentiated PCa (Gleason score, 5 to 7), and 94% in poorly differentiated PCa (Gleason score, 8 to 10) [10]. In co-culture studies, AR<sup>+</sup> stromal cells decreased the growth and invasive ability of PC3 prostate cancer epithelial cells while AR<sup>-</sup> stromal cells stimulated PC3 cell proliferation *in vitro* and increased PC3 tumor growth when xenografted into nude mice [11]. The authors hypothesized that stromal AR inhibited the growth of PCa cells, possibly through expression of androgen-regulated paracrine factors; and that the downregulation of AR promoted androgen-independent PCa growth [12]. Thus, loss of AR expression in stromal

cells may underlie, in part, the development of resistance to androgen ablation therapy for PCa [13].

### 1.1.b. Impact of the tumor microenvironment on prostate cancer progression

The TME is composed of extracellular matrix and different cell populations including fibroblasts, endothelial cells, immune cells, and smooth muscle cells [14]. A number of these cell types secrete factors that sustain normal and cancer cell survival and growth (**Fig. 1**).



For example, in prostate xenografts composed of cancer-associated fibroblasts (CAFs) and human benign prostatic epithelial cells (BPH-1) together, the CAFs “transformed” BPH-1 cells to become tumorigenic and form tumors *in vivo* even when CAFs were not included in the xenografts [15]. Two cytokines secreted by CAFs, Transforming Growth Factor  $\beta$  (TGF- $\beta$ 1) [16] and stromal cell-derived factor 1 (SDF-1), also known as C-X-C motif chemokine 12 (CXCL12), were found to promote tumorigenesis in PCa cells. Moreover, CAF-secreted SDF-1 induced the expression and localization of CXCR4 to the cell membrane in BPH-1 cells and this was dependent on TGF- $\beta$ 1, demonstrating that the crosstalk between TME cells and cancer cells were essential in driving cancer progression [17]. CAFs have also been implicated in immune evasion and poor responses to cancer immunotherapy by producing vascular endothelial growth factor (VEGF) and CXC-chemokine ligand 2 (CXCL2) which promote angiogenesis and recruit immunosuppressive cells into the TME to promote immune evasion [18-21].

The crosstalk between stromal and PCa cells is bidirectional; therefore, PCa cells can also modulate fibroblast activity. Analysis of prostate cells and fibroblasts from benign prostatic hyperplasia or aggressive carcinoma revealed that PCa cells produced interleukin-6 (IL-6) which activated adjacent fibroblasts to secrete matrix metalloproteinases (MMPs) [21]. In turn, the fibroblast-derived MMPs increased tumor formation and metastasis by promoting epithelial mesenchymal transition (EMT) and enhancing cancer stemness characteristics in PCa cells [21]. Taken together, PCa cells interact with the different elements of the prostate TME, including reactive stromal cells and the factors they secrete, to promote the development, progression, and metastatic potential of prostate cancer [22].

## 1.2. The HGF/MET signaling axis in prostate cancer and other solid tumors

Hepatocyte Growth Factor (HGF, also known as scatter factor) is a common growth factor secreted into the TME by stromal cells, and has been studied in many cancers, including PCA [23]. Binding of HGF to the HGF receptor, MET, results in the phosphorylation of the MET kinase domain and activation of numerous downstream signaling pathways, including JNK, ERK, and AKT/PI3K [24] known to regulate cancer cell survival, proliferation, motility, and invasion [24,25]. Of note, very few studies on the role of HGF in the primary prostate TME have been identified to date [26,27]. Prostate CAFs release several growth factors including HGF into the TME to stimulate PCa cell growth [28-31]; and increased HGF expression correlates with increased MET expression in PCa cells [32]. Furthermore, MET expression levels increase with tumor progression, and very high levels are detected in castration resistant prostate cancer (CRPC) [32]. This raises the question as to whether MET expression is linked to AR activity.

PCa growth and progression is initially androgen-sensitive and androgen-deprivation therapy (ADT) causes tumor regression [33]. Once ADT fails, AR activation is inhibited by second line therapies which either inhibit androgen/AR activation (e.g. enzalutamide) or the production of androgens by PCa cells (e.g. abiraterone) [33-35]. When all first-line treatments fail and PCa reoccurs, disease is often characterized as androgen-independent and classified as castration resistant prostate cancer (CRPC) [32,33]. Interestingly, the expression of MET receptor is inversely related to the levels of AR. Verras et. al. reported that AR reduced the activity of Sp1 binding to the c-Met promoter, thereby repressing c-MET transcription (**Fig. 2**) [36]. Since stromal AR inhibits the growth of PCa cells and downregulation of AR promotes androgen independent PCa growth [37], we postulate that the downregulation of AR derepresses MET expression in CRPC to drive cancer growth and metastasis.

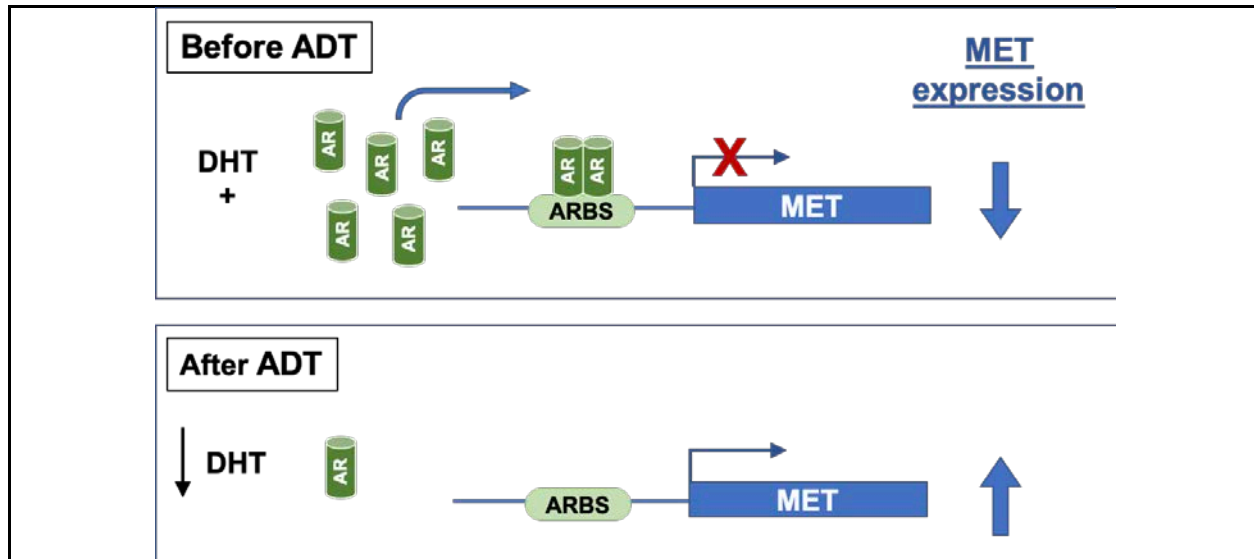


**Fig. 2. Diagram summarizing transcriptional repression of MET receptor as well as the impact of ADT on MET expression per data from Verras et al [36].**

### 1.3. HGF/MET as a target for PCa therapy

Increased levels of MET expression correlate with cancer progression and a poor prognosis [23]. Therefore, MET is of considerable interest as a pharmaceutical target as evidenced by the large number of drugs currently approved for clinical use or in clinical trial [25,38,39]. Strategies for targeting MET to inhibit cancer progression include: (1) inhibition of binding between HGF and MET by using antibodies or small molecules that bind to the HGF/MET binding pocket, (2) inhibition of MET tyrosine kinase phosphorylation and activation, and (3) the specific inhibition of downstream signaling proteins of signaling pathways shown to be upregulated in those cancers [25].

There are many types of MET inhibitors used clinically, to treat cancer where MET is overexpressed or mutated. Crizotinib is a dual-purpose c-MET and anaplastic lymphoma kinase inhibitor approved for treatment of non-small cell lung cancer (NSCLC) [25,40]. It inhibits c-MET activation through direct binding to the intracellular domain [41]. Onartuzamab is an example of

a humanized monoclonal antibody being evaluated for use against NSCLC that can bind the extra cellular domain of MET to inhibit binding and activation by HGF [41,42]. PHA-665752 is another small molecule inhibitor with a high affinity to bind c-MET and inhibit activation and downstream signaling and is being evaluated for use against neuroblastoma cells [43,44]. Finally, trivantinib is a selective small molecule inhibitor of c-MET and prevents its activation by HGF for treatment of hepatocellular carcinomas [45]. These are just a few examples of the variety of inhibitors that target the HGF/MET signaling pathway in various cancers to highlight the level of importance of this pathway as a therapeutic target.

In PCa, the recent interest in MET as a pharmaceutical target is due to the high levels of MET and HGF expression in bone metastases and its association with the development of CRPC [32]. Therefore, c-Met inhibitors such as cabozatinib and AMG 102 are currently in clinical trial for advanced CRPC [32].

#### **1.4. HGF/MET regulation of Stathmin phosphorylation**

The phosphoprotein Stathmin (STMN1) is differentially phosphorylated on 4 regulatory serine residues by a number of signaling pathways to regulate spindle formation during cell cycle progression and microtubule formation in EMT [46-59]. The p34<sup>cdc2</sup> kinase primarily phosphorylates STMN1 on serine 38 (S38) to promote entry of Jurkat T cells and HeLa cells into mitosis [60]. Phosphorylation of STMN1 occurred to a lesser extent on S25 and S16 in Jurkat T cells [61]. Since HGF/MET promotes PCa cell proliferation, we postulated that HGF/MET would phosphorylate STMN1. In lung endothelial cells, MET phosphorylation activated Rac1/Pak, resulting in the phosphorylation of STMN1 S16 [62], and S16 phosphorylation correlated with

increased cell proliferation and remodeling of microtubules (MTs) and actin filaments. In human keratinocytes, STMN1 S16 was phosphorylated by HGF to promote cell proliferation and cell migration [63]. In hepatocellular carcinoma (HCC), STMN1 expression correlated with increased proliferation, migration and drug resistance [64]. When HCCs were co-cultured with hepatic stellate cells (HSCs), STMN1 and HGF protein levels in HCC increased [64]. The upregulation of STMN1 in HCCs induced the acquisition of CAF-like characteristics in HSCs (i.e. increased HGF expression) that were critical for the development and progression of PCa [64]. Of interest was that the addition of the MET inhibitor Crizotinib significantly inhibited the crosstalk between HCCs and HSCs and decreased the rate of tumor growth *in vivo* [64].

In summary, these studies describe the role of the AR in the regulation of PCa proliferation and how the TME modulates PCa progression. While studies on the importance of HGF/MET signaling in solid tumor cancers, and as a component of the TME, have been published, there is still a great deal we do not know about the intricacies of the HGF/MET signaling pathway and how it regulates cancer progression and the development of EMT.

## **1.5. Hypothesis**

Currently, a literature search on studies investigating the role of HGF/MET in phosphorylating STMN1 and how HGF/MET-mediated phosphorylation of STMN1 regulates the cell cycle and cancer progression revealed that these types of studies had not been carried out. This knowledge gap was the impetus behind the work in this thesis.

Thus, my hypothesis was that **MET signaling phosphorylates Stathmin S16 to promote cell cycle progression and that blocking S16 phosphorylation decreases tumor cell growth without activating metastatic potential, thereby attenuating cancer progression.**

The following chapters report on the experimental strategies used in investigating this hypothesis and the findings which support that MET signaling selectively phosphorylates STMN1 S16 to promote cell cycle progression. Importantly, STMN1 S16 phosphorylation does not activate metastatic potential, suggesting that a treatment preventing STMN1 S16 phosphorylation might inhibit, or prevent, the emergence of therapeutic resistance in PCa. This work was done using human DU-145 prostate cancer cells and in normal murine mammary gland (NMuMG) cells, a known cell model used to investigate EMT [65], thus demonstrating that the mechanisms by which HGF/MET signaling regulate cell cycle progression through STMN1 S16 phosphorylation are common to epithelial cells. In conclusion, MET is an attractive therapeutic target that could be used in combination with other therapies in the treatment of epithelial cell-derived cancers.

# Chapter 2

## **HGF/MET-mediated Phosphorylation of Stathmin Serine 16 Regulates Cell Cycle Progression and Cell Proliferation**

Paul L. Deford, Andrew P. VonHandorf, Brian G. Hunt, Carissa Lester,

Susan Waltz, Katherine Burns, and Susan Kasper

In preparation for submission to Cancer Research, 2022

## 2.1. ABSTRACT

A common treatment in prostate cancer (PCa) is Androgen Deprivation Therapy (ADT). Targeting and downregulation of the Androgen Receptor (AR) by ADT typically results in the development of castration resistant prostate cancer (CRPC) which can be partially characterized by the derepression of the MET receptor, and the subsequent increase in Hepatocyte Growth Factor (HGF)/MET signaling. While HGF/MET-mediated signaling activates a variety of cellular responses in a multitude of cancers, a key pathway involves the regulation of cell cycle progression and cell proliferation. Stathmin1 (STMN1), a phosphoprotein in the HGF/MET signaling pathway, can be phosphorylated on four major serine regulatory sites (i.e., S16, S25, S38, and S63). While activation of HGF/MET can lead to differential phosphorylation of STMN1, we demonstrate, for the first time, that HGF/MET-mediated phosphorylation of STMN1 S16 in PCa cells leads to a shortening of cell cycle progression and increase in rate of cell proliferation, without inducing metastatic potential. Further, inhibition of HGF/MET-mediated signaling by the specific kinase inhibitor, AMG337, results in a decrease in the rate of cell cycle progression and cell proliferation and an increase in cell death. The data described in this study outlines a therapeutic strategy that utilizes current ADT methods in combination with the potent c-MET inhibitor, AMG337, to target both early and late stage PCa.

## **2.2. Introduction**

### **2.2.a. Role of the Tumor Microenvironment in Modulating Cancer Progression**

Androgen targeted therapy is the gold standard in the treatment of advanced PCa; however, advanced PCa will become non-responsive to androgen deprivation therapy (ADT). Second line therapies such as enzalutamide and abiraterone are used to treat PCa while it remains hormone sensitive, and chemotherapy becomes the treatment of choice once PCa progresses to castration-resistant prostate cancer (CRPC) [1,2]. The mechanisms driving therapeutic resistance remain unclear. The tumor microenvironment (TME) is an essential component of PCa and provides factors that promote cancer growth, progression, metastatic spread, and therapeutic resistance [3]. Cancer associated fibroblasts (CAFs) within the tumor stroma produce enzymes and other factors to remodel the extracellular matrix, vascular endothelial growth factor A (VEGFA) to promote angiogenesis, and chemokines and cytokines which interfere with T cell function and allow PCa cells to evade immune surveillance [4]. A growth factor secreted by CAFs is hepatocyte growth factor (HGF). HGF binds to the HGF receptor, MET, to promote tumor cell proliferation and cancer progression [5-9]. Of note, AR represses the expression of MET in a ligand-dependent manner by targeting and binding to the Sp1 region of the MET promoter to inhibit transcription by Sp1 [10]. Furthermore, downregulation of AR in response to ADT results in a derepression of MET expression in PCa cells, which increases HGF/MET signaling and drives PCa cell proliferation and metastasis [10].

### **2.2.b. Role of HGF/MET signaling in regulating STMN1 phosphorylation and tumor growth**

The phosphoprotein STMN1 regulates spindle and microtubule formation through the differential phosphorylation of four regulatory serine (S) residues in the N-terminal region, S16, S25, S38, and S63 [11]. While little is known regarding the mechanism(s) by which HGF/MET signaling

regulates STMN1 phosphorylation, cell proliferation, and PCa progression, the role of HGF/MET/STMN1 signaling has been investigated in other cancers, such as hepatocellular carcinoma (HCC) [12]. In HCC/hepatic stellate cell (HSC) co-culture experiments, HSCs secreted HGF which in turn, increased STMN1 expression in HCC cells, while the increased STMN1 expression in HCCs promoted the development of a CAF-like phenotype in HSCs [12]. In addition, the MET inhibitor crizotinib inhibited the crosstalk between HCCs and HSCs [12]. While these experiments investigated the role of STMN1 expression, they did not address the mechanisms by which STMN1 phosphorylation regulated these processes.

### **2.2.c. Therapeutics that could target HGF/MET and the phosphorylation of STMN1**

Currently, >1,000 clinical trials are being conducted, where the target of the trial is HGF/MET signaling [13]. The three primary approaches being used to block HGF/MET signaling include: inhibition of binding between HGF and MET via antibodies or small molecules that bind to the HGF:MET binding pocket (Onartuzamab), inhibition of tyrosine kinase phosphorylation/activation of the intracellular fraction of c-MET (AMG337), and the specific inhibition of downstream signaling proteins (e.g., Pak1) to target relevant signaling pathways shown to be upregulated in those cancers, namely solid tumors where MET is overexpressed (e.g. non-small cell lung cancer, PCa, hepatocellular carcinoma, etc.) (IPA-3) [14-19]. Importantly, inhibition of c-MET has shown the most positive outcomes in clinical trials [17].

In PCa (as well as in breast, renal, and lung cancers), the recent interest in MET as a pharmaceutical target is due to the high levels of MET and HGF expression in bone metastases and its association with the development of CRPC [20]. Therefore, c-Met inhibitors such as cabozatinib are currently in clinical trial for advanced CRPC [21]. A further benefit to using a MET inhibitor in combination with ADT would be that both AR(+) cancer cells, and the AR(-)

population in both local and distal disease would be eliminated. The DU-145 cell line is used for these experiments, due to its CRPC-mimicking characteristics, being an insensitivity to androgens and expressing a mutant, inactive p53 protein.

#### **2.2.d. Hypothesis**

While studies on the role of HGF/MET signaling in cancer development, and especially in PCa progression are available, minimal to no studies elucidate the role of HGF/MET-mediated phosphorylation of STMN1, and its role in cancer progression. However, previous data has demonstrated that knockdown of total STMN1 induces metastasis and is therefore not a viable treatment option. Thus, my hypothesis is that **MET signaling phosphorylates Stathmin S16 to promote cell cycle progression and blocking S16 phosphorylation decreases tumor cell growth without activating metastatic potential, thereby attenuating cancer progression.**

Here I provide the first report that MET signaling selectively phosphorylates STMN1 S16 to promote cell cycle progression. Importantly, STMN1 S16 phosphorylation does not activate metastatic potential, as has been previously reported with knocking down total STMN1, suggesting that a treatment preventing STMN1 S16 phosphorylation might inhibit, or prevent, the emergence of PCa therapeutic resistance. Thus, MET is an attractive therapeutic target that could be used in combination with ADT in the treatment of PCa.

## 2.3. MATERIALS AND METHODS

### 2.3.a. Materials

KN93 phosphate (5215/1) and KN92 (4130/1) were purchased from Tocris bioscience. Oleic Acid (S4707) was purchased from SelleckChem. Hepatocyte Growth Factor (HGF) (100-39H) was purchased from Peprotech. AMG-337 (HY-18696) was purchased from MedChem Express. Antibodies used in western blot assays are listed in **Supplementary Table 1**. Lipofectamine 2000 (11668019) was purchased from Thermo Fisher Scientific. 48-well micro chemotaxis chamber and membranes (AP48) were purchased from Neuroprobe.

### 2.3.b. Methods

#### 2.3.b.i. Analysis of HGF, MET, and STMN1 expression in tumors from men with metastatic castration resistant prostate cancer (mCPRC).

The expression microarray dataset analyzed in our study was carried out using data deposited in the Gene Expression Omnibus database, accession number GSE77930 to investigate the correlation between HGF, MET, and STMN1 expression in advanced PCa. The description of patient enrollment, tissue acquisition and processing, and approval by the Institutional Review Board (IRB) of the University of Washington and of the Fred Hutchinson Cancer Research Center are described in detail in Kumar, *et al.* [22]. Briefly, 176 primary or metastatic tumors were resected from 63 men with metastatic CRPC (mCPRC) at the time of rapid autopsy. Since tumor quantity was limited in a small subset of tumors, transcript expression by microarray hybridization was analyzed in 171 tumors from 63 men. The majority (n = 156) were adenocarcinomas, 20 tumors from two men were small-cell neuroendocrine histology, and all patients received androgen-deprivation therapy. Following disease progression, most patients also received at least

one additional AR pathway-targeted agent (most commonly bicalutamide and flutamide), and at least one systemic chemotherapy (most commonly docetaxel) [22].

### **2.3.b.ii. Cell culture**

The DU-145 (HTB-81) cell line was obtained from ATCC and the NMuMG (CRL-1636) cell line was a gift provided by Harold L. Moses, MD, Vanderbilt-Ingram Cancer Center, Nashville, TN. DU-145 cells were cultured in complete medium containing Minimum Essential Medium/Eagle with Earl's Basic Salt Solution (MEM/EBSS, Gibco), 10% fetal bovine serum (FBS) (SH30071.03, Cytiva), and 1% Penicillin/Streptomycin (15-140-148, Fisher Scientific {Gibco}). NMuMG cells were cultured in complete medium containing Dulbecco's Modified Eagle Medium (12-100-061, Gibco) containing 10% FBS and 1% penicillin/streptomycin. Transient transfection assays in DU-145 and NMuMG cells were done using the same protocol. When cells reached ~70% confluence, complete medium was replaced with serum-free medium and cells were transfected with either control pECFP and pLKO.1 plasmids or plasmids containing *STMN1* substitution mutations [S16A, S16E, S25A, S25E, S38A, S38E, S63A, S63E, S(16,38)E, S16A(25,38,63)E, S16E(25,38,63)A, S(16,25,38,63)A, and S(16,25,38,63)E] or shSTMN1 (representing total STMN1 knockdown) using the standard Lipofectamine 2000 protocol (Invitrogen). Following an incubation period of 10 hrs at 37°C, the transfection medium was removed and replaced with either complete or serum free medium as indicated for the assays being performed.

### **2.3.b.iii. Proliferation assay**

Cells were trypsinized, plated at a concentration of  $2 \times 10^4$  cells/mL/well in 24-well plates, and allowed to adhere overnight. Complete medium was replaced with either serum free medium or medium containing 1% FBS as indicated, and cells were incubated overnight. The following day,

the medium (either serum free or containing 1% FBS) was replaced with fresh medium containing growth factors without/with small molecule activators or inhibitors as indicated for each experiment. Cells were incubated for 72 hrs, trypsinized, and both viable and dead cells were counted using the Trypan Blue Exclusion method for cell viability.

#### **2.3.b.iv. Doubling time assay**

Transfected cells were transfected prior to synchronization per 2.3.c. All cells were synchronized using the double thymidine protocol to G1 phase. After synchronization, cells were plated in 24-well plates at  $7.5 \times 10^4$  cells/well and allowed to adhere to the wells overnight. The following day, serum-free treatment medium without/with small molecules were placed in the wells. Each day for 6 days, both viable and dead cells were counted using the Trypan Blue Exclusion method for cell viability.

#### **2.3.b.v. Migration and invasion assay**

The Neuroprobe migration and invasion assays were performed as described previously [11]. For the top chamber, cells were cultured in serum-free medium for 9 h, trypsinized and diluted to a final concentration of  $1.6 \times 10^5$  cell/mL. Fifty  $\mu$ L of cell suspension in serum-free medium without/with activators or inhibitors as indicated were plated per well and the apparatus was wrapped in parafilm to reduce medium evaporation and placed at 37°C and 5% CO<sub>2</sub> overnight (~18 hrs). After incubation, the polycarbonate filter was removed, cells were removed from the upper side of the membrane and the remaining migrated cells were fixed in cold 100% methanol for 15 minutes. The membrane was air-dried, then migrated cells were stained in 0.5% crystal violet + the other things in the CV staining (you can put the ingredients in here) for 15 minutes, and the stained membrane was mounted on a microscope slide [23]. Wells were photographed

(Leica DMil) and analyzed using Leica software (LAS V4.12). Invasion assays were conducted using the same protocol as the migration assay with the modification that the polycarbonate membrane was coated with a thin layer of reduced growth factor Matrigel (Corning). Matrigel was diluted to a concentration of 0.5  $\mu\text{g}/\mu\text{L}$  in sterile filtered (0.2  $\mu\text{M}$ ) coating buffer [0.01M Tris (pH 8.0), 0.7% NaCl] with a n=4 wells for each treatment per assay, and each assay was repeated at least 3 times [24].

### **2.3.b.vi. Analysis of DU-145 Conditioned Medium**

To determine whether DU-145 cells were producing and secreting HGF without co-culture with a different cell type, DU-145 cells were plated in 100 mm dishes (at ~60-70 confluence) and allowed to adhere in complete medium overnight. Following adhesion, complete medium was removed, and cells were rinsed with room temperature 1X PBS. Finally, 4 mL serum-free medium was placed on each 100 mm dish and was collected at specified time points. Following medium collection, conditioned medium was centrifuged and protein was concentrated for western blot analysis. A serial dilution of recombinant HGF protein was used as a positive control.

### **2.3.vii. Western blot analysis**

Cells were harvested using RIPA buffer (Invitrogen Inc., catalog no.: R0278) with 1% protease inhibitor cocktail (Thermo Fisher Scientific, cOmplete Protease Inhibitor Cocktail tablets/Roche, catalog no.: NC0939492) and phosphatase inhibitor cocktail (Thermo Fisher Scientific, EMD Millipore Calbiochem Phosphatase Inhibitor Cocktail Set I, catalog no.: 53-913-110VL). Lysates were centrifuged at 15,000 x g for 15 minutes to remove cell debris. Protein was quantified using BCA protein assay (Abcam ab102536). Forty or 50  $\mu\text{g}$  of protein supernatant were run on 10% SDS-PAGE gels, transferred to poly-vinylidene difluoride (PVDF) membrane, and blocked for 1

hr at room temperature in 3% non-fat dry milk in TBS-T. Membranes were then probed with primary antibody overnight at 4°C. Following 3 washes with horseradish peroxidase (HRP) conjugated secondary antibody was added at a 1:10,000 dilution for both rat and mouse antibodies for x time, before the blots were developed using the Enhanced Chemiluminescence (ECL) kit (Pierce/ThermoFisher Scientific, catalog no.: 32132). Antibodies used in this study are listed in Supplementary Table S1.

### **2.3.b.viii. Total RNA extraction, purification, and cDNA synthesis**

Total RNA extraction and purification was conducted using the Qiagen RNeasy Kit (Cat. No. / ID: 217084) according to manufacturer's instructions. To generate cDNA synthesis, the Thermo Fisher RevertAid First Strand cDNA Synthesis Kit (K1621) was used per the manufacturer's instructions.

### **2.3.b.ix. Flow Cytometry**

Cells were trypsinized and centrifuged as described above, and then washed with cold PBS before repeated centrifugation. Cells were then fixed with a 1:2 ratio of cold PBS:cold Ethanol for a minimum of 2 hrs at 4°C or a maximum of 2 weeks. Cells were then centrifuged as described above and resuspended in 1mL cold PBS, before adding 1µL RNase A and incubating at 37°C for 30 minutes before adding 100µL Propidium Iodide (PI) to stain the cells. Cells were kept in the dark on ice following staining before being analyzed by the Luminex Guava® Flow Cytometer. Sample readouts from the Guava® Flow Cytometer were analyzed using FlowJo v.10 software to create cell cycle distribution histograms for analysis.

### **2.3.b.x. Quantification and statistical analysis**

Statistical analysis and quantification of significant differences between experiments with multiple treatments were analyzed using one-way ANOVA applying Dunnett's post-hoc correction for

multiple comparisons in GraphPad Prism version 9.4.0 for Mac (GraphPad Software, San Diego, California USA).

## 2.4. RESULTS

### 2.4.a. Increased MET expression correlates with an increase in STMN1 expression in mCRPC.

Increased HGF expression correlates with increased MET expression in PCa cells [10]. Furthermore, increased MET expression levels correlate with cancer progression and a poor prognosis [14,15], with very high MET levels being detected in CRPC [10]. To determine whether STMN1 expression correlated with HGF and MET expression in mCRPC, expression microarray datasets generated from PCa tissues (171 tumors from 63 men) acquired by rapid autopsy from the prostate and from a number of metastatic sites including liver, adrenal, lung, lymph node, bone, peritoneal and bladder sites were analyzed (Gene Expression Omnibus database, accession number GSE77930) [22]. In these samples, all patients initially received androgen-deprivation therapy, and following disease progression, most patients then received at least one additional AR pathway-targeted agent (most commonly bicalutamide and flutamide), and at least one systemic chemotherapy (most commonly docetaxel) [22].

Correlation analysis determined that MET and STMN1 expression positively correlated significantly ( $p= 0.0001$ ), and that they were similarly expressed in mCRPC (**Fig. 1A, 1B**). The greatest difference in HGF expression levels were observed following chemotherapy, where HGF was more highly expressed in patients receiving chemotherapy after ADT and second line therapy (e.g., bicalutamide or flutamide) as compared to those receiving ADT and second line therapy only (**Fig. 1C**). The increase in HGF production after chemotherapy could be due to the development of CRPC post ADT and/or treatment with bicalutamide or flutamide.

Furthermore, STMN1, HGF, and MET expression remained similar in PCa samples removed from various metastatic sites, indicating that their expression levels were independent of tumor heterogeneity among men [22]. One exception occurred in PCa metastasis to the liver, where STMN1 and HGF expression was upregulated, while MET expression remained unchanged (Fig. 1D-1F), possibly suggesting that the HGF-MET-STMN1 signaling axis could be hyperactivated in secondary tumors in the liver.

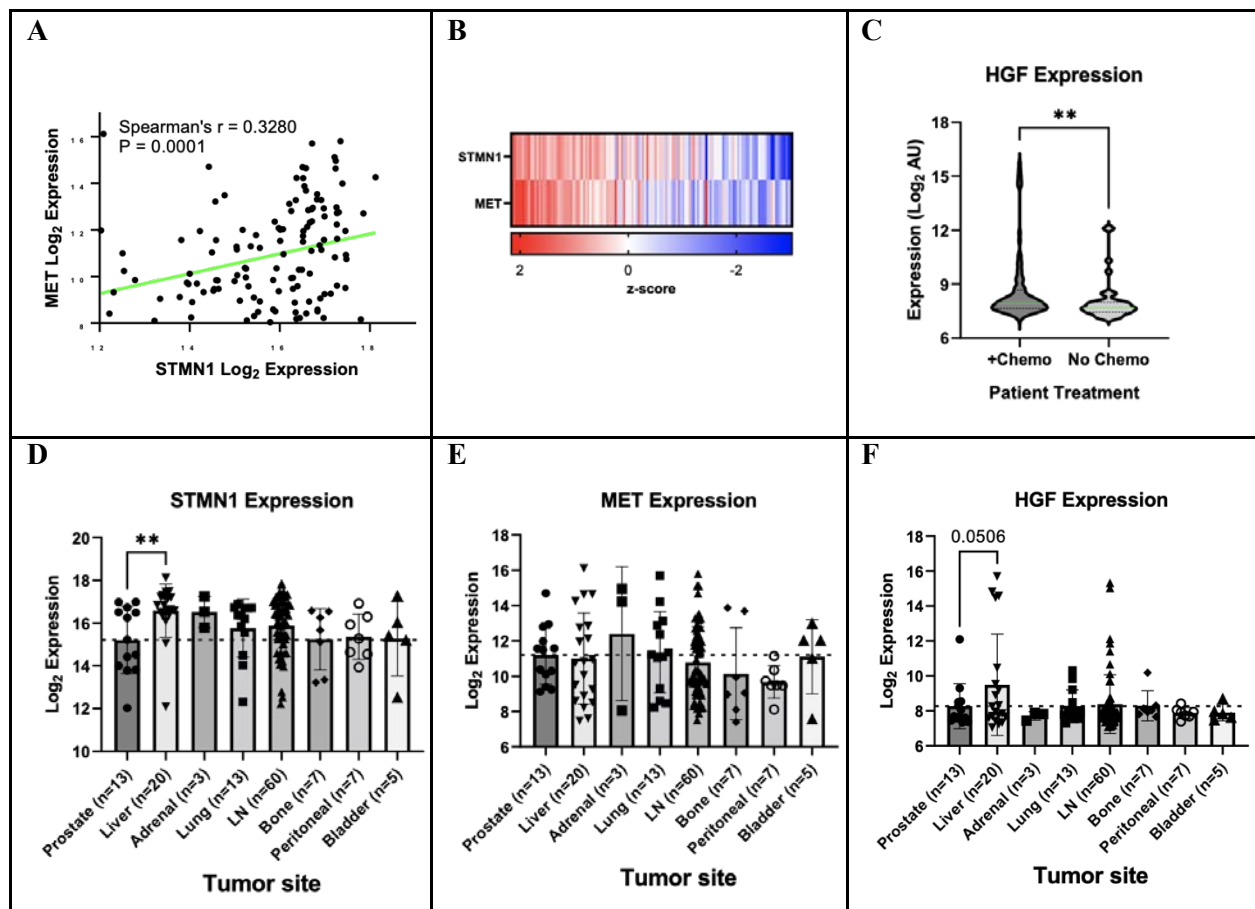


**Fig. 1. MET and STMN1 expression positively correlate with and are predictive of advanced PCa.**

**A.** Correlation analysis of MET and STMN1 expression in metastatic prostate cancer tumor samples [Gene Expression Omnibus database, expression microarray, accession number GSE77930]. **B.** Heatmap of z-scores demonstrates a high degree of similarity of MET and STMN1 expression across the tumors across distal regions (liver, adrenals, lung, lymph node (LN), bone, peritoneal cavity, and bladder). **C.** HGF expression when stratifying samples in this dataset based on whether the patient received chemotherapy or not prior to sample acquisition. HGF expression increased significantly following Chemotherapy. **D.** STMN1, **E.** MET, and **F.** HGF expression in PCa samples taken from primary or metastatic sites.

Taken together, the upregulation of HGF in response to chemotherapy could lead to increased MET activation and subsequent increased STMN1 phosphorylation that would further tumor growth and metastatic spread.

#### **2.4.b. HGF/MET signaling regulates cell proliferation**

HGF/MET signaling is associated with increased cell proliferation and upregulation of STMN1 expression, affecting a variety of cellular processes in different cancers [6-8]. To confirm that HGF promoted DU-145 cell proliferation, the protocol outlined in 2.3.c. was used to treat wild type (wt) DU-145 cells with increasing concentrations of HGF in serum-free MEM/EBSS (Gibco) medium. Cells were harvested and viable and non-viable (dead) cells were counted after 72 hrs using the Trypan Blue exclusion test for viability. Treatment of DU-145 cells with increasing doses of HGF resulted in a significant increase in cell proliferation at 25 ng/mL (**Fig. 2A**), and the number of dead cells did not change with increasing concentrations of HGF, implying that HGF, at the concentrations used, was not cytotoxic (**Fig. 2B, Supplemental Figure 1A**); however, a change in cell morphology was observed. Cells cultured in 25 ng/mL HGF retained their cobblestone-like epithelial appearance (**Supplemental Figure 1B**), but cells treated with 40 ng/mL HGF transitioned into a spindle-like mesenchymal morphology, suggesting that the highest concentration of HGF could induce EMT. Further experiments would need to be performed to determine whether this change in morphology is due to EMT [11]. Based on these observations, 25 ng/mL HGF was selected for the remainder of the study.

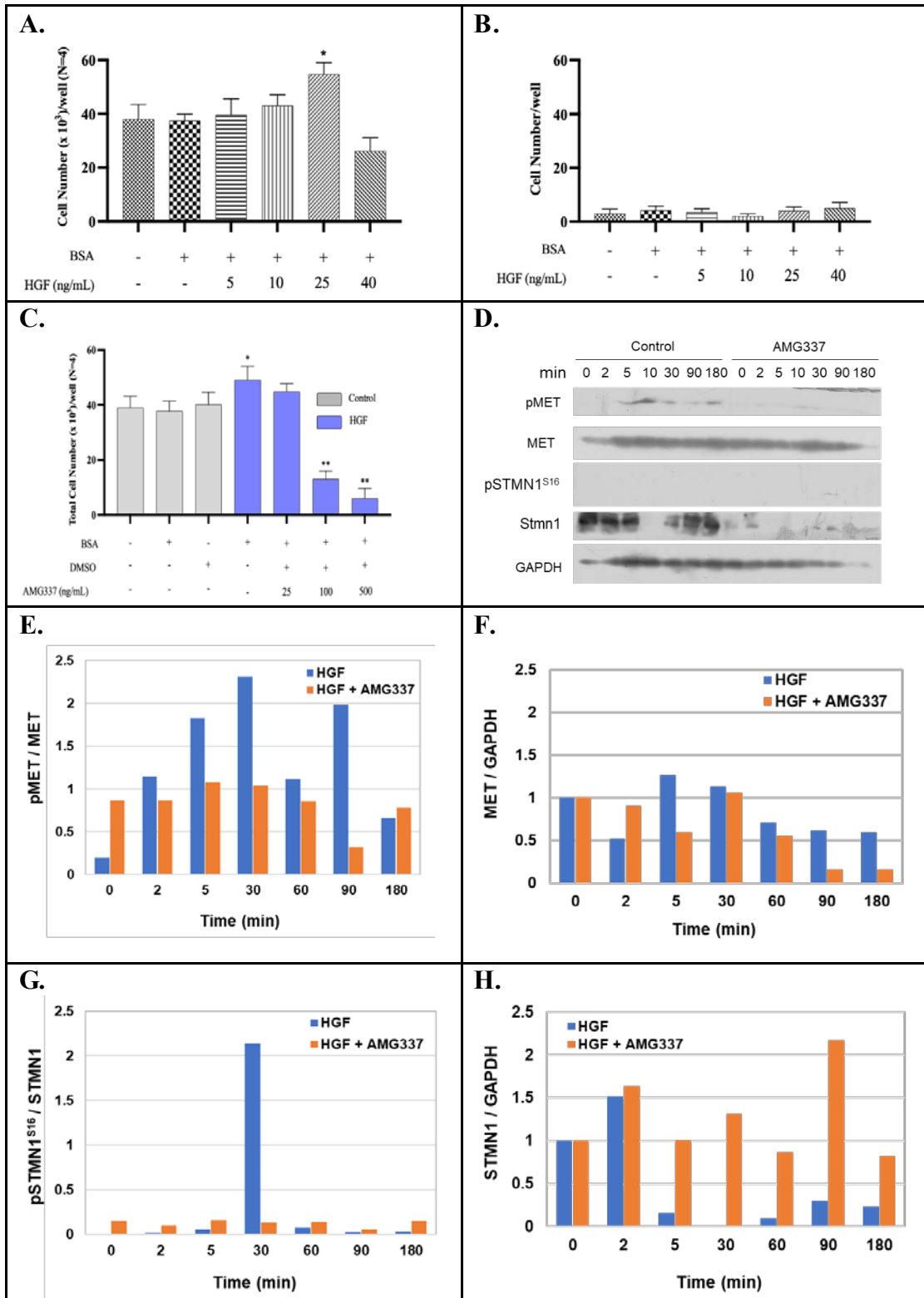
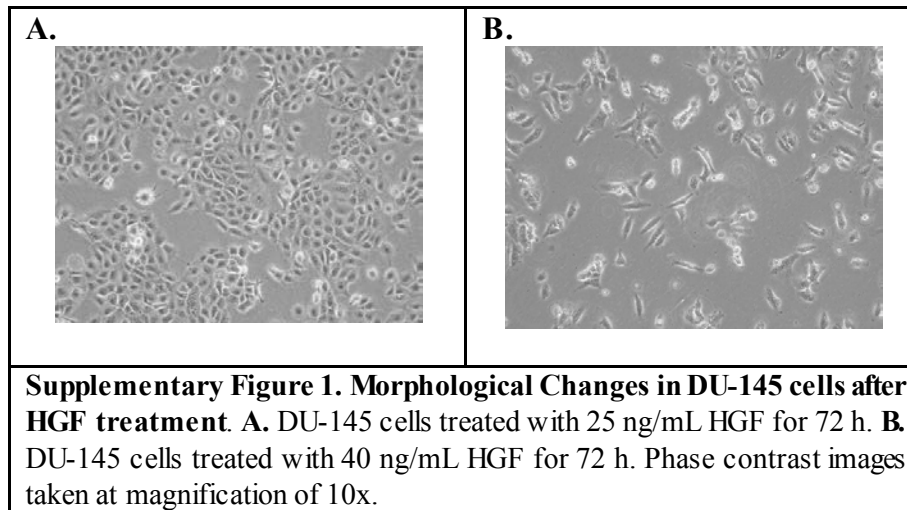
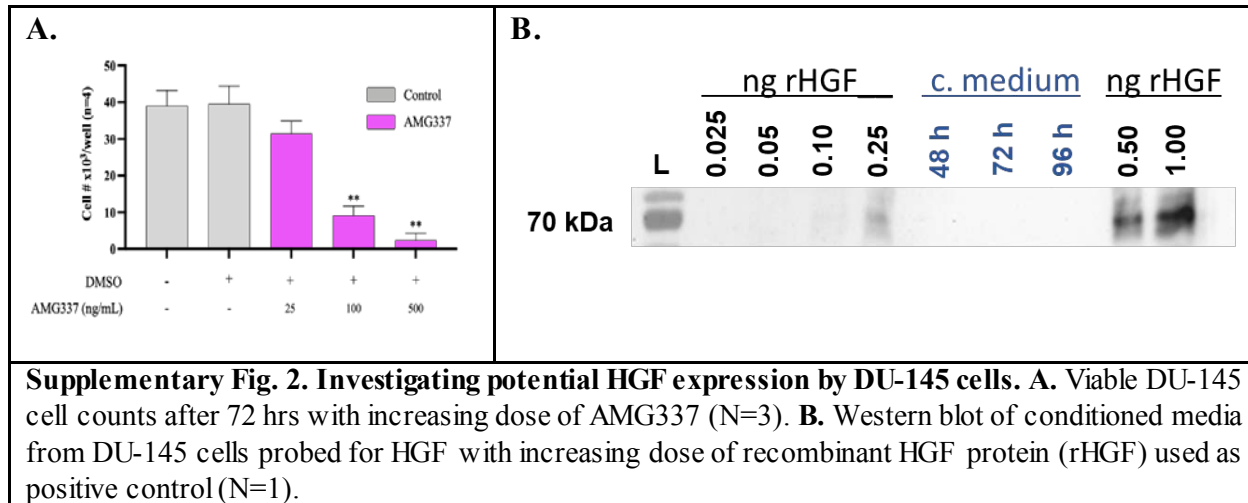


**Fig. 2. HGF/MET signaling regulates DU-145 proliferation.** Viable (A) and non-viable (B) cells in response to increasing concentrations of HGF (25ng/mL) for 72 hrs. C. Viable cells treated with increasing concentrations of the MET inhibitor AMG337 (100ng/mL) for 72 hrs. D. Western blot images of Control (Lanes 1-7) and cells treated with AMG337 (100ng/mL) alone (Lanes 8-14) over 180 min probed for pMET, total MET, pSTMN1<sup>S16</sup>, STMN1, and GAPDH. E-H. Corresponding densitometry. \* p<0.01, \*\* p<0.001 N=3



As demonstrated in **Supplementary Figure 2A**, treatment with AMG337 alone significantly inhibited DU-145 cell proliferation at 100 ng/mL and 500 ng/mL in cells treated with 25 ng/mL HGF and with AMG337 alone (**Fig. 2C**). Therefore, the concentrations of 25 ng/mL HGF and 100 ng/mL AMG337 were used, unless otherwise indicated. Cells treated with AMG337 alone (100ng/mL and 500ng/mL) exhibited a significant increase in non-viable cells, indicating toxicity at higher doses. Control cells cultured in serum-free media with no addition of HGF demonstrated phosphorylation of MET beginning at 5 min, lasting until 180 min (**Fig. 2D**).



To determine if DU-145 cells make HGF that could act in an autocrine function to activate its own MET receptor, DU-145 cells were cultured in serum-free medium for up to 96 hrs. Conditioned medium was collected, proteins were concentrated, and run on a 12% SDS-PAGE Gel and probed with anti-HGF (**Supplemental Figure 2B**). HGF was not detected in the conditioned medium. Increasing concentrations of recombinant human HGF served as positive control. While the western blot demonstrated no detectable levels of HGF in the conditioned media samples, the limit of detection in the positive control dose response demonstrated that concentrations of HGF below 0.05ng/mL were also not detected. Therefore, to confirm a lack of HGF production and secretion in DU-145 cells, RT-qPCR will be conducted to measure levels of HGF mRNA transcribed.

To understand the effect of HGF/MET signaling on STMN1 phosphorylation, cells were treated with 25 ng/mL HGF for 0 to 180 minutes (**Fig. 3A**). Phosphorylation of STMN1 S16 was detected at base line (0 minutes) with phosphorylation increasing at 10 minutes with a peak phosphorylation 90 minutes after HGF treatment (Fig 3A). At 180 mins, pSTMN1 S16 decreases to near basal levels (**Fig. 3A/B**).

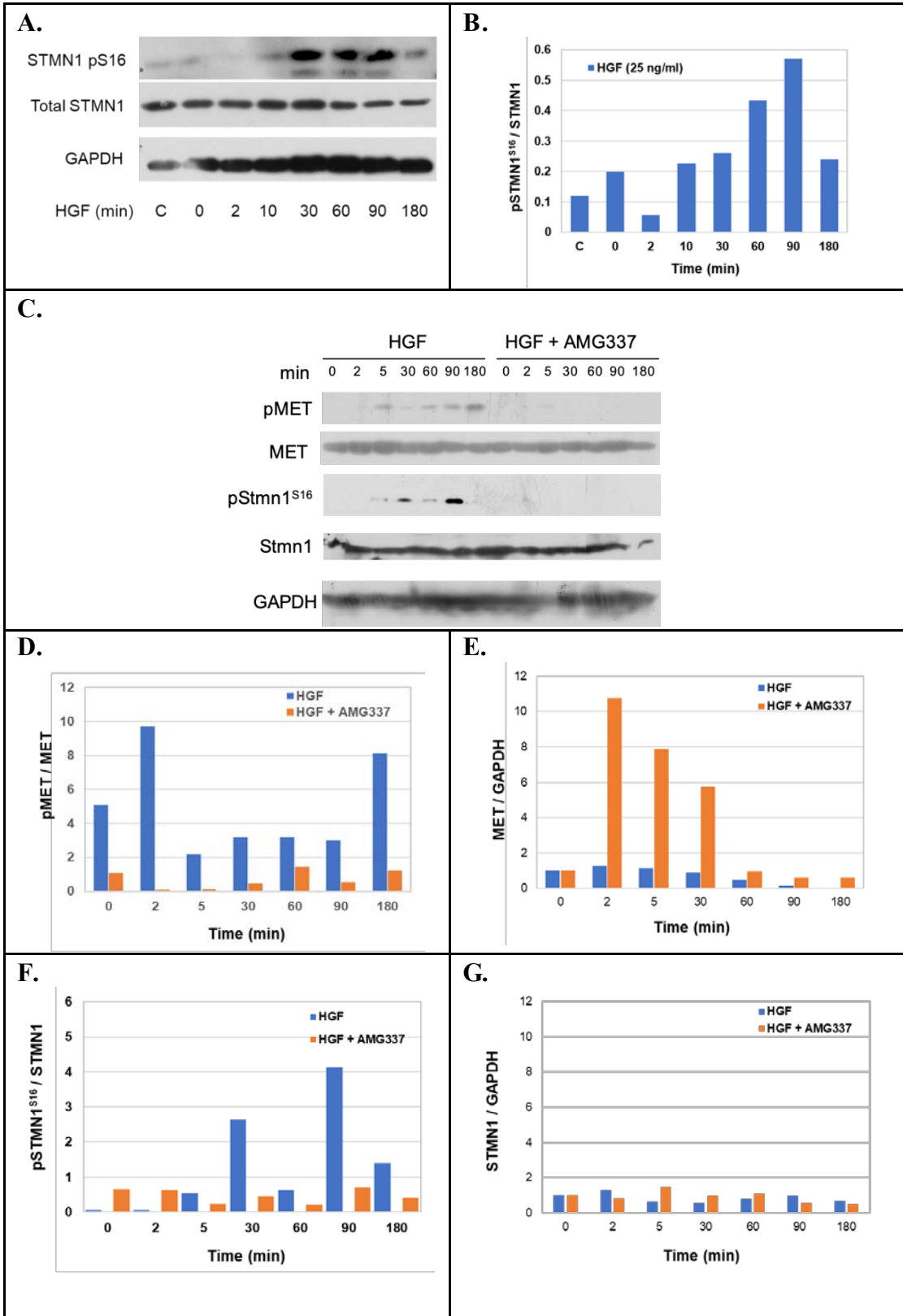
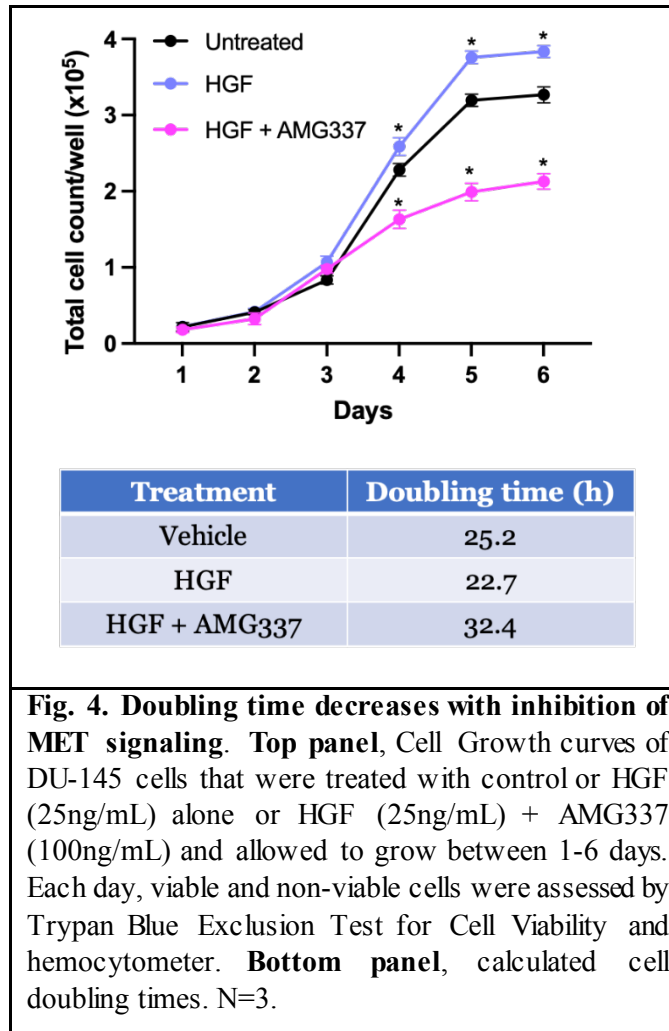


**Fig. 3. HGF treatment induces phosphorylation of MET and STMN1 S16, which is inhibited by MET inhibitor AMG337. A.** Cells treated with 25ng/mL HGF over increasing time (0-180min) before protein was isolated at each time point listed and analyzed by western blot (Lanes 8-14). Antibodies towards pSTMN1<sup>S16</sup>, total STMN1, and GAPDH used to probe membranes with densitometry in **B. C.** Western blot images of cells treated with HGF (25ng/mL) alone (Lanes 1-7) and HGF (25ng/mL) + AMG337 (100ng/mL) for 0-180 min before protein was isolated and analyzed by western blot (Lanes 8-14). Antibodies towards pMET, total MET, STMN1 pS16, STMN1, and GAPDH (from top to bottom order) used for probing membranes along with densitometry **D-G.** N = 3.

To determine the role of MET and STMN1 phosphorylation in HGF/MET-mediated regulation of DU-145 cell proliferation and cell cycle progression, cells were treated with HGF alone or with HGF + AMG337 for up to 180 minutes. Following treatment, proteins were isolated and western blots were probed for pMET, total MET, pSTMN1<sup>S16</sup>, total STMN1, and GAPDH. **Fig. 3C** supports **3A** demonstrating strong induction of pSTMN1<sup>S16</sup> at 30 minutes, peaking at 90 minutes. **Fig. 3C** also demonstrates the efficiency of AMG337 to completely inhibit phosphorylation of the HGF/MET signaling pathway at all time points.

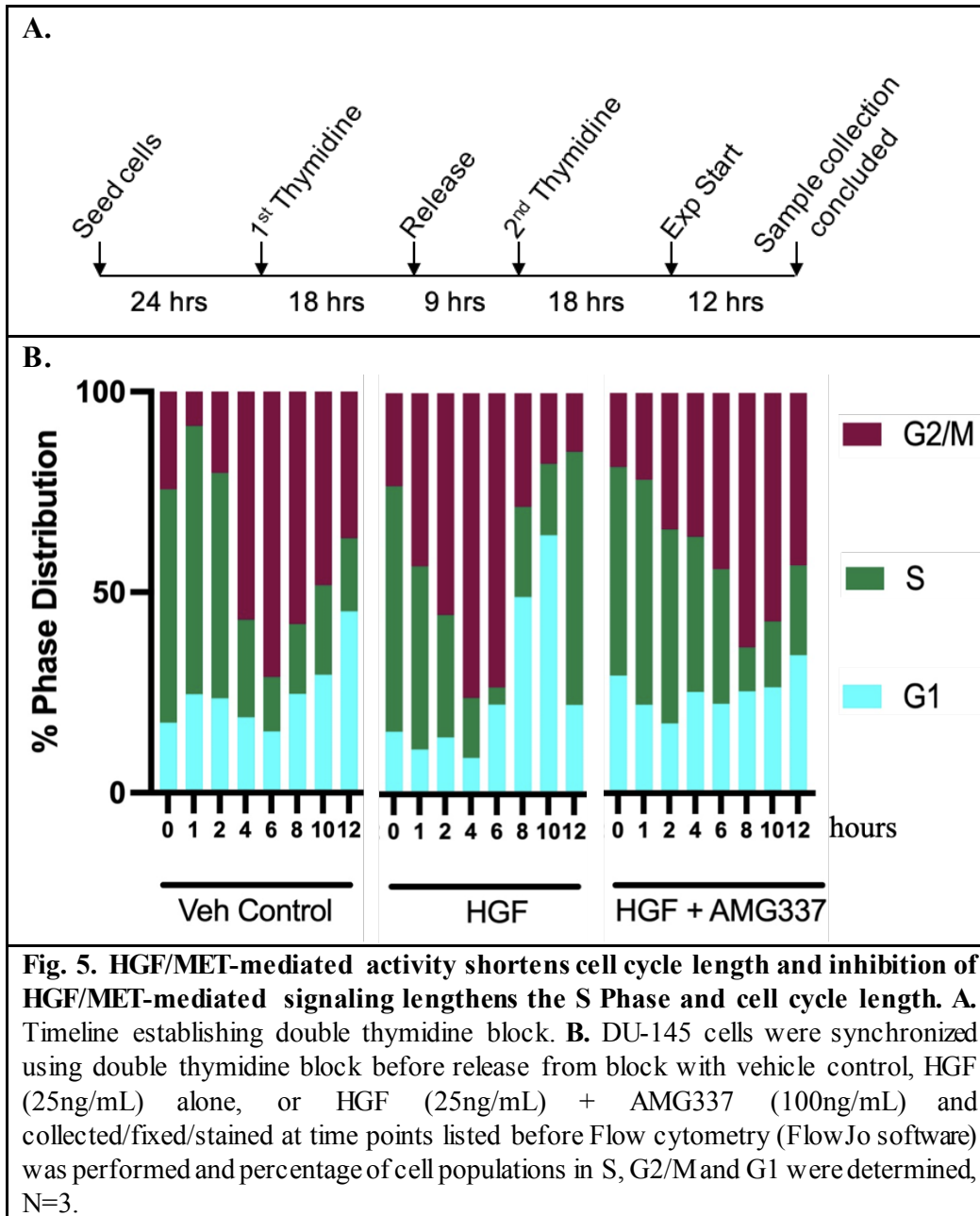
After establishing HGF/MET regulation of DU-145 proliferation, doubling time assays were conducted to quantitatively assess how/if HGF/MET regulation would impact the rate of cell doubling. As seen in **Fig. 4**, treatment with 25 ng/mL HGF + 100 ng/mL AMG337 significantly ( $p < 0.0001$ ) lengthened the doubling time from 25.2 hrs for control to 32.4 hrs for HGF + AMG337. Further supporting 25 ng/mL HGF increases cell proliferation, HGF alone shortened cell doubling time to 22.7 hrs. These data support **Supplemental Figure 2A**, which demonstrates increased DU145 cell proliferation with HGF and the inhibition of cell proliferation with 25 ng/mL HGF + 100ng/mL AMG337.



#### 2.4.c. HGF-mediated MET signaling phosphorylates Stathmin S16 and shortens cell cycle progression.

While the data in **Figures 2, 4, and Supplemental Figure 2** demonstrate that HGF/MET signaling regulates DU-145 cell proliferation, the mechanism of regulation is not known. To investigate the role of HGF/MET signaling in cell cycle progression, cells were synchronized via double thymidine block to the G1/S phase. After the block was released by treatment of cells with either vehicle, HGF, or HGF + AMG337 in serum free MEM/EBSS, cells were collected over 12 hrs,

before being fixed with cold give % here Ethanol/PBS, stained with PI, and analyzed by flow cytometry to determine DNA content and the percentage of cell cycle phase distribution.



The effects of HGF treatment on cell cycle progression are displayed in **Fig. 5**. After release from the double thymidine block, cells treated with vehicle alone exited S and entered G2/M at 4 hrs and peaked at 6 hrs with a steady decrease and entry into G1 at 12 hrs. In contrast, HGF-treated cells began to exit S enter G2/M at 1 h and peaked at 4-6 hrs with, a clear exit into G1 at 8 hrs; thus, demonstrating that HGF treatment shortened the S phase and length of the cell cycle by 4 hrs compared to the vehicle-treated group. Furthermore, in cells treated with HGF + AMG337, S phase was lengthened to 6 hrs with slow entry in G2/M that peaked at 8 hr. In addition, HGF/AMG337 treated cells did not clearly exit G2/M and the percentage of cells remaining in G1 remained consistent throughout the cell cycle, indicating that inhibition of HGF/MET activity lengthened the length of the cell cycle by approximately 4 hrs.

To determine where in the cell cycle Serine 16 was phosphorylated, DU-145 cells were synchronized at G1/S by double thymidine protocol and treated with vehicle, HGF, or HGF + AMG337 for 12 hrs (**Fig. 5**). Cells with vehicle control treatment alone showed low levels of pSTMN1<sup>S16</sup> (**Fig. 6A**). Importantly, HGF treatment induced S16 phosphorylation at 1 hr which paralleled the 1 hr timing when the cells entered G2/M (**Fig. 5**), implying that pSTMN1<sup>S16</sup> could be necessary for entry into G2/M.

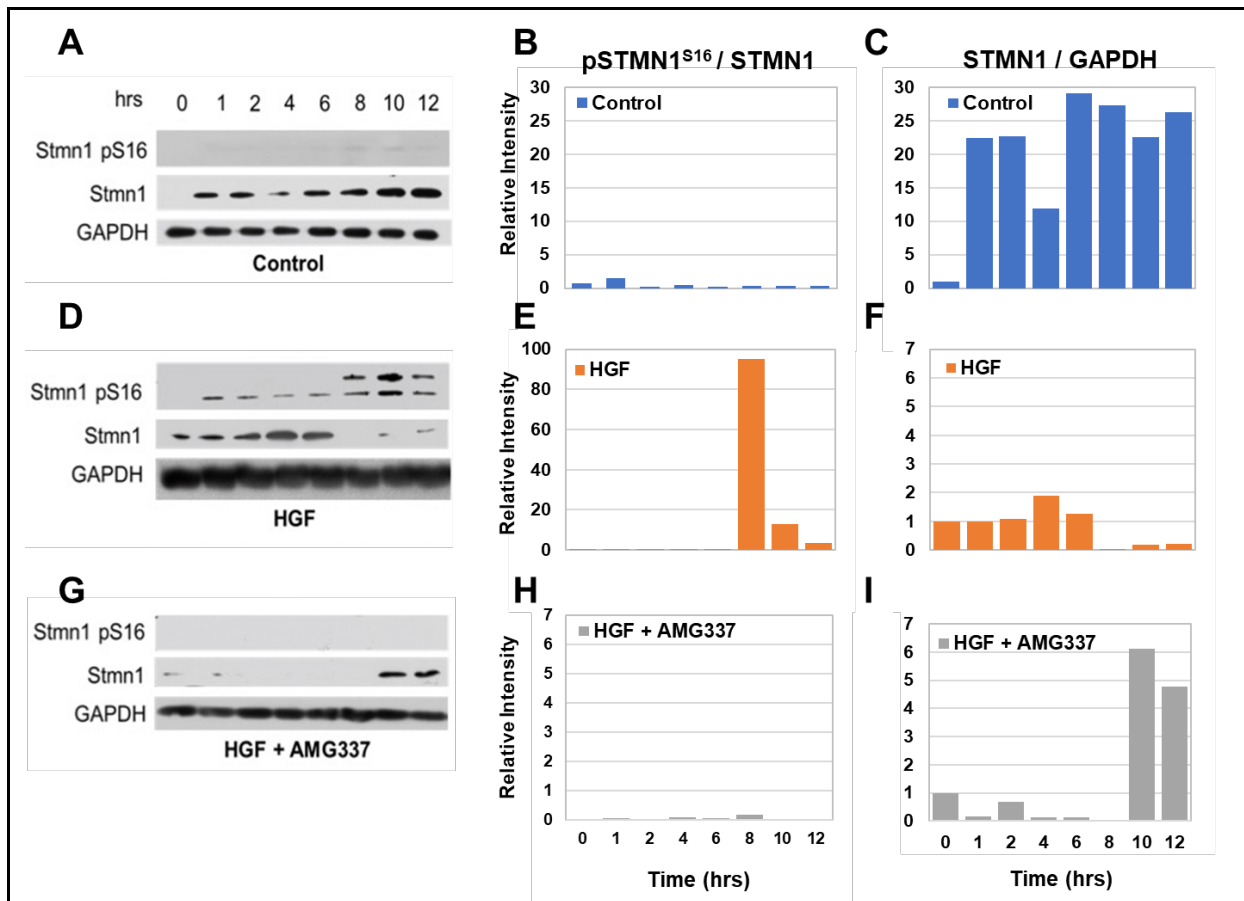


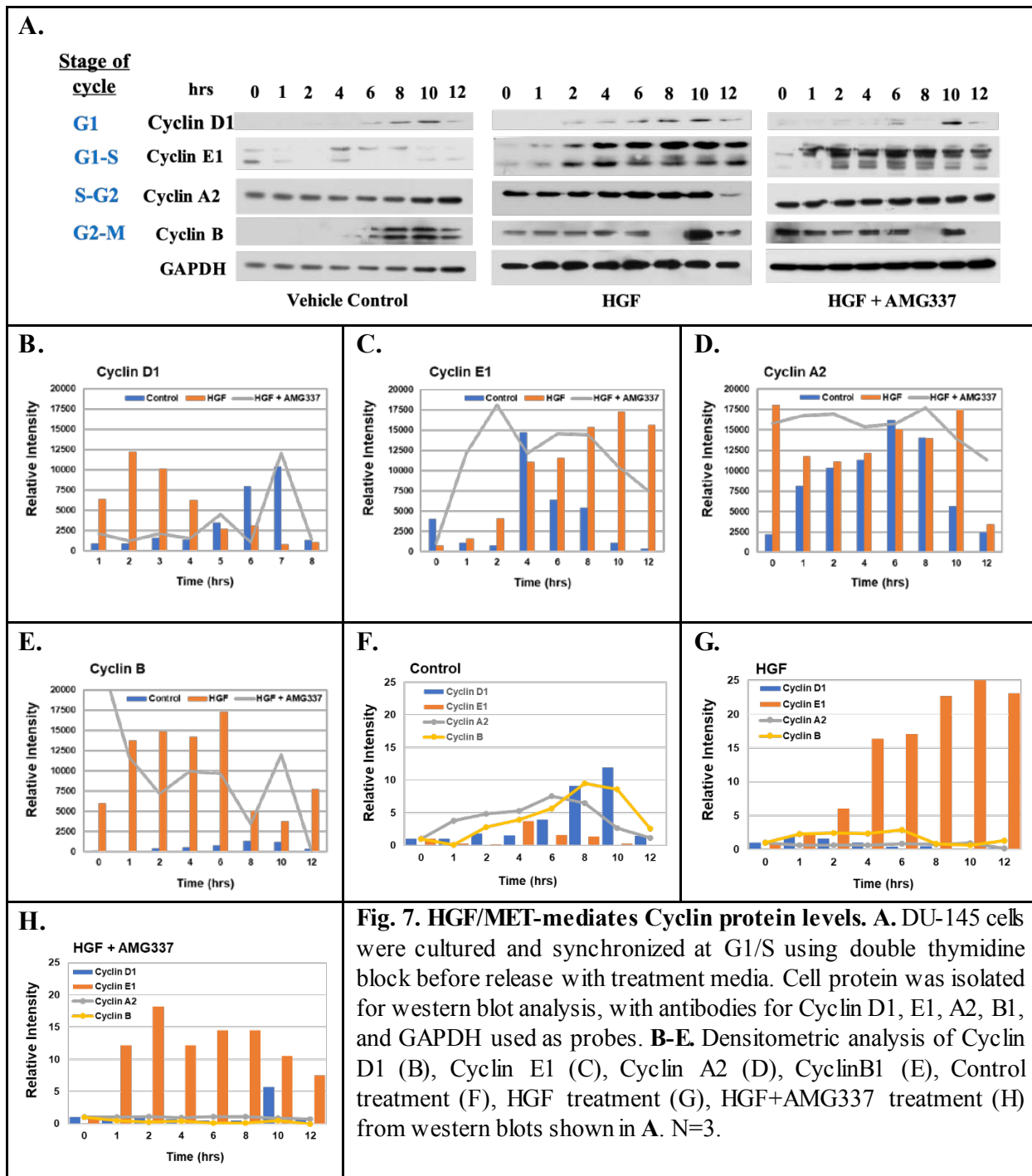
**Fig. 6. MET modulates Stathmin phosphorylation during cell cycle progression.** A. Control, DU-145 cells synchronized using double thymidine block to G1/S before release with vehicle for 0-12 hrs. Protein samples were collected and analyzed by western blot before being probed with antibodies against pSTMN1<sup>S16</sup>, STMN1, and GAPDH. B/C densitometric analysis of A; D. Same protocol as (A) with release from block with HGF (25ng/mL) and densitometric analysis E/F; G. Same protocol as (A) with release from block with AMG337, 100ng/mL, and densitometric analysis H/I. N=3.

In addition, pSTMN1<sup>S16</sup> increased greatly until most of STMN1 was phosphorylated when cells were entering G1 at 8 and 10 hrs (Fig 6D). The loss of total STMN1 between 8 to 12 hrs could indicate that the total STMN1 antibody does not recognize phosphorylated STMN1. The concurrent appearance of a shifted upper band at 8, 10, and 12 hrs indicates that other STMN1 serine residues are likely phosphorylated to mediate this band shift (Fig. 6D); however, the requirement of additional serine phosphorylation for transition into interphase remains to be determined. Interestingly, total STMN1 protein levels were below detectable levels when DU-145

cells were treated with HGF + AMG337 (**Fig. 6G**), but STMN1 was present at 10 and 12 hrs when cells began to enter G1. Moreover, STMN1 S16 phosphorylation was not detected at any time points, including once total STMN1 was present.

#### **2.4.d. HGF/MET signaling regulates cyclin expression during cell cycle progression**

The following western blot analyses were performed to determine the levels of cell cycle regulators in parallel with STMN1 S16 phosphorylation (**Fig. 7A**)



Cyclin D1 was induced at 6 hrs when most cells were in G2/M and increased as cells began to transition into G1 at 8-10 hrs compared to vehicle-treated cells (**Fig. 7B**). HGF treatment induced Cyclin D1 levels 4 hrs earlier (at 2 hrs) compared to vehicle-treated cells, and HGF +

AMG337 inhibited Cyclin D1 expression 4 hrs later (at 10 hrs) compared to vehicle-treated cells, thus corresponding to the shortened cell cycle observed with **Fig. 5**, where DU-145 cells progressed more rapidly through G2/M to G1.

Cyclin E1 levels were highest from 4 to 8 hrs in cells treated in control cells (**Fig 7C**). In contrast, HGF treatment began to cause an increase in Cyclin E1 expression at 1 hr, and expression continued to increase as cells re-entered G1 at 8-10 hrs, followed by a modest decrease as cells re-entered S phase at 12 hrs, confirming a shortened cell cycle as observed with **Fig. 5**. Treatment with HGF + AMG337 only modestly decreased Cyclin E1 levels over time.

Cyclin A2 levels were observed immediately following release from the double thymidine block, and levels increased modestly at 10-12 hrs. Following HGF treatment (**Fig. 7D/G**), Cyclin A2 expression increased with the highest levels at 6-10 hrs, while Cyclin A2 levels remained constant with HGF + AMG337 treatment (**Fig. 7H**).

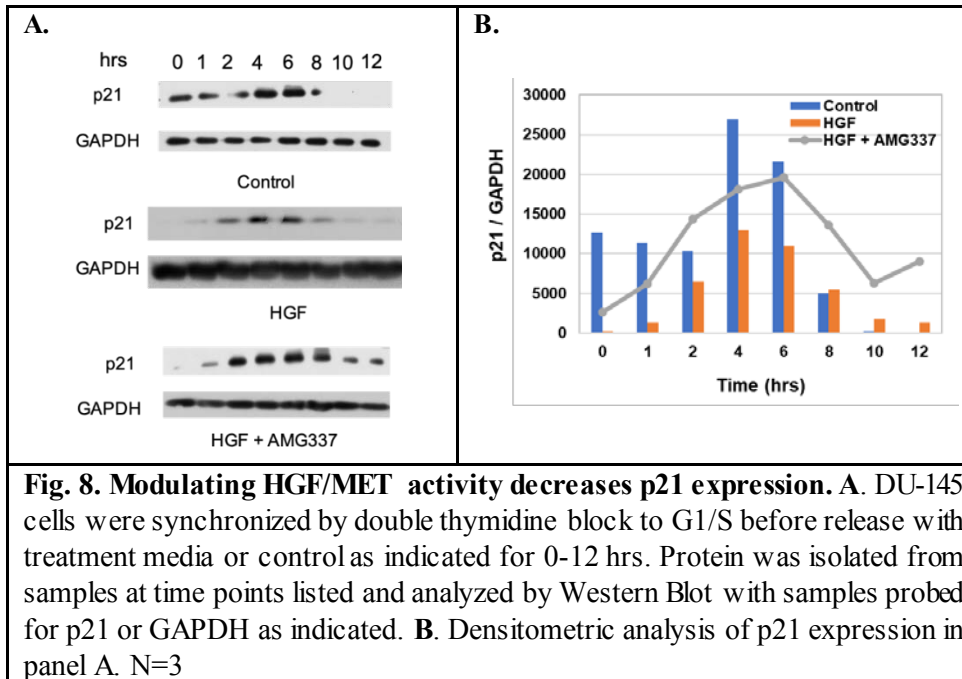
In cells treated with vehicle, Cyclin B1 levels increased in G2/M and decreased as cells began to enter G1 (6-12 hrs). In contrast, HGF treatment upregulated Cyclin B1 when the cells were released from the double thymidine block (0 hrs), and levels remained relatively constant until they dropped at 8 hrs, spiked at 10 hrs, and then dropped back down to basal levels at 12 hrs. Treatment with HGF + AMG337 resulted in a similar pattern of Cyclin B1 levels, with the exception that levels did not spike at 10 hrs, and expression was absent at 12 hrs. Of note, the loss of Cyclin B1 expression was observed at 8 hrs in both HGF and HGF + AMG337 treatment groups. The cause of this loss of Cyclin B1 is currently unclear.

The treatment composite graphs in **Fig. 7F-H**, demonstrate changes in the family of cyclin protein expression as a result of treatment. The overall levels of cyclin protein expression in control

cells were equal across 12-hour treatment period (**Fig. 7F**); however, in both HGF alone and HGF + AMG337, levels of Cyclin E1 are increased as compared to the control. In summary, HGF/MET signaling modulates pSTMN1<sup>S16</sup> and the expression of Cyclins D1, E1, A2, and B, resulting in the shortening of the cell cycle and increased cell proliferation.

#### **2.4.e. HGF/MET mediates a decrease in p21 levels in G2/M**

A key regulator of cell cycle progression is p21. Cyclin/CDK binding is required for the progression through each phase of the cell cycle, and p21 inhibits this process by disrupting cyclin/CDK binding [25]. This commonly occurs when an error in DNA replication causes an activation of p21 that halts the cell cycle, allowing the replication error to be repaired before inhibition is removed and the cell progresses to the next phase of the cell cycle [25]. HGF+AMG337 dual treatment increased levels of p21 expression compared to control cells and cells treated with HGF alone. This rise in p21 in HGF+AMG337 treated cells could contribute to the lengthening of the cell cycle when HGF/MET signaling is inhibited by delaying progression from one phase of the cell cycle to the next.

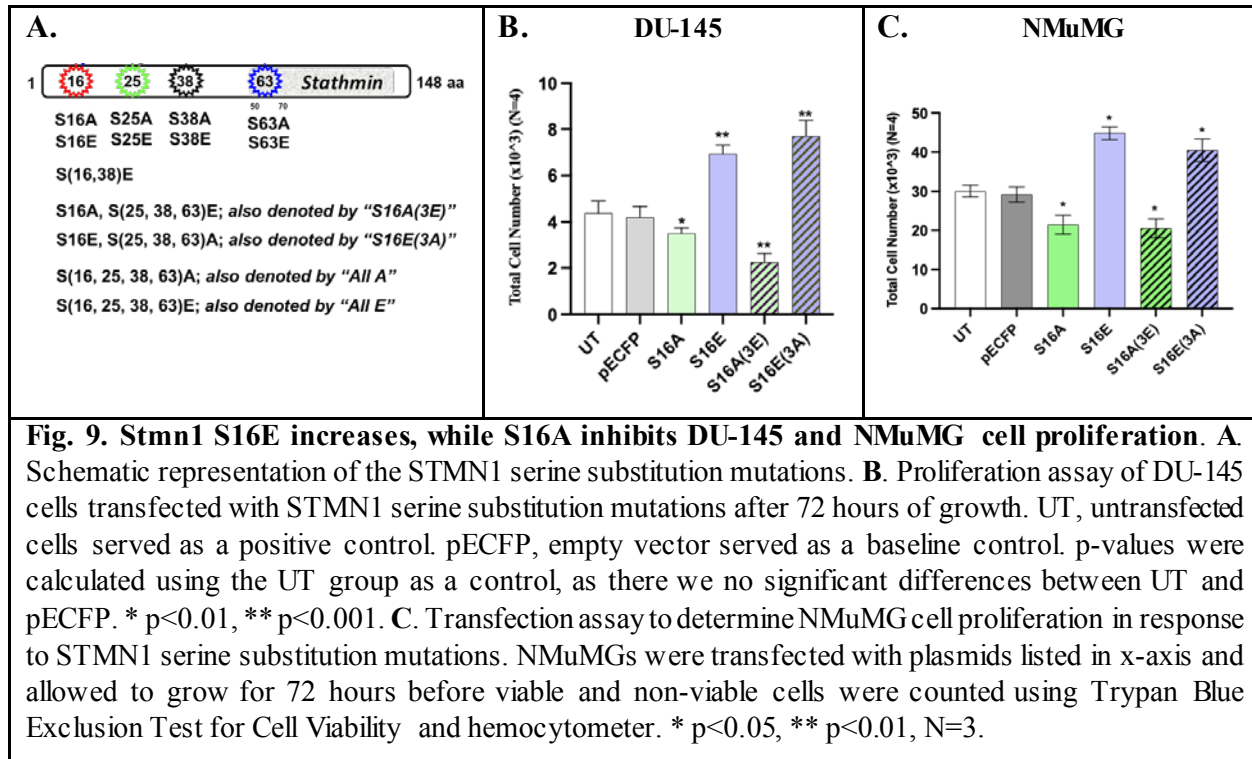


In summary, these data demonstrate the effect of HGF/MET signaling induction and inhibition, where HGF induces a shortening of the cell cycle, thereby shortening the cell doubling time and increasing overall cell proliferation; while inhibition of HGF/MET signaling lengthens the cell cycle, thereby lengthening the cell doubling time and inhibiting overall cell proliferation.

#### 2.4.f. STMN1 S16 phosphorylation selectively regulates cell cycle progression

To study the direct effect of STMN1 differential phosphorylation, transient transfections were used to induce mutant STMN1 protein containing substitution mutations at each of the four regulatory serine residues, either alone or in combination. Schematic of mutant plasmids generated (**Fig. 9A**). Glutamic Acid (E) was substituted in place of Serine (S) to mimic constitutive phosphorylation, while Alanine (A) was substituted in place of S to mimic dephosphorylation. Proliferation rates of DU-145 cells transfected with plasmids expressing mutant STMN1 S16A or STMN1 S16E (**Fig. 9B**). STMN1 S16A inhibited proliferation and inhibition to cellular proliferation was greater with STMN1 S16A(25,38,63)E, suggesting that S16 dephosphorylation was sufficient to inhibit

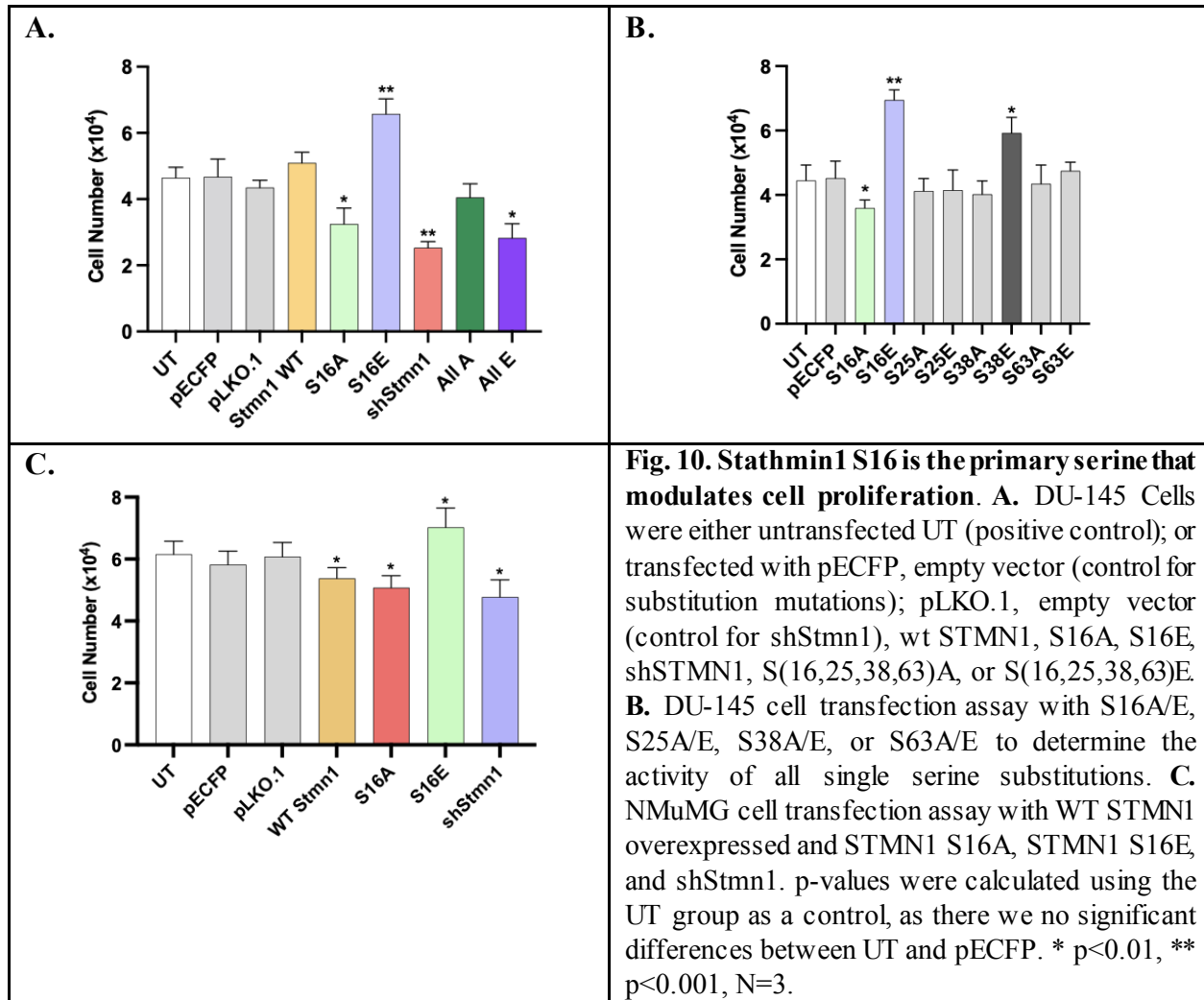
proliferation. In contrast, both STMN1 S16E alone and STMN1 S16E(25,38,63)A promoted cell proliferation, suggesting that S16 phosphorylation was sufficient to drive proliferation.



Stathmin's effect on cell proliferation is not restricted to prostatic cells or cancerous cells. Therefore, the transfection assays involving S16A/E and S16A(3E)/S16E(3A) were repeated in another epithelial cell line, Normal Murine Mammary Gland (NMuMG, **Fig 9C**) where results from **Fig. 9B.** were repeated, implying that pSTMN1<sup>S16</sup> status was critical for regulating STMN1 function during epithelial cell division.

Cells were transfected with wild type (WT) STMN1 to determine whether regulation of DU-145 proliferation via S16A/E transfected cells was a consequence of pSTMN1<sup>S16</sup> or merely a response to increased levels of STMN1 from transfected plasmids (**Fig 10**). Compared to STMN1

S16A or STMN1 S16E-regulated proliferation, overexpression of the WT STMN1 protein did not change proliferation (**Fig. 10A**). Our previous work reported that transfection with shSTMN1 knocked down STMN1 protein expression and decreased the rate of cell proliferation [11]. STMN1 S(16,25,38,63)E represents a total functional knockdown, as all serines are phosphorylated and therefore unable to bind tubulin, while STMN1 S(16, 25, 38, 63)A represents fully dephosphorylated STMN1 that will bind tubulin. Transfection with STMN1 S(16,25,38,63)E significantly inhibited cell proliferation, similarly to shSTMN1 transfected cells (**Fig 10A**). Indeed, there were no statistically significant differences between the inhibitory effects of STMN1 S16A, shSTMN1, and STMN1 S(16,25,38,63)E, supporting our findings that S16 phosphorylation status was essential for regulating cell proliferation.



Next, all single serine substitutions were tested to determine whether S25, S38, and/or S63 modulated proliferation (**Fig. 10B**). The only other single serine that increased proliferation was STMN1 S38E, albeit not as strongly as STMN1 S16E. This observation was not entirely surprising, as the kinase cell cycle protein cdc2 (CDK1) is known to phosphorylate STMN1 S38 [26]. Finally, WT STMN1 and shSTMN1 were transfected into the NMuMG cells, which showed a significant ( $p < 0.05$ ) inhibition in growth with the WT overexpression, and the knockdown of endogenous STMN1 via shSTMN1 (**Fig. 10C**). We therefore determined whether S38 in combination with S16 also regulated cell doubling time.

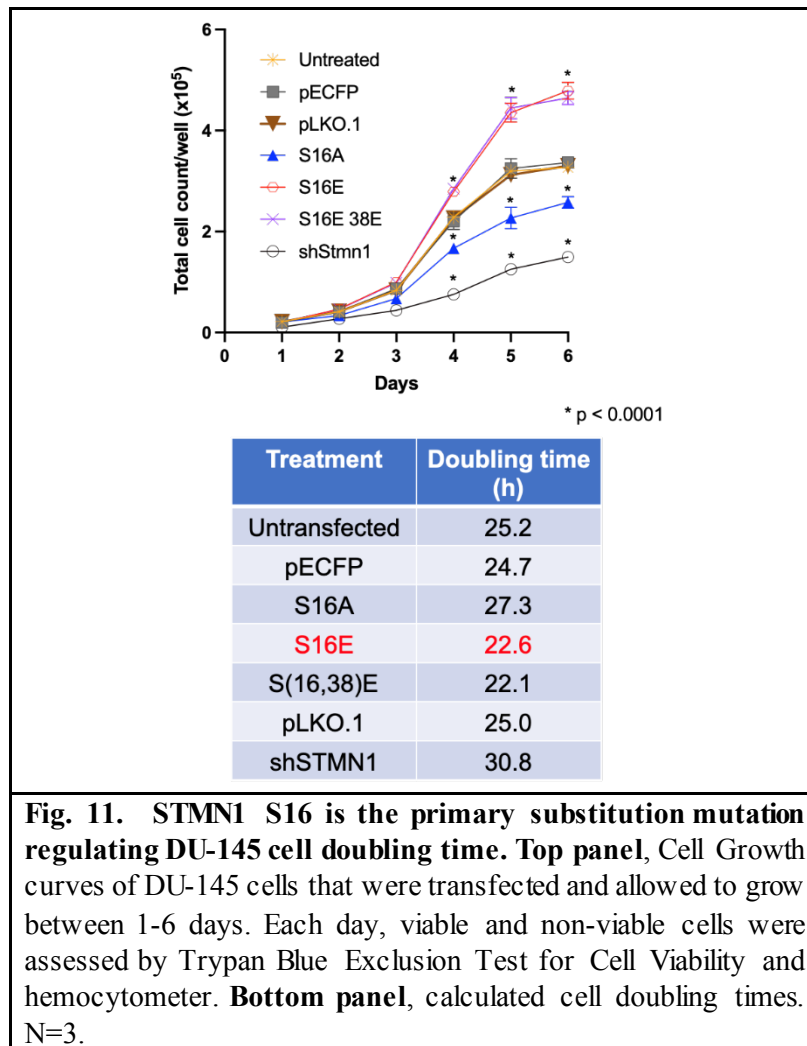
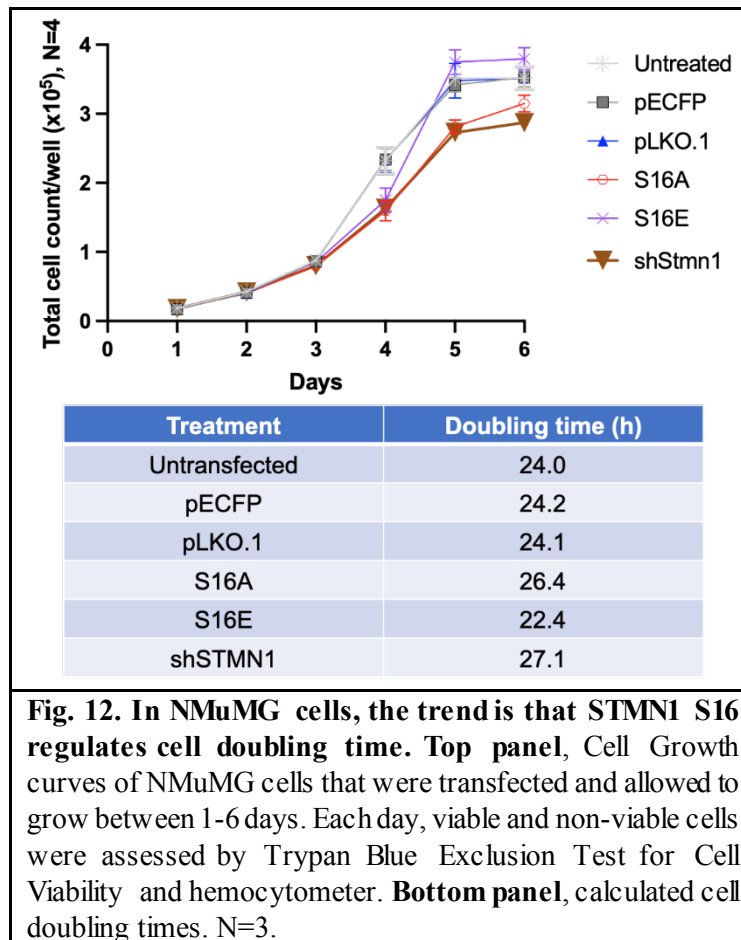


**Fig. 11. STMN1 S16 is the primary substitution mutation regulating DU-145 cell doubling time. Top panel,** Cell Growth curves of DU-145 cells that were transfected and allowed to grow between 1-6 days. Each day, viable and non-viable cells were assessed by Trypan Blue Exclusion Test for Cell Viability and hemocytometer. **Bottom panel,** calculated cell doubling times. N=3.

Cells transfected with the pECFP control or the pLKO.1 control did not significantly alter the rate of cell doubling time compared to untransfected cells (**Fig 11**). STMN1 S16A lengthened cell doubling time by 2.6 hrs compared to the pECFP control, and expression of shSTMN1 lengthened cell doubling time by 5.8 hrs compared to the pLKO.1 control, supporting the observations that shSTMN1 was more effective in inhibiting cell proliferation compared to STMN1 S16A. In comparison, STMN1 S16E shortened cell doubling time by 2.6 hrs, while STMN1 S(16,38)E shortened cell doubling time by 3.1 hrs. The modest difference of 0.5 hrs was

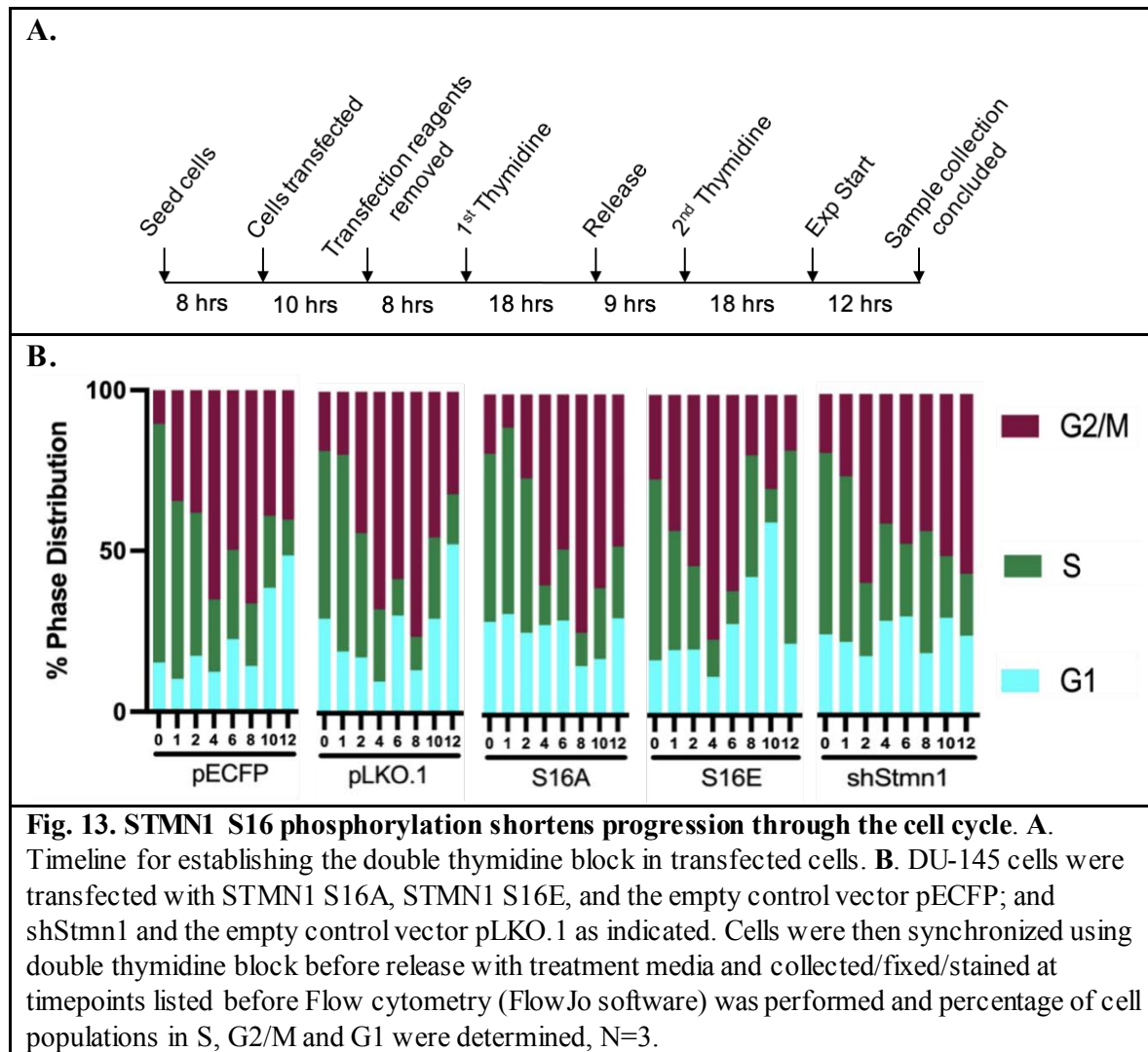
not statistically significant, indicating that STMN1 S16 remained the primary serine involved in regulating cell proliferation.

To validate the effect of mutant STMN1 protein effects on cell doubling time, the assays were repeated in the NMuMG cells (**Fig 12**), which displayed similar trends as DU-145 cells (**Fig 11**). Cells transfected with STMN1 S16E resulted in a 2 hr shortening in cell doubling time as compared to cells transfected with STMN1 S16A. Similar to the results in the DU-145 transfected cells, STMN1 S16A and shSTMN1 transfected NMuMG cells showed comparable doubling times. This suggests that pSTMN1<sup>S16</sup> results in a shortening of cell doubling time, which leads to an overall increase in cell proliferation.



#### **2.4.g. Phosphorylation of STMN1 S16 shortens the time of progression through the cell cycle.**

Flow cytometry was performed to determine whether STMN1 S16 phosphorylation-controlled time in mitosis. DU-145 cells were transfected with either control plasmids or plasmids expressing mutant STMN1 protein before being synchronized at G1/S using double thymidine block. They were then released, to be collected over 12 hrs and then analyzed via Flow Cytometry to determine the percent distribution of cells in S, G2/M and G1 phases (**Fig. 13**). After release from the double thymidine block, cells transfected with the empty vectors pECFP or pLKO.1 entered G2/M at 1-2 hrs to peak between 4-8 hrs, followed by entry into G1 at 10-12 hrs. However, cells expressing STMN1 S16A showed a delayed entry into G2/M by 4 hrs and nearly 50% of cells remained in G2/M at 12 hrs. In addition, the percent distribution of cells in G1 did not change significantly throughout the 12 hrs. In contrast, cells expressing STMN1 S16E entered G2/M at 1 hr, peaked at 4 hrs and exited at 8 hrs. Furthermore, the percentage distribution of cells in G1 began to increase at 6 hrs, peak at 10 hrs and exit at 12 hrs, at which time most cells were already in S phase, similar to that observed at the time of release from the double thymidine block, demonstrating that the cells had completed one cell cycle within 12 hrs. Finally, shSTMN1-mediated knockdown of endogenous STMN1 disrupted the cell cycle, as shown by the percentage of cells in G2/M and G1 that did not change significantly during the 2 to 12 hr time period. This delay in cell cycle progression is supported by the observation that STMN1 knockdown lengthened cell doubling time by 5.8 hrs.



After establishing the impact of transfected protein on the progression of the DU-145 cells through the cell cycle, cells were synchronized, and protein was isolated at the same time points to evaluate the effect of the transfected protein on cell cycle protein expression and overall STMN1 levels.

#### 2.4.h. STMN1 S16 phosphorylation regulates the expression of factors during cell cycle progression

While the phospho-S16 STMN1 antibody recognized pSTMN1<sup>S16</sup> (Figs. 5A/C, 6D), its lack of binding to transfected STMN1 cells confirms its specificity towards pSTMN1<sup>S16</sup> and not merely

the presence of a negative charge in the 16<sup>th</sup> amino acid of STMN1 (**Fig. 14A**). In cells expressing STMN1 S16A (**Fig. 14A**), the pattern of total STMN1 expression was similar to that observed in control cells (**Fig. 6**) at the early time points, with one difference in that STMN1 levels did not increase at 10-12 hrs as seen in the controls (**Fig. 14A/C**). However, when cells expressed STMN1 S16E, total STMN1 levels decreased significantly at 4 hrs and continued to decrease to nearly undetectable levels by 12 hrs, implying that STMN1 S16 phosphorylation was critical in regulating total STMN1 levels (**Fig. 14A/D**).

In contrast, STMN1 S16E expression upregulated cyclins overall compared to STMN1 S16A transfected cells. Notably, Cyclin E1 expression was increased by 2.2-fold increase at 1 hr in STMN1 S16E transfected cells as compared to cells expressing STMN1 S16A (**Fig. 14E**); however, a similar level of Cyclin E1 expression was observed from 2 hrs onward for both STMN1 S16E (**Fig 14F**) and S16E expression (**Fig. 14 B**). In comparison, Cyclin A2 levels in cells expressing STMN1 S16A were nearly 3.9-fold greater at 0 hr and 2.2-fold at 1 hr as compared to cells expressing STMN1 S16E, but again, Cyclin A2 expression remained similar between both groups from 2 hrs onward. Most significantly, levels of Cyclin B1 in cells transfected with STMN1 S16E were expressed at a greater level than cells transfected with S16A between 2-6 hrs, which could represent an earlier entrance of STMN1 S16E transfected cells into M-phase compared to cells transfected with STMN1 S16A.

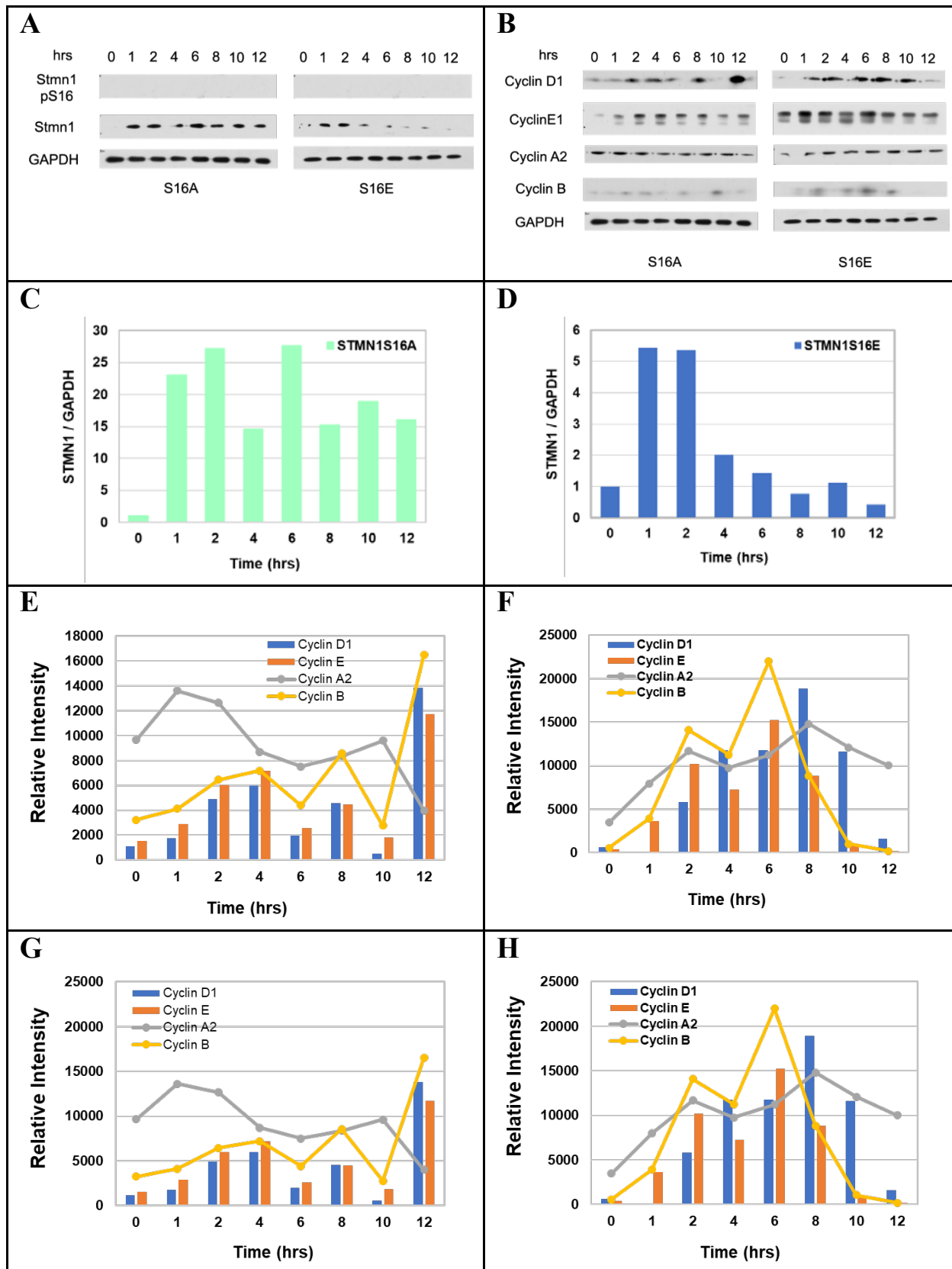
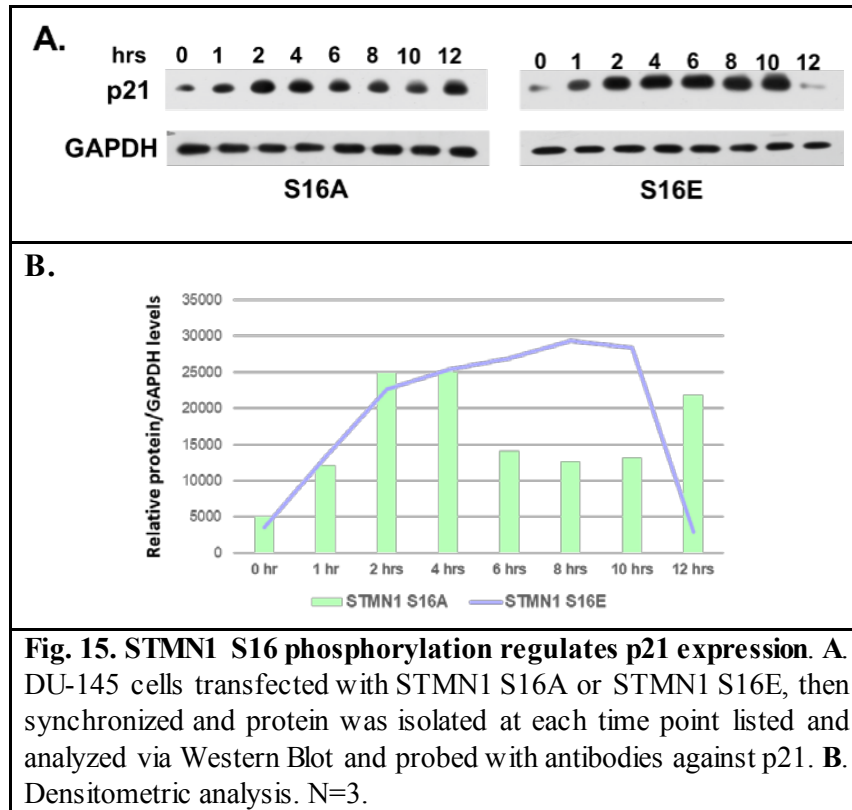


**Fig. 14. STMN1 phosphorylation regulates total STMN1 and Cyclin expression.** **A.** Cells were transfected, synchronized to G1/S, and collected over 12 hrs and analyzed by Western Blot before being probed with antibodies towards STMN1 pS16 and total STMN1. **B.** Identical protein samples as were harvested in **A** while probing for Cyclins D, E, A, and B. **C and C/D.** Densitometry of STMN1/GAPDH for S16A (**C**), and S16E (**D**). **E/F.** Densitometry of cyclin proteins compared to GAPDH for S16A (**E**), and S16E (**F**). **G/H.** Densitometry of cyclin proteins compared to control (from **Fig. 7.**) for S16A (**G**) and S16E (**H**). N=3.

In summary, these observations demonstrate for the first time that S16 phosphorylation modulates total STMN1 expression levels through a yet unknown mechanism. Since the time from transfection to the end of the double thymidine block was 63 hrs, any effects due to expression of the substitution mutations would have already been established prior to the release of the thymidine block. Alternative mechanisms could include a decrease in STMN1 protein stability as cells progress through the cell cycle and/or a down-regulation of STMN1 transcription upon release from the double thymidine block. In addition, Cyclin E1 regulates the transition from G1 to S phase while Cyclin A2 regulates S to G2 phase and Cyclin B1 regulates G2 to M phase. Whether this function accounts for the differential levels of Cyclin E1 and Cyclin A2 at G1/S (synchronized by the thymidine block) or Cyclin B1 at G2/M remains to be determined.

To determine whether STMN1 S16A or STMN1 S16E regulated p21 expression during the cell cycle, protein samples were probed for levels of p21 from the previously described data (**Fig. 14**).

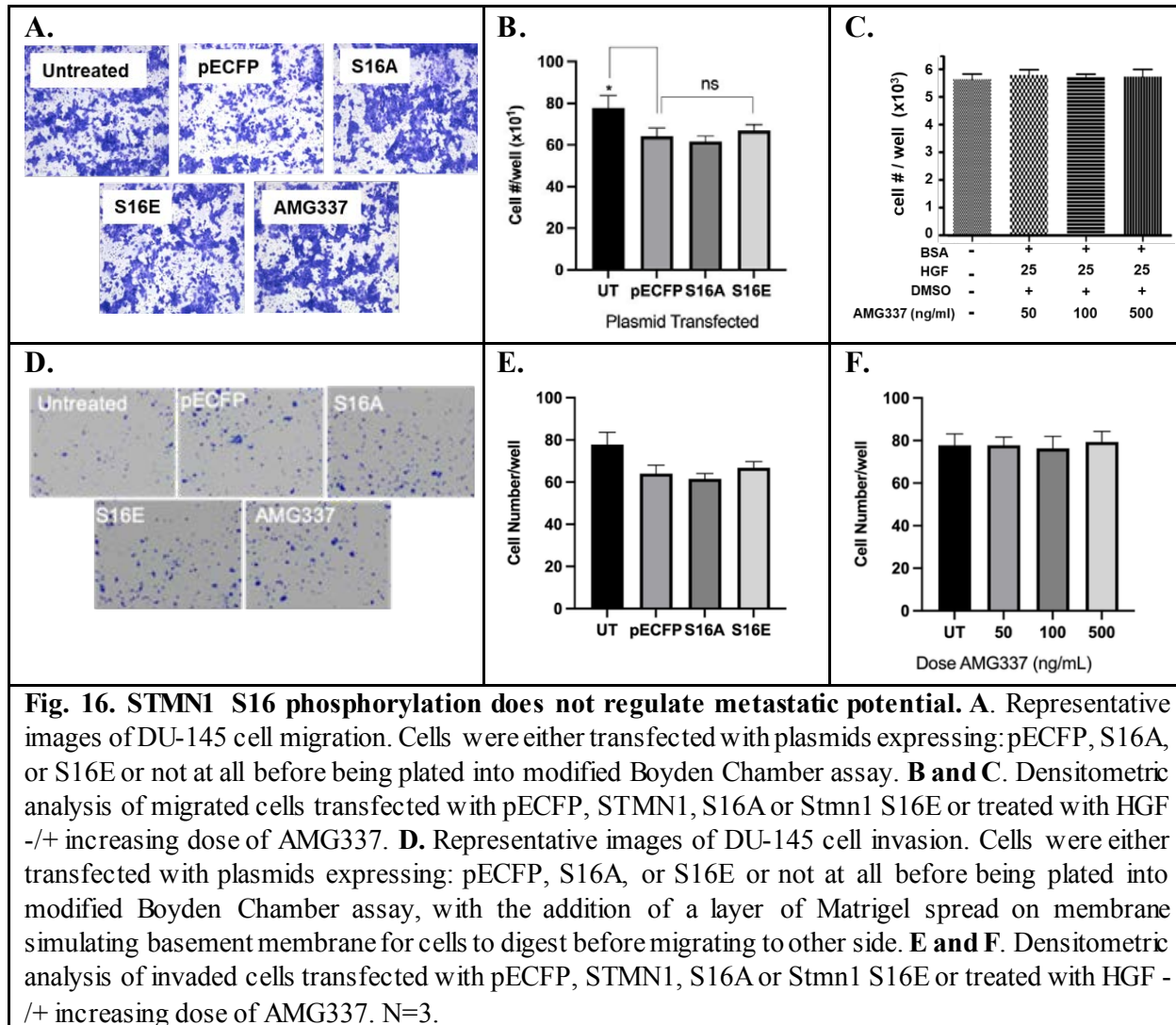


In STMN1 S16A expressing cells, p21 levels were highest from 2 to 4 hrs, and again at 12 hrs, correlating with the delayed exit from G2/M when nearly 50% cells remained in G2/M at 12 hrs. However, in STMN1 S16E expressing cells, the defined rise and decrease of p21 expression back to basal levels at 12 hrs supports our finding that cells expressing STMN1 S16E had completed the rest of the cell cycle (from being synchronized at G1/S) within 12 hrs. Taken together, these observations support that S16 phosphorylation is a key regulator of DU-145 cell cycle progression and cell proliferation.

#### 2.4.i. STMN1 S16 phosphorylation does not regulate metastatic potential

Cell migration assays and cell invasion assays through Matrigel are used to determine whether cancer cells exhibit motility or metastatic potential, respectively. To determine whether STMN1 S16 phosphorylation regulated these functions, DU-145 cells were treated with HGF + AMG337

or transfected with pECFP, STMN1 S16A, or STMN1 S16E, and migration and invasion assays performed as outline in 2.3.e. As seen in **Fig 16B**, neither STMN1 S16A nor STMN1 S16E increased cell migration compared to the pECFP vector control.



As observed previously, the vector control expressing ECFP (used as a marker for transfection efficiency) inhibited cell migration as compared to the untransfected cell control; however, no significant difference was observed in cells transfected with STMN1 S16A or

STMN1 S16E compared to pECFP, indicating that the pECFP-induced inhibition was due to the control plasmid itself. In addition, DU-145 cells treated with increasing concentrations of the MET inhibitor AMG337 did not induce cell migration (**Fig. 16C**). Similarly, there is no significant difference in invasion with STMN1 S16A nor STMN1 S16E-transfected cells without/with inhibition of HGF/MET signaling (**Fig 17**).

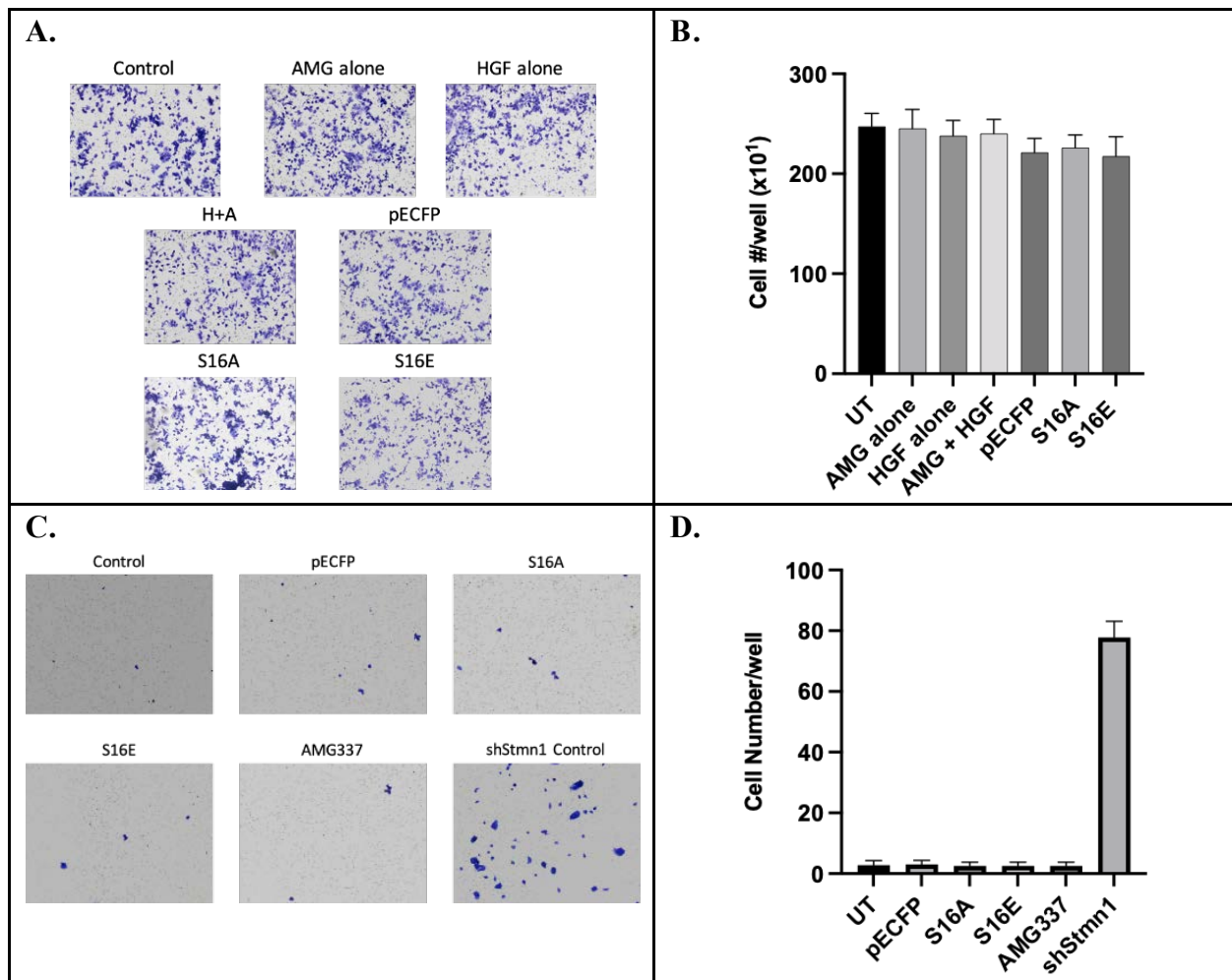


**Fig. 17. STMN1 S16 phosphorylation does not regulate metastatic potential in NMuMG cells. A.** Representative images of NMuMG cell migration. **B and C.** Densitometric analysis of migrated cells transfected with pECFP, STMN1, S16A or Stmn1 S16E or treated with HGF +/- increasing dose of AMG337. **D.** Representative images of NMuMG cell invasion. **E and F.** Densitometric analysis of invaded cells transfected with pECFP, STMN1, S16A or Stmn1 S16E or treated with HGF +/- increasing dose of AMG337. N=3.

To assess the ability of pSTMN1<sup>S16</sup> to affect metastatic processes in normal cells, NMuMG cells were treated or transfected as described above for the DU-145 cells. Similar to the results from **DU-145 cells**, the NMuMGs were not impacted by treatment or phosphorylation/dephosphorylation mimetics of STMN1 in the migration and invasion assays (**Fig 17**). The invasion assays with the NMuMGs yielded such a low number of invaded cells, that a control condition was added (DU-145 transfected with shSTMN1) which had been shown previously to induce invasion [11].

In conclusion, these data support the overarching hypothesis that STMN1 S16 phosphorylation selectively regulates cell proliferation, but not metastatic potential, and that inhibition of STMN1 S16 phosphorylation induces apoptosis and cancer cell death. Furthermore, we determined that the stromal factor HGF activates the MET receptor expressed on PCa cells to phosphorylate STMN1 S16, resulting in the modulation of cyclins and p21, a shortening of the cell cycle which led to increased cell proliferation. Treatment with a selective MET inhibitor, AMG337, inhibited these processes and induced cell death. Taken together, these observations indicate that a MET inhibitor may be used in combination with ADT to decrease overall tumor growth without stimulating metastatic spread.

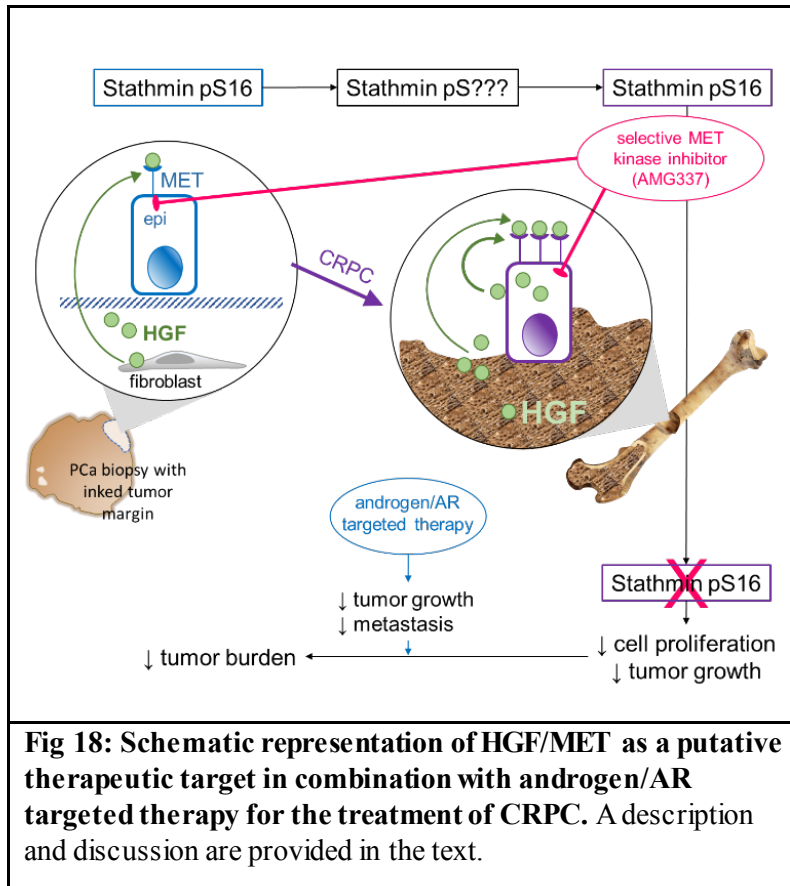
## 2.5. DISCUSSION

The role of HGF/MET-mediated phosphorylation of STMN1 on cancer progression (especially in PCa) remains poorly understood. Our study provides, for the first time, evidence that HGF/MET-mediated phosphorylation of STMN1 S16 promotes cell cycle progression and cell proliferation without inducing metastasis in PCa. Further, treatment with a c-MET inhibitor, AMG337, delayed cell cycle progression which lengthened cell doubling time, inhibited cell proliferation, and induced prostate cancer cell death.

Current literature demonstrates HGF/MET-mediated phosphorylation of STMN1 and the varied effects that can have on cellular processes. Tian et. Al. shows HGF/MET-mediated phosphorylation of STMN1 (likely at S16) through activation of Rac1 (a kinase known to regulate transcription factor activation, proliferation, transformation, apoptosis, etc. [27]), resulting in an increase in the pool of free tubulin, which encourages stable MTs and maintenance of intact barriers in endothelial cells [28]. Additionally, in primary human keratinocytes, HGF phosphorylation of STMN1 S38 led to a 2-fold increase in cell proliferation [29]. While not directly linked to phosphorylation, increases in STMN1 expression in hepatocellular carcinoma increased MET expression in HCCs and HGF production in hepatic stellate cells HSCs grown in co-culture [4,30]. HGF/MET-mediated phosphorylation of STMN1 S16 led to earlier expression of Cyclin D1, Cyclin E1, and Cyclin B1 compared to control cells and those treated with HGF+AMG337. This earlier increase in cyclin expression correlates with the shortening in time of progression through the cell cycle, as DU-145 cells progressed through G2-M-G1 phases. This resulted in an overall significant increase in cell proliferation of the DU-145 cells.

HGF plays a significant role in prostatic TME. The expression of HGF by cancer associated fibroblasts (CAFs) was correlated with an increase in MET expression and overall progression of PCa [5,30]. The Cunha Laboratory demonstrated *in vivo* that factors secreted by CAFs (including HGF) transformed normal prostatic epithelial cells into cancerous cells in mouse xenografts, even in the absence of CAFs in the xenograft [31]. While Cunha's study demonstrated the impact of HGF/MET-mediated phosphorylation of STMN1 S16 on cell proliferation and cell cycle progression, our data demonstrate that phosphorylation of STMN1 S16 does not play a role in regulating metastatic processes. These data separate the function of differential phosphorylation of STMN1, indicating that S16 phosphorylation by HGF does not contribute towards PCa progression and development of EMT, and may be a viable candidate for therapeutic targeting.

Inhibitors targeting MET are currently being investigated to treat a variety of solid tumors [9,14,15,32-35]. As described above, treatment of PCa patients with chemotherapy resulted in increased levels of HGF expression, which could be due to the development of CRPC post ADT and/or treatment with bicalutamide or flutamide. The increase of HGF in response to chemotherapy could lead to MET activation and downstream STMN1 phosphorylation which would further tumor growth and metastatic spread.



Due to increased levels of MET and HGF expression in the bone that contributes to the development of CRPC, interest in developing a therapeutic strategy to target HGF/MET signaling in PCa is particularly high [20]. AMG337 is a potent c-MET inhibitor that restricts activation and downstream signaling of the HGF/MET signaling pathway [18]. It is currently being used to treat gastric and esophageal cancer in adult patients with MET amplified tumors [36], and is being considered for applications with other solid tumors that exhibit increased levels of MET [37]. We show here that not only does AMG337 inhibit HGF-increased growth of PCa cells, but also induces cell death. When treating cells with HGF+AMG337, phosphorylation of MET and the downstream signaling protein, STMN1, is inhibited. STMN1 inhibition led to an overall lengthening of cell doubling time, and delayed progression through the cell cycle and overall inhibition of cell

proliferation. The diagram above demonstrates a therapeutic strategy that utilizes ADT and AMG337 to target both early and late stage PCa cells. It is important to note that the DU-145 cells do not express AR, therefore the impact of AMG337 on these cells would mimic effects seen on CRPC. Taken together, these data indicate a therapeutic role for AMG337 to be utilized with traditional ADT to eliminate both AR(+) and AR(-) PCa cells in both local and metastatic disease.

### **Supplementary Table S1. Primary antibody list**

<b>Antibody</b>	<b>Company</b>	<b>Product Code</b>	<b>IgG Species</b>	<b>Conjugate</b>	<b>Dilution</b>
<b>Cyclin A2</b>	Cell Signaling	4656	Rabbit	None	1:1000
<b>Cyclin B1</b>	Cell Signaling	4135	Rabbit	None	1:1000
<b>Cyclin D1</b>	Santa Cruz	8396	Mouse	None	1:1000
<b>Cyclin E1</b>	Cell Signaling	4129	Rabbit	None	1:1000
<b>GAPDH</b>	Peprtech	60004-1	Mouse	None	1:2000
<b>HGF</b>	Cell Signaling	52445	Rabbit	None	1:1000
<b>Met</b>	Cell Signaling	8198	Rabbit	None	1:1000
<b>pMET</b>	Cell Signaling	3077	Rabbit	None	1:750
<b>p21</b>	Cell Signaling	2947	Rabbit	None	1:1000
<b>p27</b>	Cell Signaling	3686	Rabbit	None	1:1000
<b>STMN1</b>	Santa Cruz	55531	Mouse	None	1:1000
<b>STMN1 pS16</b>	Thermo Fisher	PA5-17091	Rabbit	None	1:250

# Chapter 3

The Role of CAMKII in Regulating STMN1

S16 Phosphorylation, Proliferation, and

Metastatic Potential

### **3.1. ABSTRACT**

Stathmin (STMN1) is a phosphoprotein whose function is dictated by the phosphorylation status of its four regulatory serine sites, S16, S25, S38 and S63. Calmodulin Kinase II (CAMKII) has been shown to regulate cell proliferation and to phosphorylate STMN1 on S16. Furthermore, knockdown of total STMN1 decreased cell proliferation, but induced epithelial to mesenchymal transition (EMT). To determine the specific function(s) of differential phosphorylation of STMN1, experiments were designed to stimulate or inhibit the four regulatory serines of the STMN1 molecule. Being that the focus of this project centered on the role STMN1 plays in regulating cell cycle progression and cell proliferation, each of the four regulatory serines were stimulated or inhibited via small molecules to assess the impact they have on cell proliferation. In summary, inhibition of CAMKII, CDK1, and PKA demonstrated significant inhibition of DU-145 cell proliferation, while only stimulation of CAMKII significantly increased proliferation.

## 3.2. INTRODUCTION

STMN1 is increased in many cancers including prostate cancer, and several studies have investigated the role of STMN1 in PCa progression [1-3]; however, the role of STMN1 S16 phosphorylation in regulating PCa proliferation and growth has yet to be investigated. Therefore, we reviewed the role of STMN1 S16 phosphorylation in other cancers and cell types to gain knowledge that would assist in predicting the role of STMN1 S16 phosphorylation in PCa cells.

### 3.2.a. CAMKII-mediated phosphorylation of STMN1 S16 in breast cancer

CAMKII expression is increased in cancer, including breast, colon and gastric cancers, and glioblastoma [4,5]. For example, CAMKII activity increases the rate of breast cancer cell proliferation and tumor growth while inhibiting apoptosis [4-6]. Phosphorylation of CAMKII on Thr286 was detected in primary breast cancer tissue sections and metastatic breast cancer lesions in lymph nodes, indicating that the autophosphorylation of CAMKII is indicative of breast cancer progression [5-7]. STMN1 has also been shown to be expressed highly in breast cancer cells and is prognostic of poor outcome and overall survival [5,6]. In cell culture, CAMKII phosphorylated STMN1 S16 in breast cancer cells [7,8]. While overexpression of STMN1 did not alter cell viability, treatment with the microtubule-depolymerizing agent eribulin markedly decreased cell viability when STMN1 was overexpressed, suggesting that high STMN1 levels were required for the antitumor activity of eribulin [9]. Furthermore, STMN1 S16 was phosphorylated by eribulin and dephosphorylated by the CaMKII inhibitor KN62, implying that CaMKII phosphorylated STMN1 S16 [9]. In summary, these studies imply that the CAMKII-mediated phosphorylation of STMN1 S16 is essential in promoting breast cancer cell proliferation and cancer progression to metastasis [9-12].

### **3.2.b. CAMKII phosphorylation of STMN1 S16 in dendrites**

In addition to cell cycle progression and cell proliferation, STMN1 phosphorylation is correlated with dendritic arborization in neurons. Arborization or branching of neuronal dendrites is largely dictated by microtubule formation and is critical to the development of neuronal pathways [13,14]. Interestingly, CAMKII-mediated phosphorylation of STMN1 S16 plays a stimulatory role in the arborization of dendrites [13,14]. The phosphorylation of STMN1 S16 by CAMKII results in the downregulation of STMN1 binding to tubulin dimers and has been seen in the early phases of neuronal development, which aids in establishing neuronal branching and arborization [13]. The downregulation of total STMN1 expression in early neuronal development results in a similar outcome to phosphorylation of STMN1 by CAMKII in established neurons undergoing later stage branching and arborization [13]. CAMKII is activated by an increase in intracellular  $Ca^{2+}$  facilitated by voltage gated calcium channels and the metabotropic glutamate receptor 1 [13]. In addition to STMN1, SCLIP (also known as STMN3) has been shown to regulate Purkinje cell arborization and development [14]. The inhibition of SCLIP restricts formation of early stages of postnatal neuronal cell development and the elongation and branching of Purkinje cells at later stages of development. While SCLIP is a STMN1-like protein, its function and necessity in the establishment and arborization of Purkinje dendritic cells mimics the effects seen with STMN1 regulation in Purkinje cells [14].

### **3.2.c. CAMKII phosphorylation of STMN1 S16 in hepatoma cells (HepG2)**

In certain cell types, STMN1 expression is differentially regulated to limit the risk of carcinogenesis [15]. In normal liver cells, STMN1 is differentially phosphorylated to maintain normal cell cycle progression and cell proliferation [16]; however, in HepG2 cells derived from a well-differentiated hepatocellular carcinoma [17], overexpression of STMN1 is correlated with

increased tumor growth and overall cancer progression [15,16]. Tseng et al. reported that STMN1 negatively regulated the levels of thyroid hormone receptor (THR) and that THR bound to the promoter region of the STMN1 gene to inhibit STMN1 transcription [16]. Moreover, increased levels of the thyroid hormone T<sub>3</sub> inhibited STMN1 and suppressed HepG2 cell proliferation and xenograft tumor growth in mice [16]. Li and others have shown that in the HepG2, HeLa, and MCF7 cells, Piwi Like RNA-Mediated Gene Silencing 1 (PIWIL1) binds STMN1 at S16 to inhibit CAMKII phosphorylation [18]. In HepG2 cells, the binding activity of PIWIL1 serves two distinct functions: first to inhibit CAMKII phosphorylation which leads to an increase in microtubule destabilization, and secondly to increase the cellular levels of STMN1 protein via inhibition of STMN1 degradation by the Ring Finger Protein, LIM (RLIM) E-3 ligase [19]. These studies demonstrate that STMN1 is regulated at a transcriptional and post-translational level to balance its function in regulating cell cycle progression against its potential to promote metastasis. Herein, we report that in PCa cells, CAMKII regulates proliferation, but not metastatic potential through a STMN1 S16 independent mechanism.

## **3.3 MATERIALS AND METHODS**

### **3.3.a. Materials**

Oleic Acid (Cat. No. S4707) was purchased from SelleckChem. KN93 (Cat. No. 1278), KN92 (Cat. No. 4130), Okadaic Acid (Cat. No. 1136), Anisomycin (Cat. No. 1290), SB203580 hydrochloride (Cat. No. 1402), Roscovitine (Cat. No. 1332), 8-bromo-cAMP (Cat. No. 1140) and H89 Dihydrochloride (Cat. No. 2910) were purchased from Tocris. Each of the small molecules was prepared according to manufacturer recommendations to the highest stock concentration possible in the least toxic vehicle to minimize the effect of vehicle control on the assay.

### **3.3.b. Methods**

#### **3.3.b.i. Proliferation Assays**

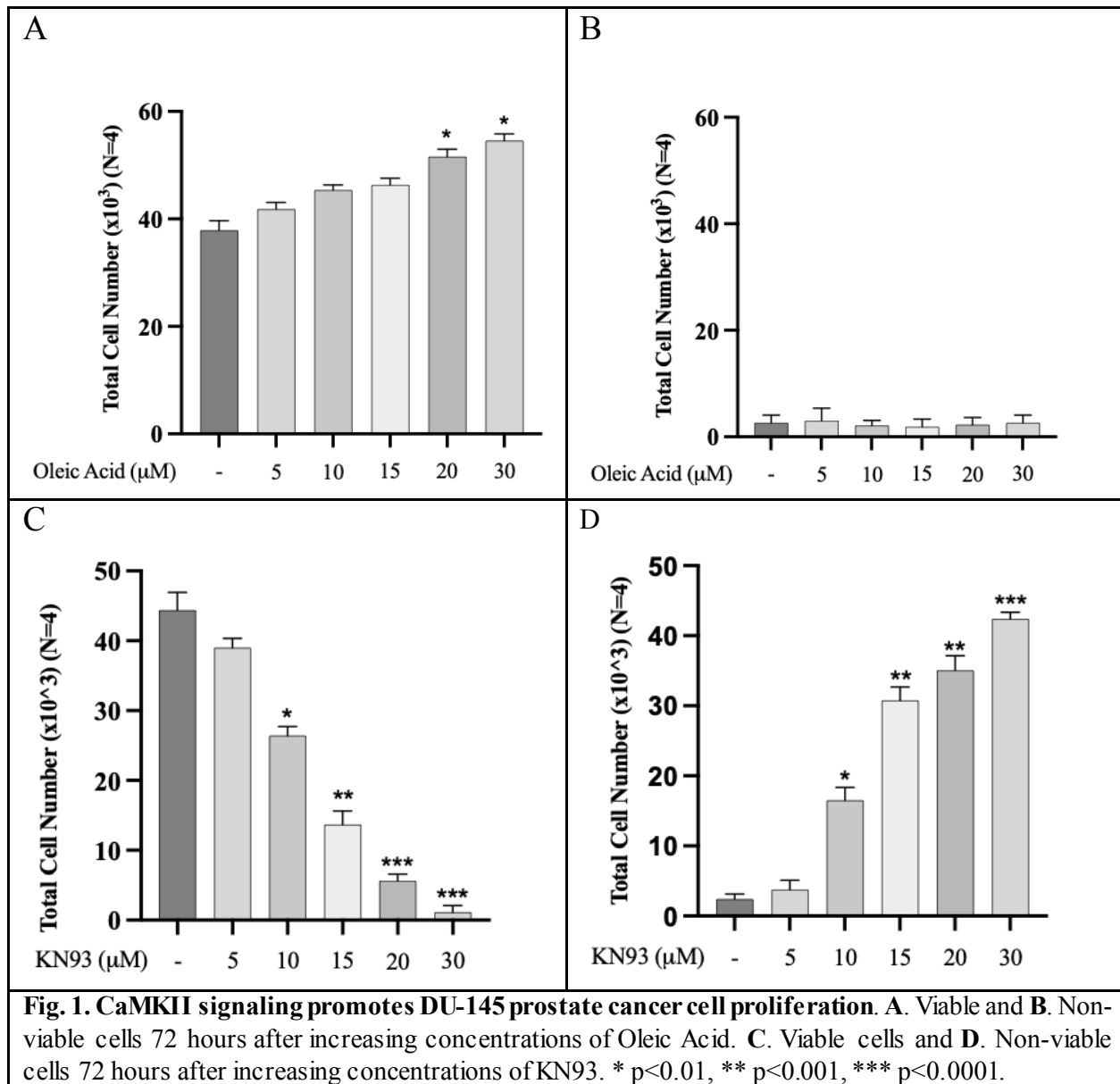
Proliferation assays were conducted as described in Chapter 2.1.b.3.

#### **3.3.b.ii. Migration and invasion Assays**

Migration and invasion assays were conducted as described in Chapter 2.1.b.4.

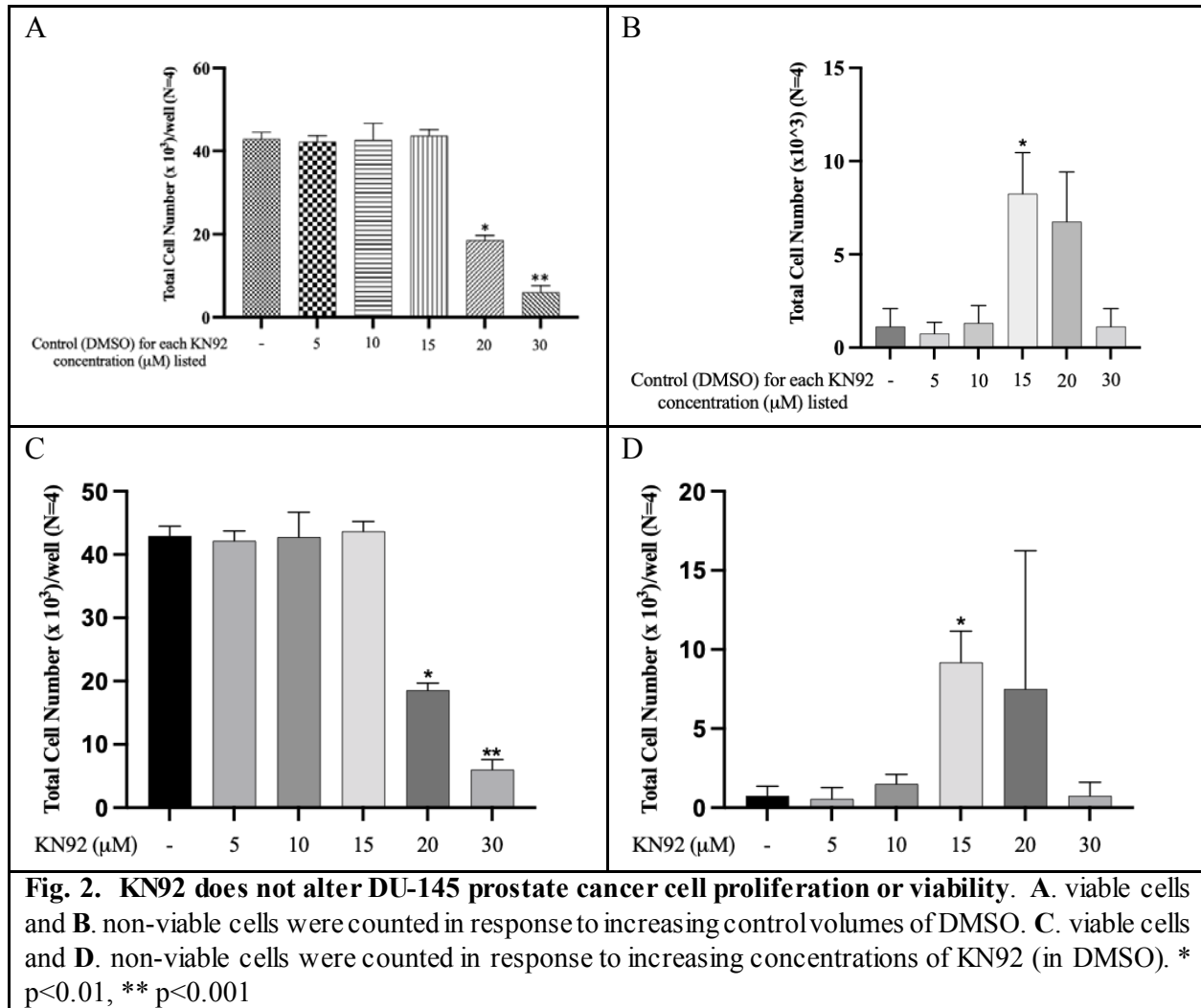
## 3.4. RESULTS

**3.4.a. CAMKII promotes cell proliferation but does not induce EMT.** Andre Sobel, and others have documented that CAMKII phosphorylates STMN1 on S16 [20-22]. Since little is known of the role of STMN1 S16 phosphorylation in PCa, especially via CAMPKII, we performed proliferation, migration, and invasion assays using the DU-145 cell line. To study the effect of CAMKII activity on DU-145 cell proliferation, DU-145 cells were treated for 3 days with increasing concentrations of the CaMKII activator oleic acid or increasing concentrations of the CaMKII inhibitor KN93 as indicated, and the Trypan Blue exclusion assay for viability was used to determine the number of viable and non-viable cells after treatment (**Fig. 1**).



In comparison to untreated groups, the vehicle control of ethanol did not significantly alter cell proliferation (Fig. 1A, 1C). Treatment with 20 and 30 μM oleic acid significantly increased DU-145 cell proliferation (Fig. 1A) without inducing cell death (Fig. 1B). In contrast, treatment with KN93 decreased the numbers of viable DU-145 cells in a dose-dependent manner (Fig. 1C), as observed by the corresponding increase in non-viable cells (Fig. 1D).

KN92 is an inactive isomer of KN93. Therefore, KN92 was used to determine its effectiveness in stimulating (or not stimulating) DU-145 cell proliferation. Unlike KN93 which is soluble in ethanol, KN92 is only soluble in DMSO, but DMSO has been shown to be a microtubule oligomerization-stimulating agent that could lead to cell death at higher concentrations [23]. Therefore, to achieve the same concentrations of KN92 that were used in the KN93 proliferation assay, 40  $\mu\text{L}$  of DMSO was used to generate the 20  $\mu\text{M}$  dose and 60  $\mu\text{L}$  of DMSO was used to generate the 30  $\mu\text{M}$  dose. Since DMSO was required to dissolve KN92, the Trypan Blue exclusion assay for viability was performed to test for toxicity. While DMSO alone did not affect cell growth at lower concentrations (**Fig. 2A**), the sharp decrease in viable cell number at the higher volumes of DMSO determined that DMSO was toxic at those levels (**Fig. 2B**). Similarly, the addition of KN92 did not affect cell growth at lower concentrations (**Fig. 2C**). However, cell viability decreased sharply at 20 and 30  $\mu\text{M}$  KN92 (**Fig. 2D**), indicating that this decrease was due to DMSO-induced toxicity. Indeed, cell death was so high that cells lifted off the culture plate and fragmented before they could be harvested and counted



### 3.4.b. CaMKII does not promote cell migration or invasion.

As described in 2.1.b.4., DU-145 cells were treated without/with Oleic Acid and KN93 to regulate CAMKII activity and the Neuroprobe chemotaxis chamber was used to determine whether CAMKII signaling regulated DU-145 cell migration. As shown in **Fig. 3**, both Oleic Acid and KN93 had no effect on promoting or inhibiting DU-145 cell migration respectively.

Similarly, the Neuroprobe chemotaxis chamber was also used to determine whether CAMKII signaling promoted DU-145 cell invasion, with the modification that the Neuroprobe

membrane was coated with Matrigel. Only cells producing enzymes that promote Matrigel digestion would be able to invade through the membrane and be counted as described above.

Again, neither Oleic Acid nor KN93 stimulated DU-145 cell invasion (**Fig. 4**).

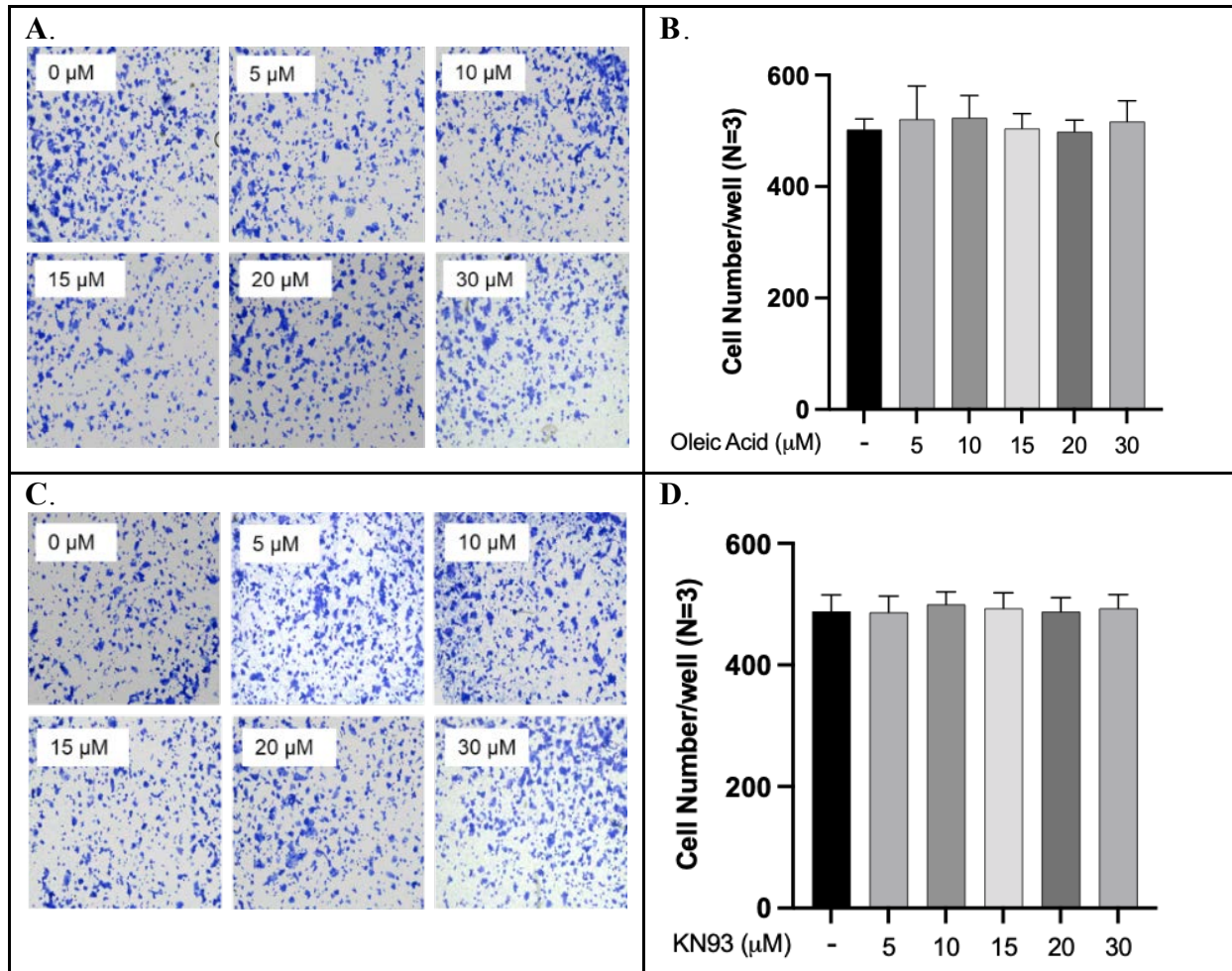


**Fig. 3. CaMKII signaling does not promote cell migration.** **A.** Representative images of crystal violet staining of DU-145 cells treated with increasing concentrations of Oleic Acid. **B.** Analysis of Oleic Acid-mediated cell migration. **C.** Representative images of crystal violet staining of DU-145 cells treated with increasing concentrations of KN93. **D.** Analysis of cell migration in response to KN93 treatment.

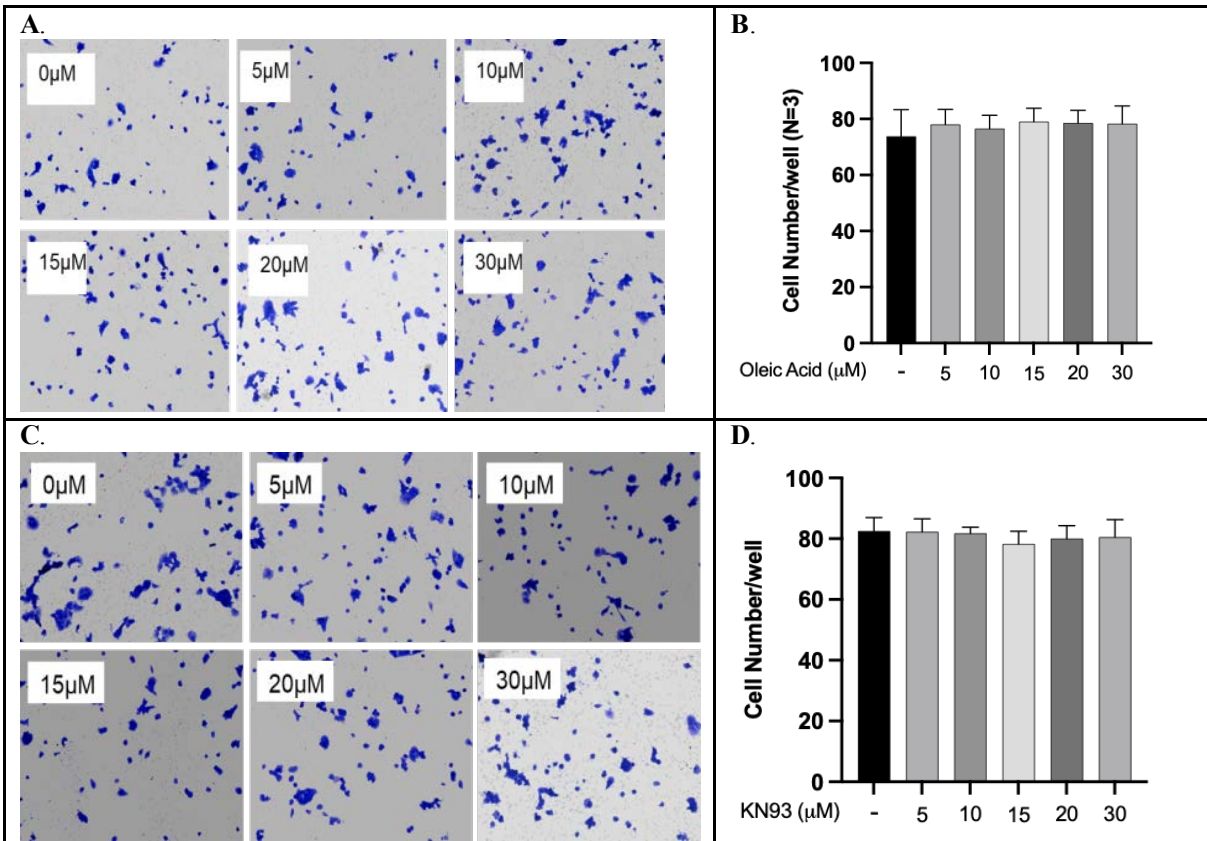


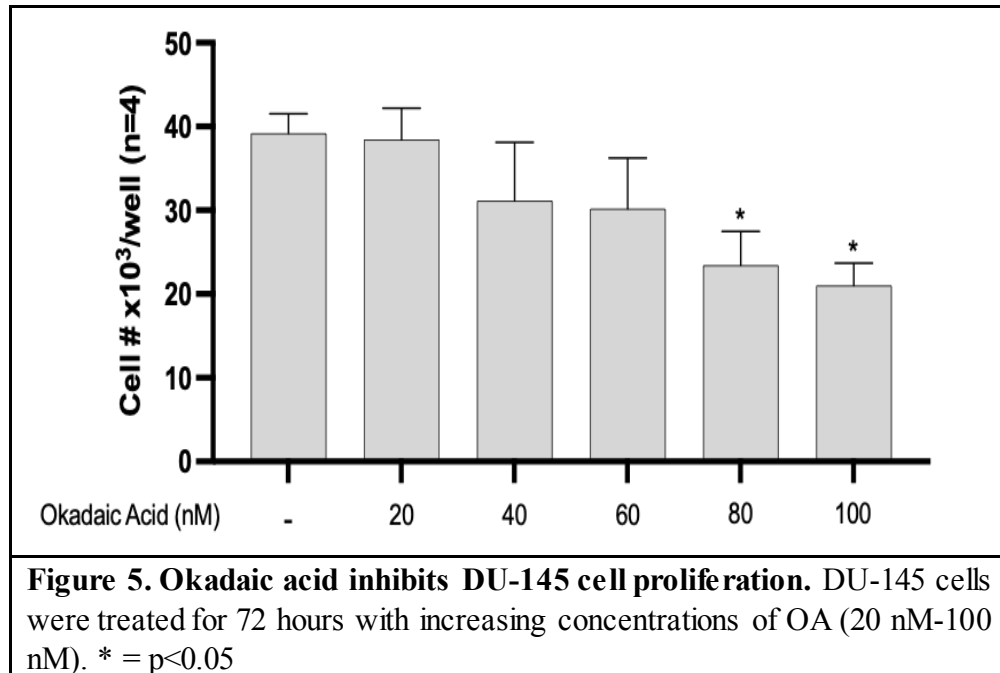
**Fig. 4. CaMKII signaling does not promote cell invasion.**

**A.** Representative images of crystal violet staining of DU-145 cells treated with increasing concentrations of Oleic Acid. **B.** Analysis of Oleic Acid-mediated cell invasion. **C.** Representative images of crystal violet staining of DU-145 cells treated with increasing concentrations of KN93. **D.** Analysis of cell invasion in response to KN93 treatment.

### 3.4.c. PP2A inhibits DU-145 cell proliferation.

Proliferation assays utilizing the Protein Phosphatase 2A (PP2A) inhibitor okadaic acid (OA) were conducted to investigate the effect of PP2A inhibition on DU-145 cell proliferation. PP2A functions to allow for normal cell cycle progression by dephosphorylating STMN1 after completion of cytokinesis; therefore, inhibition of PP2A should lead to an inhibition of cell proliferation. Cells treated with OA alone demonstrate that at 80 nM and 100 nM, DU-145 cells

were significantly inhibited from proliferating over 72 hours, as numbers of non-viable cells did not significantly change with increasing dose of OA.

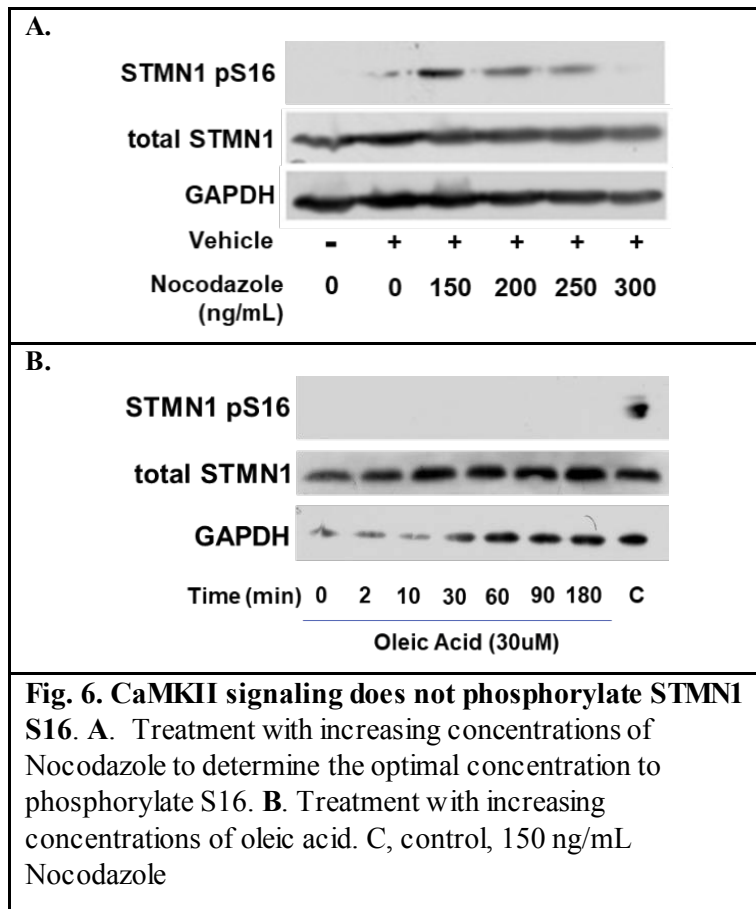


The inhibition in DU-145 proliferation at 80 and 100nM OA was could have been due to the cells inability to properly transition from mitosis to G1 of the next phase of the cell cycle, as a phosphorylated STMN1 protein is not capable of binding free tubulin to facilitate breakdown of cell spindles and a transition into the next phase of the cell cycle.

#### 3.4.d. CaMKII does not phosphorylate STMN1 S16

Western blot analysis was performed to determine whether activation of CAMKII resulted in downstream phosphorylation of STMN1 S16. Nocodazole is an agent that binds tubulin to inhibit polymerization which results in halting cell cycle progression and is used by Cell Signaling Technology to phosphorylate S16 and validate their Phospho-Stathmin (Ser16) Antibody #3353.

DU-145 cells treated with increasing concentrations of Nocodazole showed that the optimal concentration of Nocodazole for S16 phosphorylation was 150 ng/ml (**Fig. 6A**). Therefore, 150 ng/ml Nocodazole was used as a positive control for inducing S16 phosphorylation. DU-145 cells treated with increasing concentrations of Oleic Acid showed that STMN1 S16 was not phosphorylated by increasing CAMKII activity, as was anticipated through treatment with increasing dose of Oleic Acid (**Fig. 6B**). This observation was unexpected given that several studies report that CAMKII phosphorylated STMN1 S16 in Jurkat T, HeLa, HepG2, and MCF7 cells [24-26]. Our study suggests that CAMKII-mediated S16 phosphorylation is cell-type specific.

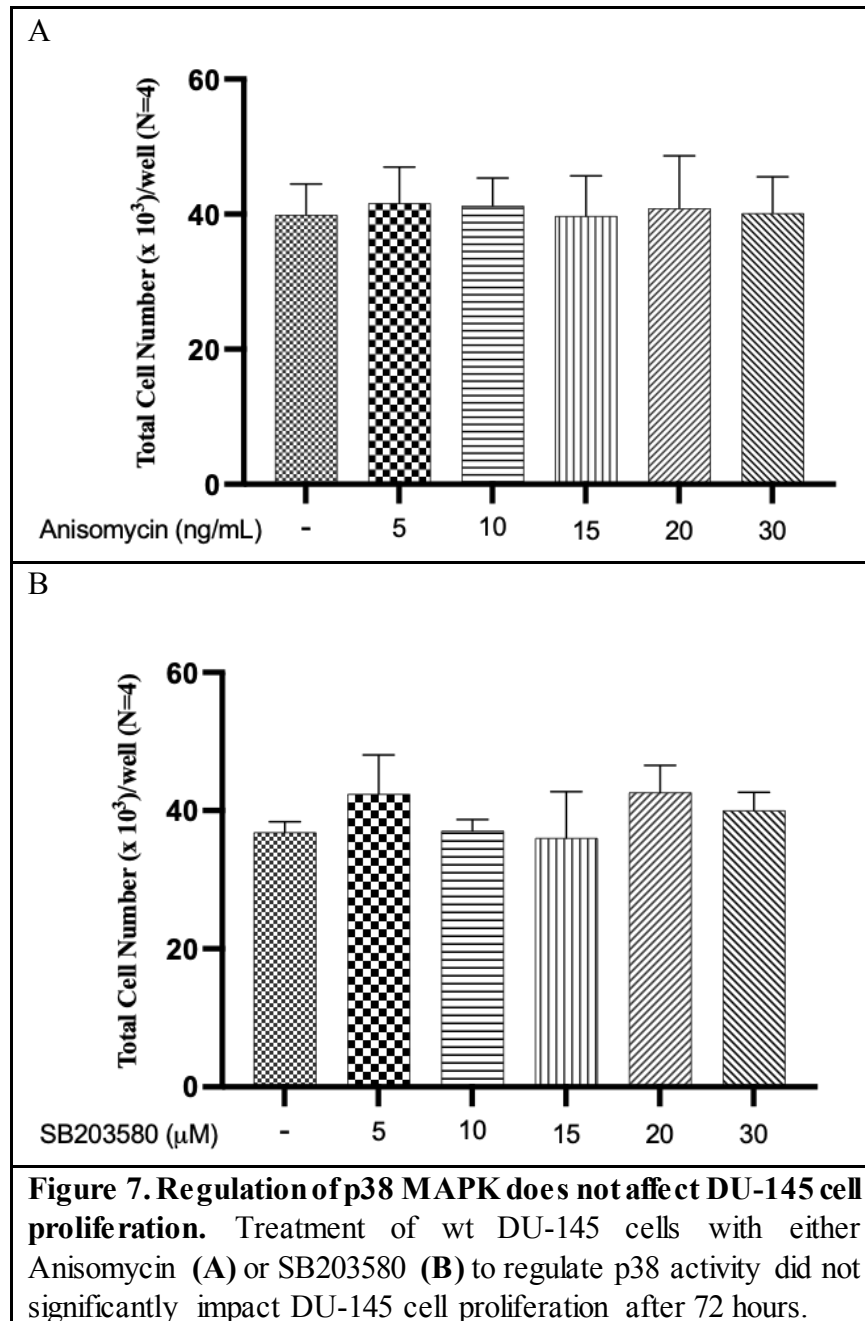


Taken together, these observations indicated that CAMKII activity promoted DU-145 cell proliferation, but not through the phosphorylation of STMN1 S16. Furthermore, CAMKII signaling did not promote metastatic potential in DU-145 cells, as observed by a lack of activity in the migration and invasion assays.

In conclusion, the experiments above outline the effect of CAMKII regulation on DU-145 cell proliferation, migration, and invasion. While CAMKII was not linked to phosphorylation of STMN1 S16 in DU-145 prostate cancer cells, these data demonstrate the complexity in the regulation of cell proliferation and that the role of CAMKII and STMN1 phosphorylation may be dependent on tissue and cell type.

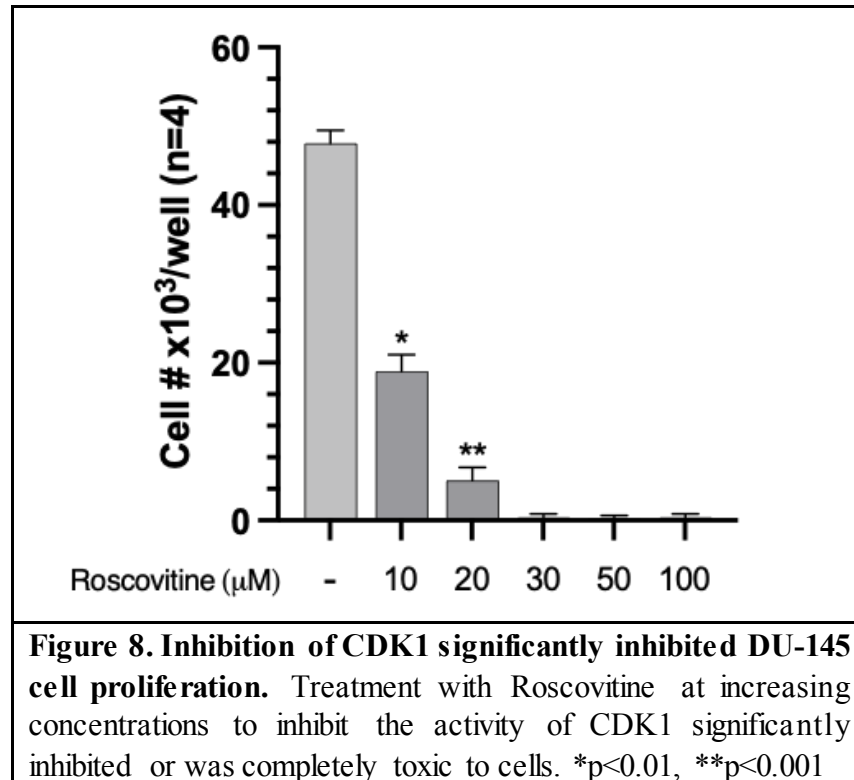
#### **3.4.e. The effect of small molecules targeting STMN1 S25, 38, and 63 on cell proliferation**

After completing the initial proliferation assays as demonstrated in 3.3.a., additional proliferation assays were conducted with small molecules that have been reported to regulate phosphorylation of STMN1 S(25,38,63). We hypothesized that regulation of STMN1 S25 would promote migration and invasion, but not proliferation; therefore, it was not predicted that treatment with Anisomycin (MAPK activator) or SB203580 (MAPK inhibitor) would have an impact on wt DU-145 cell proliferation.



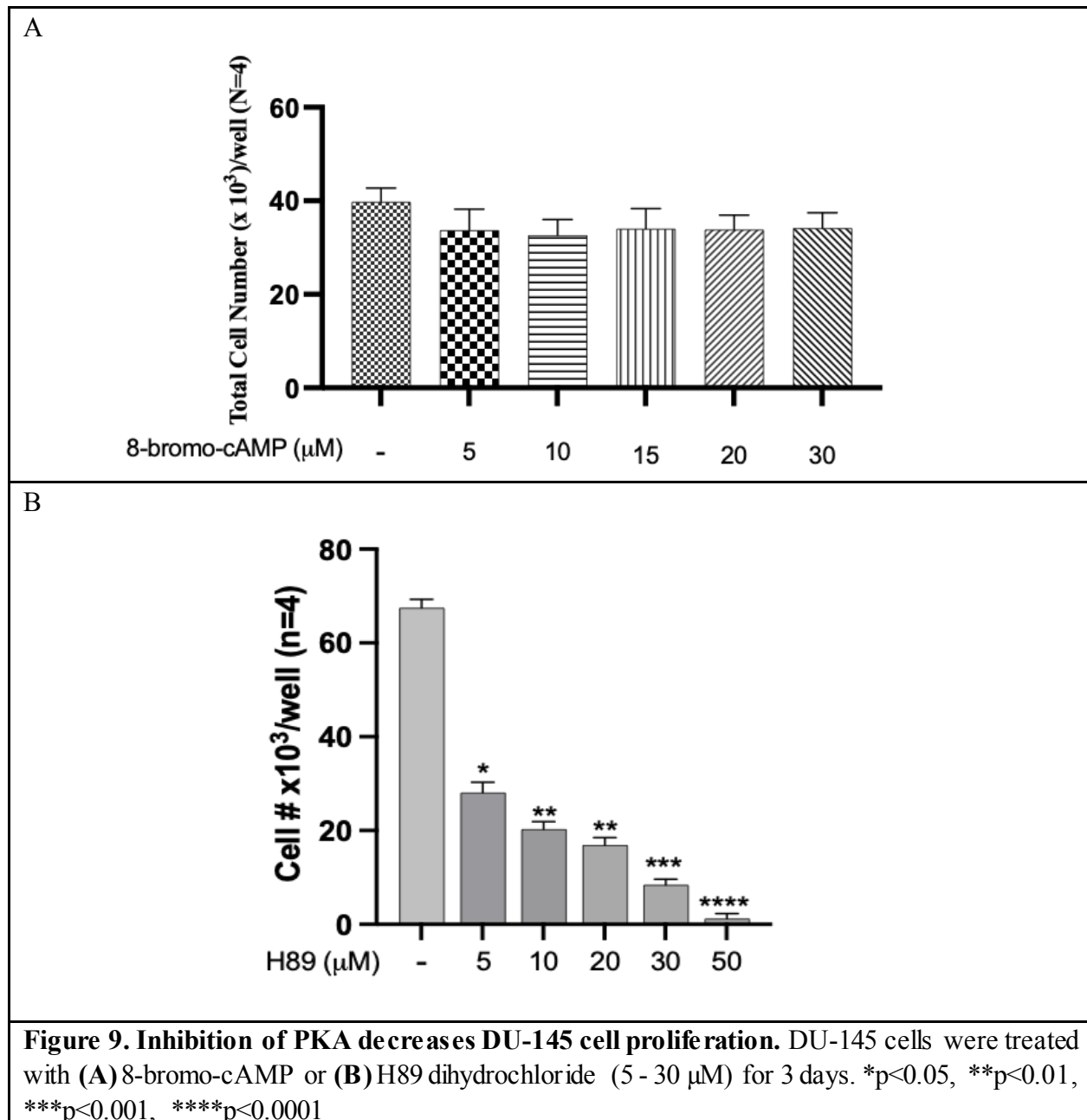
Regulation of MAPK via either the activator Anisomycin, or SB203580 did not alter DU-145 cell proliferation at any dose tested over 72 hours (Fig. 7). This could indicate that the role of

STMN1 S25 is more closely related to regulation of migration/invasion pathways and be more involved with metastatic potential than with cell proliferation.



Currently, small molecules known to specifically induce CDK1 activity are not available. Thus, we used Roscovitine, a pan cyclin-dependent kinase (cdk) inhibitor, to inhibit CDK1 (cdc2) to determine the effect(s) of inhibition of STMN1 S38 phosphorylation on DU-145 cell proliferation [27]. Roscovitine inhibited DU-145 cell proliferation, likely due to the inhibition of CDK1 and cell cycle progression as compared to the inhibition of STMN1 S38 phosphorylation. However, as observed in Chapter 2, Section 2.1.c.5. in Figure 16, expression of the STMN1 S38A mutant protein mimicking constitutively dephosphorylated S38 did not significantly alter DU-145 cell proliferation, while transfection of STMN1 S38E mutant protein mimicking constitutively

phosphorylated S38 significantly increased DU-145 cell proliferation, implying that STMN1 S38 phosphorylation regulated DU-145 cell proliferation.



In evaluating the results seen in **Fig.9**, it is evident that stimulation of PKA, which has been previously shown to phosphorylate STMN1 S63, does not increase proliferation in DU-145 cells; however, treatment with the PKA inhibitor H89 dihydrochloride has a drastic effect on proliferation/cell viability over 72 hours. In prostate cancer cell lines, it was reported that activation of the cAMP/PKA/CREB pathway leads to an increase in cell proliferation [26]. Therefore, it is likely that the lack of significant change with 8-bromo-cAMP treatment, which has been shown to stimulate PKA, is due to the pathway already being stimulated at a high-level basally, while inhibition of the pathway (**Fig. 9**) would have a more dramatic impact, unrelated to STMN1 S63 phosphorylation [28]. Finally, as seen in Section 2.1.c.5 in Figure 16, transfection of STMN1 S63E/A into DU-145 cells to mimic either permanent phosphorylation or permanent dephosphorylation, respectively, does not alter cell proliferation alone. Thus, this leads to the conclusion that regulation of the PKA pathway has a STMN1-independent effect that regulates cell proliferation.

### 3.5. DISCUSSION

CAMKII is reported to phosphorylate STMN1 S16 and regulate cell proliferation in a number of different cell lines [20-22]. Our study shows for the first time that CAMKII promotes DU-145 cell proliferation, however CAMKII activity does not induce metastasis. Further, CAMKII does not phosphorylate STMN1 S16 as was previously shown in other cell lines, indicating that CAMKII-mediated DU-145 cell proliferation is independent of STMN1 S16 phosphorylation, and that CAMKII phosphorylation of STMN1 S16 is cell-type-specific.

STMN1 phosphorylation on S16 by CAMKII has been published to increase cell proliferation in Jurkat T cells, with Okadaic Acid (OA) further stimulating prolonged phosphorylation on all 4 serine sites by inhibiting PP2A activity [21]. While our data demonstrates increase in proliferation with stimulation of CAMKII by Oleic Acid, the utilization of the PP2A inhibitor OA was found to inhibit cell proliferation in a dose-dependent manner. This inhibition is likely due to the inability of the cell to progress through the cell cycle in its entirety, as STMN1 is maintained in the phosphorylated state due to lack of PP2A activity.

A novel aspect of the work presented here demonstrates the ability of CAMKII to regulate cell proliferation without inducing metastasis, and that the effects of CAMKII on cancer cells are cell-type-specific. Liu *et al.*, demonstrated that CAMKII activity induces NFkB and MMP-9 production in gastric cancer cells leading to the induction of metastasis [23]. Our work demonstrates for the first time that CAMKII activation or inhibition had no effect on DU-145 cell

migration or invasion, while stimulation of CAMKII by Oleic Acid and inhibition by KN93 both significantly increased and decreased cell proliferation, respectively, in dose-dependent manners.

An extensive literature base exists regarding the effect of CAMKII on a variety of cancers ranging from breast to gastric, to osteosarcoma, to prostate, and many more [6]. While each cancer has its own unique characteristic, the differences between cell lines in each cancer type results in varied outcomes to CAMKII regulation [6]. The work reported here could help to further advance the current understanding of the differential role CAMKII plays in PCa progression.

# Chapter 4

## Constant Degradation of the AR by MDM2 Conserves Prostate Cancer Stem Cell Integrity

Premkumar Vummidi Giridhar <sup>#1</sup>, Karin Williams <sup>#2</sup>, Andrew P VonHandorf <sup>#3</sup>, Paul L Deford <sup>3</sup>, Susan Kasper <sup>4</sup>

Cancer Res. 2019. 79:1124-1137.

doi: 10.1158/0008-5472.CAN-18-1753

- <sup>1</sup> Department of Neonatology and Pulmonary Biology, Cincinnati Children's Hospital and Medical Center, Cincinnati, Ohio.
- <sup>2</sup> Translational Radiation Biology, Wolfson Wohl Cancer Research Centre, Institute of Cancer Sciences, College of Medical, Veterinary & Life Sciences University of Glasgow, Glasgow, Scotland.
- <sup>3</sup> Department of Environmental Health, University of Cincinnati College of Medicine, Cincinnati, Ohio.
- <sup>4</sup> Department of Environmental Health, University of Cincinnati College of Medicine, Cincinnati, Ohio. [susan.kasper@uc.edu](mailto:susan.kasper@uc.edu).

# Contributed equally.

## 4.1 Abstract

Prostate cancer stem cells (CSCs) are implicated in tumor initiation, cancer progression, metastasis, and the development of therapeutic-resistant disease. It is well known that the bulk of prostate cancer (PCa) cells express androgen receptor (AR) and that androgens are required for PCa growth, progression and emergence of castration-resistant disease. In contrast, the small subpopulation of self-renewing CSCs exhibit an AR-negative (-) signature. The mechanisms underlying the absence of AR are unknown. Using CSC-like cell models isolated from clinical biopsy tissues, we identify the E3 ligase MDM2 as a key regulator of prostate CSC integrity. First, unlike what has been reported for the bulk of AR(+) tumor cells where MDM2 regulates the temporal expression of AR during transcriptional activity, MDM2 in CSCs promoted the constant ubiquitination and degradation of AR, resulting in sustained loss of total AR protein. Second, MDM2 promoted CSC self-renewal, the expression of stem cell factors, and CSC proliferation. Loss of MDM2 reversed these processes and induced expression of full-length AR (and not AR variants), terminal differentiation into luminal cells, and cell death. Selectively blocking MDM2-mediated activity in combination with androgen/AR-targeted therapy may offer a novel strategy for eliminating AR(-)CSCs in addition to the bulk of AR(+) PCa cells, decreasing metastatic tumor burden and inhibiting the emergence of therapeutic resistance.

## 4.2 Introduction

While the androgen receptor (AR) is a master regulator of prostate development and disease, it is commonly believed that normal prostate stem cells and prostate cancer stem cells (CSCs) express no/low AR and that their growth is androgen-independent [1]. Our previous study demonstrated that AR(-) pluripotent CSCs isolated from patient biopsies differentiated into prostatic glandular structures containing all three epithelial cell types including AR(+) luminal secretory cells and AR(-) basal and neuroendocrine cells when engrafted with embryonic mesenchyme under the renal capsule [2]. Similarly, other studies report that AR(-) normal prostate stem-like cells differentiate into three prostatic epithelial cell lineages [3]. This pattern of AR(-) expression mimics that observed in human and rodent prostate development where AR(-) epithelial anlagen grow into the urogenital mesenchyme until AR protein is induced by, as yet unknown mechanisms, to initiate glandular lumen formation, epithelial cell specification, and androgen-mediated secretory activity [4,5]. Qin and colleagues determined that Prostate Specific Antigen (PSA)-/lo cells, a subpopulation isolated from LNCaP and LAPC9 prostate cancer (PCa) cell lines, were AR-/lo and exhibited stem-like properties including self-renewal and the ability to regenerate PSA+ cells (6). PSA-/lo LAPC9 cells developed into therapeutic-resistant tumors [6].

Together, these observations imply that an AR(-) phenotype is essential for maintaining CSC and normal prostate stem cell homeostasis and for promoting castration resistant prostate cancer (CRPC). The mechanisms underlying this AR(-) phenotype are unknown. Our previous study showed that biopsy-derived PCa CSCs, referred to as HPET (human prostate epithelial cells expressing hTERT), expressed AR mRNA but not AR protein, suggesting that expression was regulated at the posttranscriptional level (2). The Qin study reported that in PSA-/lo cells, both AR mRNA and protein were down-regulated, implying that AR expression was regulated at the

transcriptional level [6]. Whether inhibition of AR protein expression occurs at the transcriptional and/or posttranscriptional level remains to be established.

Evidence from non-CSC, AR(+) PCa cell lines suggests that the ubiquitin-proteasome system (UPS) modulates the steady state of AR expression. For example in AR(+) LNCaP, CWR-R1, and CWR22Rv1 cells, the E3 ligase MDM2 (mouse double minute 2 homolog) transiently modulates AR stability during transcriptional activity [7]. Other E3 ligases, including NEDD4 (neural precursor cell expressed developmentally down-regulated protein 4) [8], CHIP (C-terminus of Hsp70-interacting protein) [9], and SKP2 (S-Phase Kinase-Associated Protein 2) [10] also regulate AR protein degradation in LNCaP, C4-2B and CWR22Rv1 cells. Whether AR(-) CSCs use these same ligases to block total AR expression remains to be explored.

The recent discovery of AR splice variants (AR-Vs) provides insight into the mechanisms promoting emergence of CRPC. These naturally occurring AR-Vs are identified in clinical PCa biopsy specimens and non-CSC PCa cell lines (reviewed in [11,12]). AR-Vs contain the N-terminal and DNA binding domains; however, they lack a ligand binding domain, resulting in constitutive activation. Several reports demonstrate that AR-Vs are highly expressed in CRPC, metastasis, and PCa cell lines not requiring androgens for cell growth. The most commonly expressed variant AR-V7 (a.k.a. AR3) is associated with development of CRPC and drug resistance. Furthermore, AR-V7 promotes epithelial mesenchymal transition (EMT) and induces expression of signature stem cell genes, including Nanog in LNCaP cells and Lin28B in DU-145 cells [13]. Interestingly, MDM2 induces AR-V7 ubiquitination and protein degradation [14]. Whether CSCs express AR-Vs remains to be investigated.

Prostate cells with CSC-like properties have typically been isolated as side populations (~0.1–0.3% of PCa cells) from established cell lines, e.g., PC-3 [15], DU-145 [16], and LNCaP [17] cells,

and from biopsy tissues [18]. Here we use two CSC-like cell models to investigate the AR(-) signature of prostate CSCs. Both HPET (2) and HuSLC (human stem like cells; previously termed HPE for human prostate epithelial) [19] cell lines were isolated from high grade Gleason 9 biopsy tissues from two unrelated individuals. Of note is that the HuSLC line arose spontaneously. Both cell lines express AR mRNA but not AR protein, and exhibit stem-like properties including pluripotency in vivo, differentiating into the three prostatic epithelial cell lineages, i.e., luminal secretory AR(+) cells, basal cells and neuroendocrine cells [2,19]. Using these CSC-like cell models, we report that MDM2 is critical for conserving an AR(-) signature and promoting stemness, while loss of MDM2 induces full-length AR expression, terminal CSC differentiation into AR(+) luminal epithelial cells, and cell death.

## 4.3 Materials and Methods

### 4.3.1 Materials

Prostate cancer cells LNCaP, PC3, 22RV1 and VCaP were purchased from American Type Culture Collection (ATCC). Proteasome inhibitors MG132 (cat.#: 3175-v), MG115 (cat.#: 3170-V) and Epoxomicin (cat#: 4381-v) were purchased from the Peptide institute, Osaka, Japan. Matrigel (BD Biosciences, cat.#:10828028) was batch-tested by the Pluripotent Stem Cell Facility at Cincinnati Children's Hospital Medical Center. The human full-length wild type (wt) AR expression vector pSVAR<sub>0</sub> was a gift from Dr. S. Liao, Chicago. Additional materials and reagents are indicated below.

### 4.3.2 Methods

#### 4.3.2.a. Cell culture

The parental HPET cell line was established by transducing primary human prostate epithelial cells (passage 2) cultured from de-identified human prostate cancer surgical waste material (Gleason 9, undifferentiated PCa,) using pLenti-particles expressing the *hTERT-EGFP* gene [2]. The HPET cell lines and their prostate epithelial and stem cell characteristics were authenticated both *in vitro* and *in vivo* as described in detail in Gu *et al.* [2]. Vials containing HPET passage 73 were thawed and passaged approximately 5 times to complete this current study. A second cell line, termed HuSLC line arose spontaneously from Hcells cultured from de-identified biopsy tissue (Gleason 9, undifferentiated PCa) from an unrelated male donor. Their HPE-like and PCa-generating characteristics were authenticated both *in vitro* and *in vivo* in detail in Williams *et al.*

[Figure 6 (19)]. They were initially named “HPE”, but subsequently renamed “HuSLC” because of their stem-like characteristics. Vials containing HuSLC passage 32 and 34 were thawed and passaged approximately 5 to 6 times to complete this study. Cell lines were recently tested (June, 2018) and found to be negative for mycoplasma (Lonza MycoAlert™ Mycoplasma Detection Kit, cat.#: LT07-218; Lonza Mycoalert™ Mycoplasma Assay Control Set, cat.#: LT07-518).

Both the HPET and HuSLCs cell lines were cultured in under embryonic stem (ES) cell conditions using defined ESC medium, DMEM-F12 (ThermoFisher Scientific, cat.#: 11320033) supplemented with KnockOut™ Serum Replacement (ThermoFisher Scientific, cat.#: 10828028) and 4ng/ml recombinant bFGF (ProSpec, cat.#: CYT-218) on Matrigel coated plates. Prostate cancer cells LNCaP, PC3, 22RV1 and VCaP were purchased from American Type Culture Collection (ATCC) and cultured as recommended by ATCC. Cells from the company were expanded through approximately 4 to 5 passages and frozen down as stock vials. Stock vials were thawed and cells were passaged approximately 2 to 4 times to complete this study.

#### **4.3.2.b. Sphere formation assay**

HPET or HuSLC cells were trypsinized using Trypsin-EDTA Solution (ThermoFisher Scientific, cat.#: 25200056), centrifuged for 5 minutes at 300 x g and the cell pellet resuspended in defined ESC medium (described above). Cells were seeded at 2,500 cells/ml in 6-well ultra-low attachment plates (FisherScientific, Corning™ Costar™ 3471, cat.#: 07-200-601) and cultured for 10 days. Wells were photographed using phase contrast and total number of spheres/well were counted using NIH ImageJ software.

#### **4.3.2.c. Proliferation Assay**

Cells were plated at  $5 \times 10^3$  cells/well using 24 well plates and either transfected with control plasmid or pSVARo to induce exogenous AR protein expression or treated with MG132 to induce endogenous AR, and treated with/without  $10^{-8}$  M dihydrotestosterone (DHT) with/without  $10^{-5}$  M hydroxyflutamide (OHF) or vehicle control (95% ethanol) as indicated in each assay. Cell numbers were determined using the Trypan Blue Viability assay (ThermoScientific, HyClone™ Trypan Blue Solution, 0.4%, cat.# SV3008401).

#### **4.3.2.d. Western Blot Analysis**

Cells were harvested using RIPA buffer (Invitrogen Inc., cat.#: R0278) with 1% protease inhibitor cocktail (FisherScientific, cOmplete™ Protease Inhibitor Cocktail tablets/Roche, cat.# NC0939492) and phosphatase inhibitor cocktail (FisherScientific, EMD Millipore™ Calbiochem™ Phosphatase Inhibitor Cocktail Set I, cat.# 53-913-110VL). Lysates were centrifuged at 4°C for 10 min at  $14,000 \times g$ ; 50 µg protein from each supernatant was subjected to 10% SDS-PAGE, transferred to PVDF membrane and blocked and probed with primary antibody overnight at 4°C. Peroxidase-conjugated secondary antibody was added at a 1:4500 dilution and blots were developed using the Enhanced Chemiluminescence (ECL) kit (Pierce™/ThermoFisher Scientific™, cat.#: 32132).

#### **4.3.2.e. Immunoprecipitation**

Cells were lysed in 300 µL of cold lysis buffer [1% Triton X-100, 150 mmol/L NaCl, 10 mmol/L NaHPO<sub>4</sub> (pH 7.2), 5 mmol/L NaF, 2 mmol/L EDTA, 1x HALTTM protease inhibitor cocktail (ThermoFisher Scientific, cat.#: 78440)] at 4°C in a cold room. Lysates were cleared by

centrifugation and immunoprecipitation was performed by incubating 500 µg total protein with 10 µg rabbit anti-AR antibody or 5 µg mouse anti-hemagglutinin (HA) antibody (Santa Cruz Biotechnology, cat # sc-816 and cat.# sc-805 respectively) overnight at 4°C. ImmunoPure Immobilized Protein G beads (Pierce Biotechnology, cat.#:44667) were used to pull down protein complexes. The immunoprecipitates were washed in 1x phosphate buffered saline (PBS), resuspended in 1x Laemmli buffer and subjected to Western blot analysis.

#### **4.3.2.f. Luciferase Assay**

Cells were transfected with the ARR2PB-luc reporter [20] and Renilla luciferase vectors (Promega, cat.#: E2231) and either treated with increasing concentrations of MG132 (to induce endogenous AR) or co-transfected with increasing concentrations of pSVARo (to induce exogenous AR). Twenty-four hours post AR induction, cells were treated with vehicle control (ethanol) or DHT (10<sup>-8</sup> M) with/without OHF (10<sup>-5</sup> M) for 24 h, as described previously [21]. Cells were lysed and luciferase activity was determined using the Promega Dual-Luciferase® Reporter Assay System kit and protocol (Promega, cat.#: E1910) according to the manufacturer's protocol. Cell lysate protein concentrations were determined using the Protein BCA Assay kit (Pierce™/ThermoFisher Scientific™, cat.#: 23225).

#### **4.3.2.g. Total RNA Extraction, Purification, and cDNA Synthesis**

Total RNA was extracted from HPET and HuSLCs using TRIzol reagent (Invitrogen™/ThermoFisher Scientific™, cat.#: 15596018) following the manufacturer's protocol. Total RNA concentrations (260/280 nm) were determined using the NanoDrop system (NanoDrop Technologies Inc., Wilmington, DE). RNAs were treated with DNase I (Invitrogen Inc., cat.#: AM2222) to remove any traces of DNA contamination and cDNAs were synthesized

from 1 µg of RNA per sample using the Fermentas Revertaid kit (Fermentas™/ThermoFisher Scientific™, cat.#: K1621), according to the manufacturers' protocols.

#### **4.3.2.h. Quantitative Polymerase Chain Reaction and Data Analysis**

Primers used in this study are listed in Supplementary Tables S2 and S3. One (1) µg of synthesized cDNA was added to 1µM random-specific primers (synthesized by IDT Inc.), and 12.5 µl of 2x Power SYBR® Green PCR Master Mix (Applied Biosystems™/ThermoFisher Scientific™, cat.#: 4309155) to a final volume of 25 µl. PCR amplification was performed using an Applied Biosystems 7300 Real-Time PCR System [one cycle at 50°C for 2 min, one cycle of 95°C for 10 min, followed by 40 cycles of 15 sec at 95°C and 1 min at 60°C]. The dissociation curve was completed with one cycle of 1 min at 95°C, 30 sec of 55°C, and 30 sec of 95°C. Non-reverse transcription control and no template control were included in the PCR program for quality control.

#### **4.3.2.i. Quantification And Statistical Analysis**

GraphPad Prism v4.0 was used for all statistical analyses. Statistical parameters, including the types of tests, number of samples (n), descriptive statistics and p values are reported in the figure legends.

## 4.4 Results

### 4.4.a. Inhibition of the proteasome induces AR expression in CSC-like PCa cells.

Previously, we reported that HPET cells recapitulated the AR(-) phenotype reported for CSCs [2] (Figure 1A) and similarly, the HuSLC line also expressed AR mRNA but not AR protein (Figure 1B). To determine whether AR protein was constitutively being degraded, HPET and HuSLCs were transfected with increasing concentrations of pSVARo, which expresses human full-length/wt AR at low concentrations ( $\leq 4 \mu\text{g}$ ) [23]. Unexpectedly, 30  $\mu\text{g}$  pSVARo were required for detectable AR protein expression in HPETs (Figure 1A;  $p < 0.0001$ ). Moreover, addition of (DHT,  $10^{-8}$  M) appeared to stabilize AR protein levels. Similarly, 40  $\mu\text{g}$  pSVARo were required to induce detectable AR protein in HuSLCs (Figure 1B;  $p < 0.0001$ ), suggesting that at lower pSVARo concentrations, AR protein was actively being degraded.

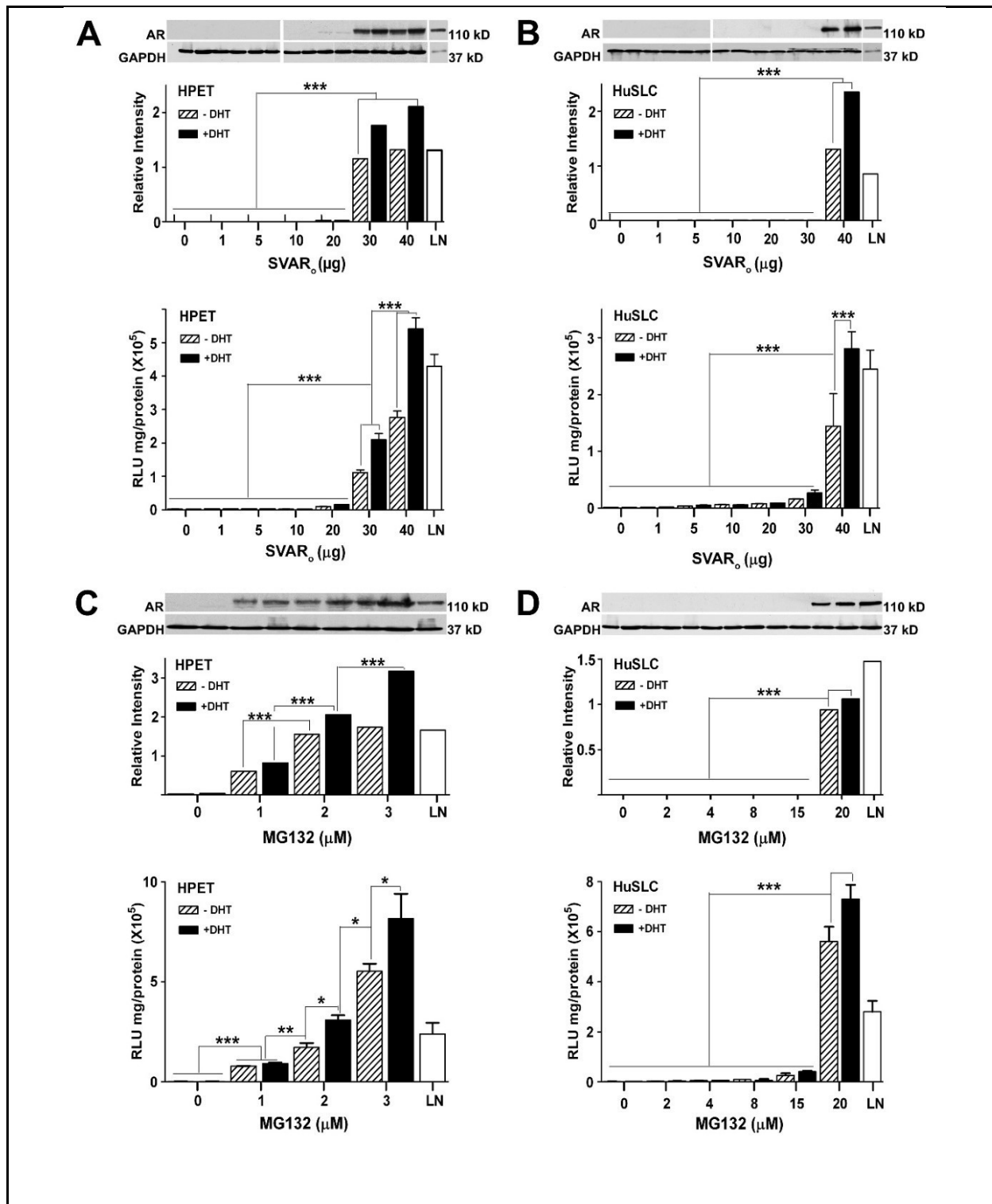


**Figure 1. AR expression in CSC-like PCa cells is modulated by the proteasome.**

**(A, B) AR expression and transcriptional activity are only induced following transfection with high concentrations of pSVAR<sub>o</sub> plasmid.** HPET cells (A) and HuSLCs (B) were transfected with increasing concentrations of pSVAR<sub>o</sub> plasmid (expressing full-length, wt human AR). AR protein levels were analyzed by Western blot and semi-quantified by Densitometry. Cells were transfected with ARR<sub>2</sub>PB-

*luc* (24,49) and *Renilla* luciferase reporter genes. Luciferase activity was determined using the Promega Dual-Luciferase® Reporter Assay System kit and protocol (Promega, cat.#: E1910). **(C, D) Proteasomal inhibition initiates AR expression and transcriptional activity.** HPET cells (C) and HuSLCs (D) were treated with increasing concentrations of MG132 with/without addition of 10<sup>-8</sup> M DHT and dual luciferase activity was determined as above. Abbreviations: wt, wild type; DHT, dihydrotestosterone. Data are expressed as mean ± SEM; *n* = 4. \*, *p*<0.01; \*\*, *p*<0.001; \*\*\*, *p*<0.0001.

To determine whether AR protein levels were down-regulated by proteasomal degradation, HPET cells (Figure 1C) and HuSLCs (Figure 1D) were treated with increasing concentrations of the proteasome inhibitor MG132. In HPET cells, endogenous full-length AR protein was already detected at the lowest concentration of MG132 (1 μM) tested. Similarly, AR protein was induced in HuSLCs following MG132 treatment (20 μM). Furthermore, treatment with other proteasome inhibitors, MG115 and Epoxomicin, confirmed these observations (Supplementary Figure S1). In transfection assays using the androgen-regulated probasin promoter linked to the luciferase reporter gene (ARR2PB-luc) (24), AR-mediated transcription was only induced when exogenous (Figure 1A, 1B) or endogenous (Figure 1C, 1D) AR protein was expressed.

The E3 ligase MDM2 is reported to regulate AR levels in PCa cells [7]. Therefore, MDM2 expression was analyzed in HuSLC and HPET cells and compared to two standard PCa cell lines, LNCaP (where MDM2 modulates AR levels in a temporal manner to regulate AR-mediated transcription) and DU-145 (which do not express AR). Both HuSLC and HPET cells expressed higher levels of MDM2 (2.16- and 1.74-fold respectively) as compared to LNCaP and DU-145 cells (Supplementary Figure S2). Furthermore, MDM2 levels were highest in HuSLCs, implying that AR degradation in HuSLCs was greater than in HPET cells. This is supported by the findings that more AR plasmid and higher amounts of proteasome inhibitor were required to induce HuSLC AR expression. Taken together, these observations support an active role for the proteasome in conserving the AR(-) CSC signature.

#### 4.4.b. HPET and HuSLCs express full-length AR but not AR-Vs

Published primer sets spanning the genomic region from which AR-Vs are transcribed were used to determine whether HPET cells and HuSLCs expressed AR-V transcripts [25,26]. A universal forward primer, P1/P2/P3 (F), located in AR exon 2 was paired with one of three reverse primers (P1R, P2R, and P3R) located within in each variant exon (as outlined in **Supplementary Table S2**). This approach provided coverage for the known AR variants. 22Rv1 and VCaP cell lines served as positive controls.

Both HPET cells and HuSLCs expressed full-length AR transcript (AR-fl) (**Figure 2A**); however, they did not express any of the other recognized AR-V transcripts (**Figure 2, Supplementary Figure S3**). We then determined whether androgen-mediated activity was required for induction of AR-V expression. AR-V1 and AR-V7 transcripts were not detected under any conditions tested (**Figure 2B and 2C**). In contrast, full-length AR mRNA was expressed at similar levels regardless of treatment with vehicle or dihydrotestosterone (DHT) with/without OHF (**Figure 2A**). Western blot analysis using an AR antibody towards the N-terminal (which recognizes AR-fl and AR-Vs) determined that HPET cells and HuSLCs expressed full-length 110 kDa endogenous AR following MG132 treatment, however an 80 kDa band corresponding to AR-Vs [27] was not detected in either cell line under any condition tested (**Supplementary Figure S4**). Several bands at lower molecular weights (<68 kDa) were observed in HPET cells, however they did not correspond to any known AR-Vs. Since these bands were already present prior to induction of AR expression, they may represent degraded/non-functional AR or non-specific antibody interactions. In summary, CSC-like HPET cells and HuSLCs did not express AR-Vs, but instead, conserved expression of full length AR.

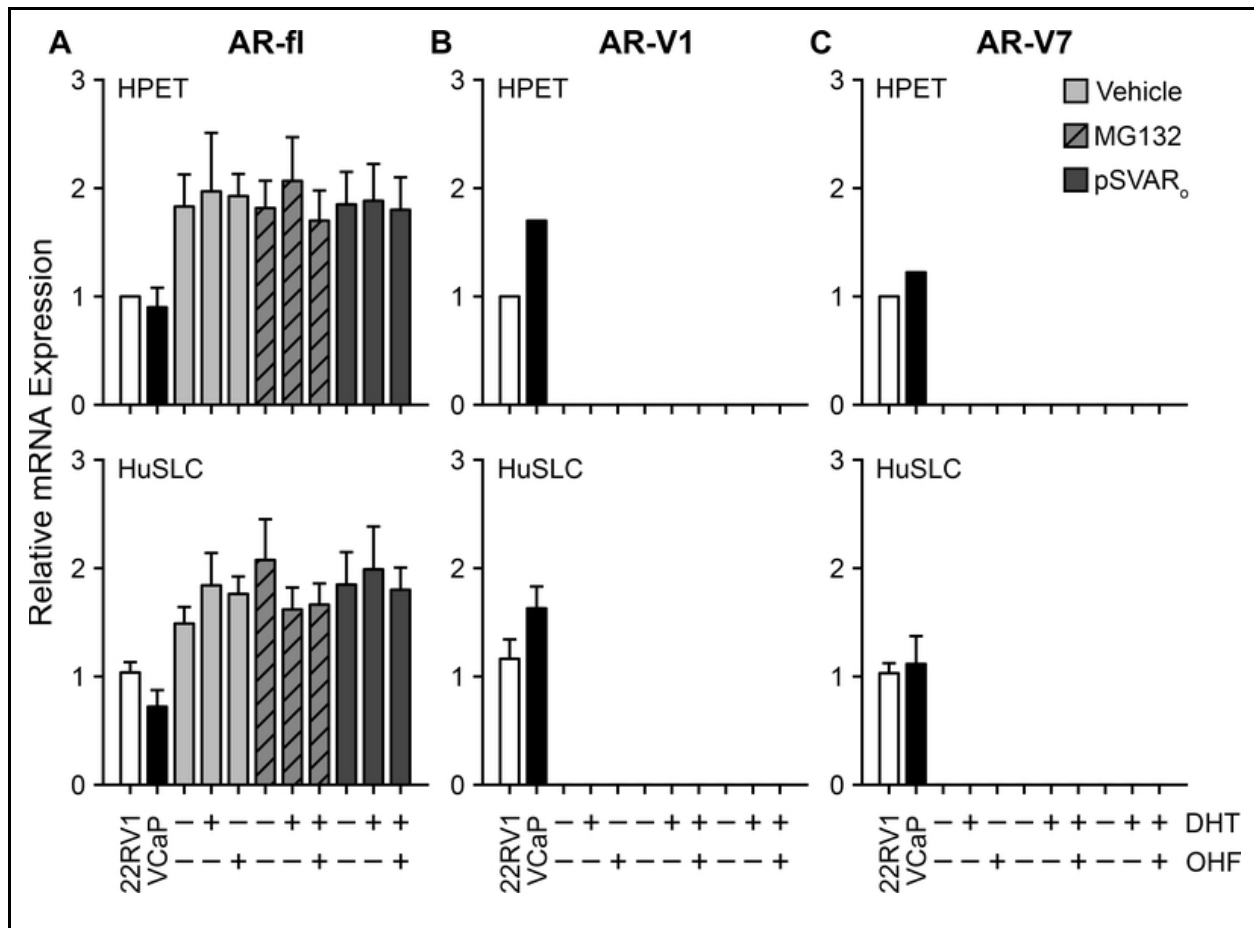


**Figure 2. CSC-like HPET cells and HuSLCs express full-length AR, but not AR-Vs.**

**(A) RT-qPCR analysis of endogenous HPET and HuSLC AR-fl following treatment with DHT with/without OHF.** HPET cells (upper panel) were treated with 2  $\mu$ M MG132 to induce endogenous AR, or 30  $\mu$ g pSVAR<sub>o</sub> to express exogenous AR-fl, and treated with 10<sup>-8</sup> M DHT with/without 10<sup>-5</sup> M OHF. Vehicle control, 95% ethanol. HuSLCs (lower panel) were treated with 20  $\mu$ M MG132 to induce endogenous AR, or 40  $\mu$ g pSVAR<sub>o</sub> to express exogenous AR-fl, and treated with 10<sup>-8</sup> M DHT with/without 10<sup>-5</sup> M OHF. Vehicle control, 95% ethanol. VCaP and 22RV1 cell lines served as control PCa cell lines for AR-fl, AR-V1 and AR-V7 expression. Primer sets used to characterize AR-V expression are listed in Supplementary Table S2. Only data for AR-fl, AR-V1 and AR-V7 are shown since HPET and HuSLCs did not express any of the other AR-Vs tested (data not shown).

**(B-C) RT-qPCR analysis of endogenous AR-V1 and AR-V7 following treatment with DHT with/without OHF.** HPET cells (upper panel) and HuSLCs (lower panel) were treated as in (A). In both HPET and HuSLCs, AR-V1 and AR-V7 expression was not observed under any conditions tested. Abbreviations: fl, full-length; V, Variant; DHT, dihydrotestosterone; OHF, hydroxyflutamide. Data are expressed as mean  $\pm$  SEM;  $n = 4$ .

#### **4.4.c. An AR(-) phenotype is essential for prostate CSC self-renewal and proliferation**

A standard sphere formation assay was performed to determine whether AR signaling inhibited CSC stemness. HPET cells (**Figure 3A**) and HuSLCs (**Figure 3B**) were treated with MG132 with/without DHT to induce AR protein expression and activate AR-mediated signaling. Sphere formation was absent upon AR expression, and remained unaltered by DHT treatment. In contrast, sphere formation was rescued by addition of OHF. Similarly, exogenous expression of pSVAR<sub>o</sub> inhibited sphere formation; and this could be rescued by OHF treatment (**Figure 3C, 3D**). Furthermore, induction of AR dramatically decreased cell proliferation within 48 h, and addition of DHT decreased cell proliferation even further down to baseline levels. In contrast, OHF-mediated inhibition of AR activity restored cell proliferation (**Figure 3C, 3D**).

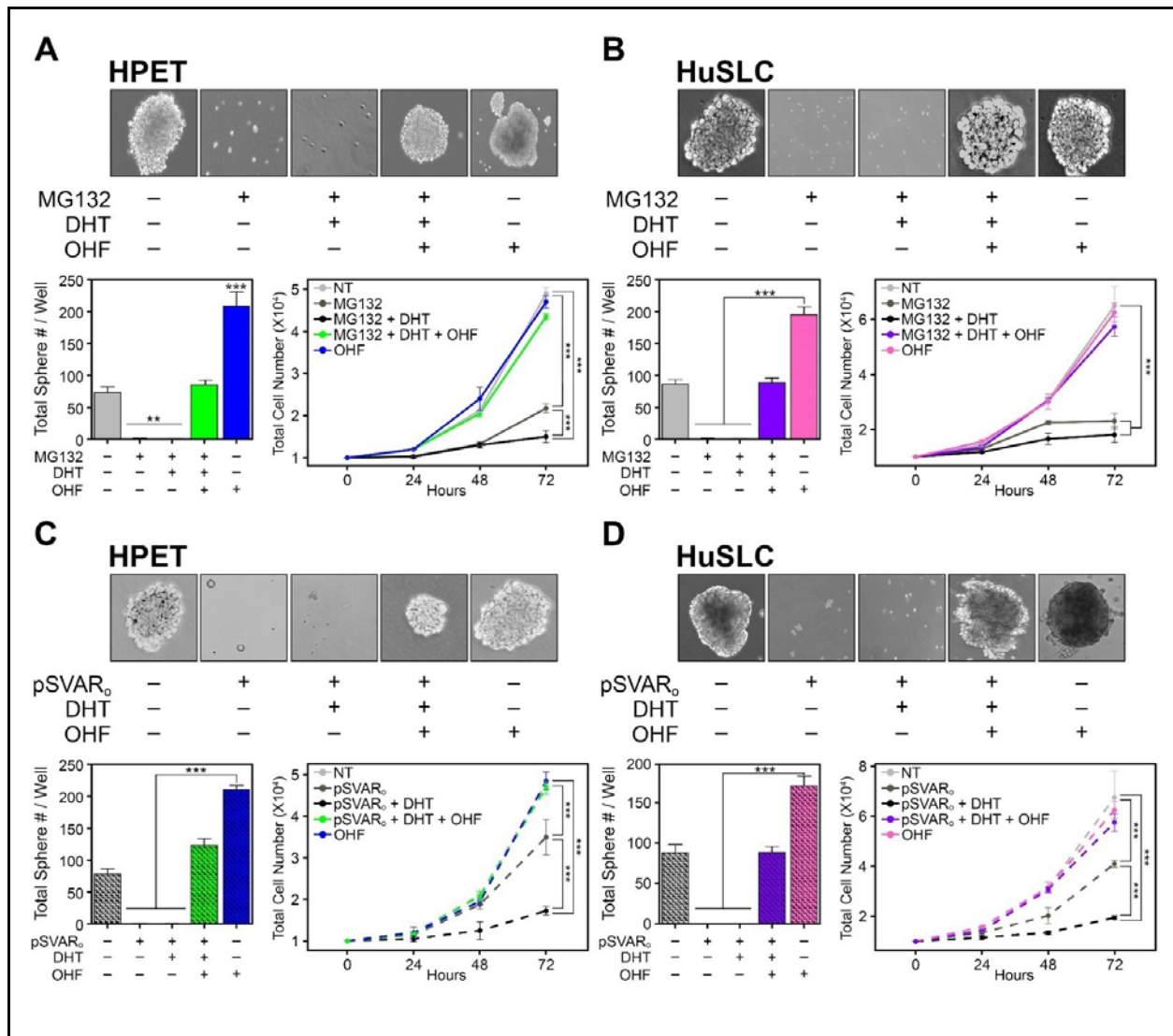


**Figure 3. Induction of AR protein down-regulates sphere formation and cell proliferation.**

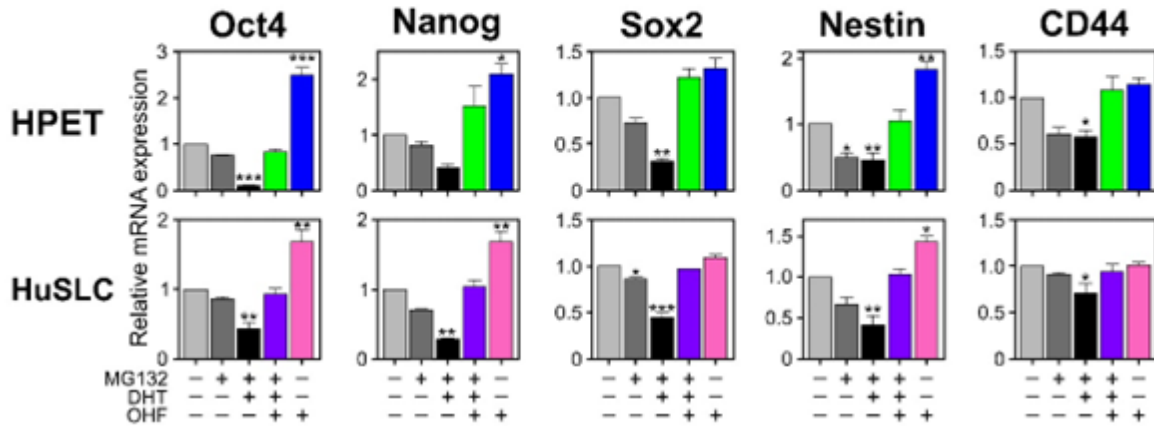
(A) Top panel, sphere formation assay (2). HPET cells were treated with 2  $\mu$ M MG132 to induce endogenous AR and  $10^{-8}$ M DHT with/w without  $10^{-5}$ M OHF to increase or inhibit AR activity respectively. Vehicle control, 95% ethanol. Phase contrast images, 20x. Bottom left panel, quantification of the number of spheres/well. Bottom right panel, proliferation assay (19). HPET cells were treated as described in the top panel and total cell numbers/well were determined using the Trypan Blue Viability assay. AR expression inhibited sphere formation and cell proliferation which could be rescued by treatment with OHF. (B). Assays in HuSLCs were performed as described in (A) with HuSLCs being treated with 20  $\mu$ M MG132 to induce endogenous AR. (C) Assays in HPET cells were performed as described in (A) with the modification that AR was exogenously expressed following transfection with 30  $\mu$ g pSVAR<sub>0</sub> plasmid. (D) Assay in HuSLCs cells were performed as described in (A) following transfection with 40  $\mu$ g pSVAR<sub>0</sub> plasmid. Data are expressed as mean  $\pm$  SEM;  $n = 4$ . \*\*,  $p < 0.001$ ; \*\*\*,  $p < 0.0001$ .

Collectively, these observations infer that an AR(-) phenotype is essential for prostate CSC self-renewal and proliferation. Moreover, treatment with OHF alone is sufficient to significantly promote sphere formation. Therefore, absence of AR protein and the potential of antiandrogens to exert as yet undiscovered AR-independent effects on stimulating prostate CSC self-renewal and proliferation could facilitate the emergence of therapeutic resistance.

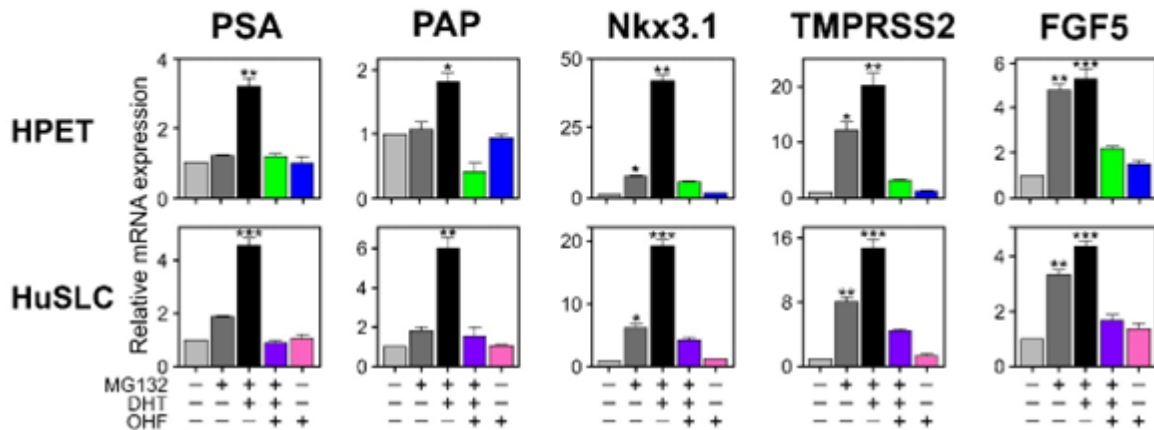
#### **4.4.d. Induction of AR down-regulates stem/progenitor characteristics and promotes luminal epithelial cell fate**

HPET and HuSLCs express numerous stem/progenitor cell markers, including the transcription factors Oct-4, Nanog, and Sox2 which regulate pluripotency and self-renewal in human and mouse embryonic stem cells [2]. They also express the progenitor cell markers Nestin and CD44 (2). To determine whether AR restricted their expression, cells were treated with MG132. As seen in Figure 4A, induction of endogenous AR decreased Oct-4, Nanog, Sox2, Nestin, and CD44 expression following DHT treatment ( $p < 0.05$ ). In contrast, inhibition of AR signaling by OHF restored their expression. Transfection of HPET and HuSLCs with pSVARo confirmed these observations (Figure 5A). Moreover, in both MG132-treated and pSVARo-transfected cells, OHF alone could up-regulate these factors with Oct4, Nanog, and Nestin increasing  $>2$ -fold ( $p < 0.05$ ) as compared to the vehicle control group, suggesting that antiandrogens might exert, as yet, unknown AR-independent activities that support CSC expansion.

### A. Expression of stem cell factors



### B. Expression of prostate luminal epithelial cell factors



### C. Expression of prostate basal and neuroendocrine factors

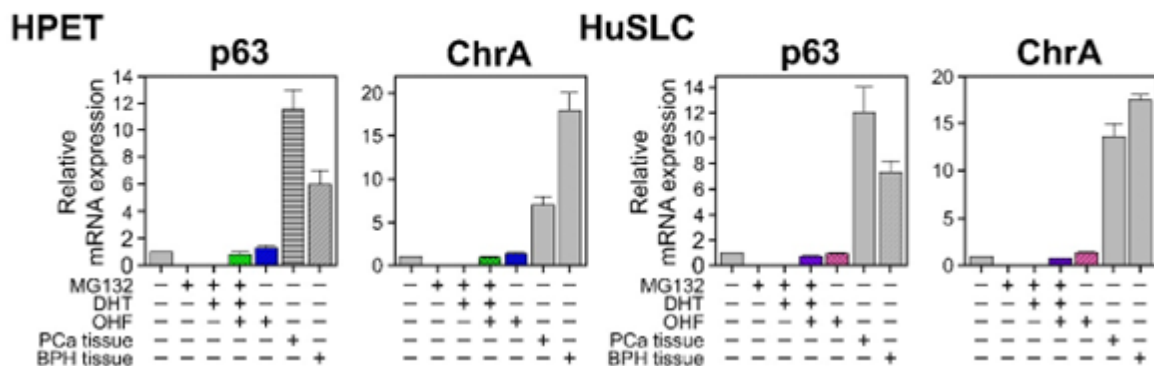
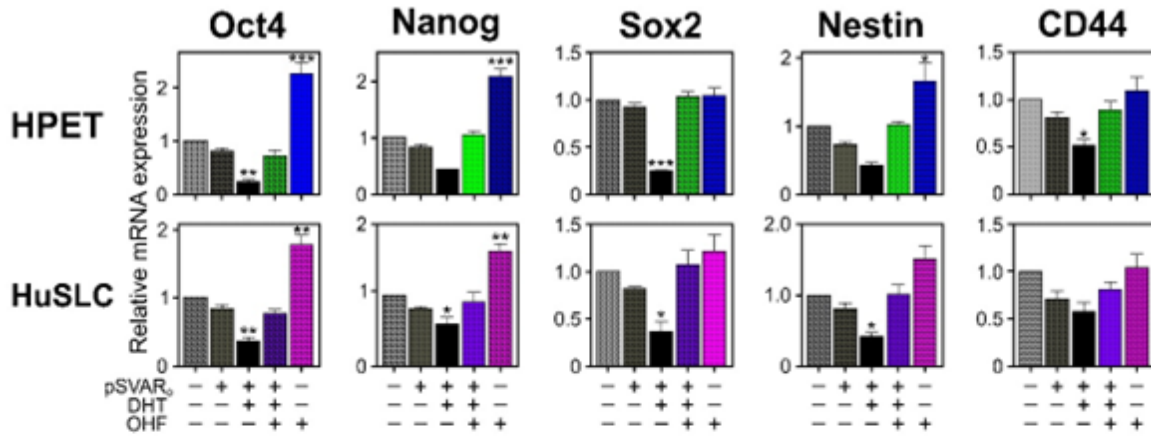


**Figure 4. MG132 treatment down-regulates expression of stem cell-associated markers and promotes luminal epithelial cell fate.**

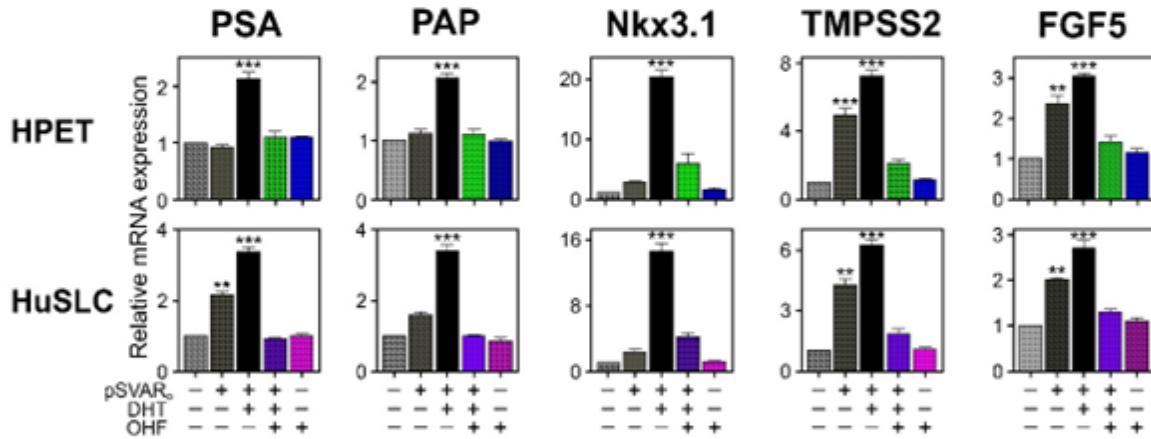
(A) HPET cells and HuSLCs were treated with 2  $\mu$ M and 20  $\mu$ M MG132 respectively and expression of the stem cell factors Oct4, Nanog, Sox2, Nestin and CD44 were determined by RT-qPCR. (B) Cells were treated with 2  $\mu$ M and 20  $\mu$ M MG132 respectively and expression of prostate luminal epithelial

cells factors PSA, PAP, Nkx3.1, TMPRSS2 and FGF5 were determined by RT-qPCR. (C) Cells were treated with 2  $\mu$ M and 20  $\mu$ M MG132 respectively and expression of p63 and ChrA were determined by RT-qPCR. Primer sets to characterize expression of all of these factors are listed in Supplementary Table S3. Data are expressed as mean  $\pm$  SEM;  $n = 4$ . \*,  $p < 0.01$ ; \*\*,  $p < 0.001$ ; \*\*\*,  $p < 0.0001$ .

### A. Expression of stem cell factors



### B. Expression of prostate luminal epithelial cell factors



### C. Expression of prostate basal and neuroendocrine factors

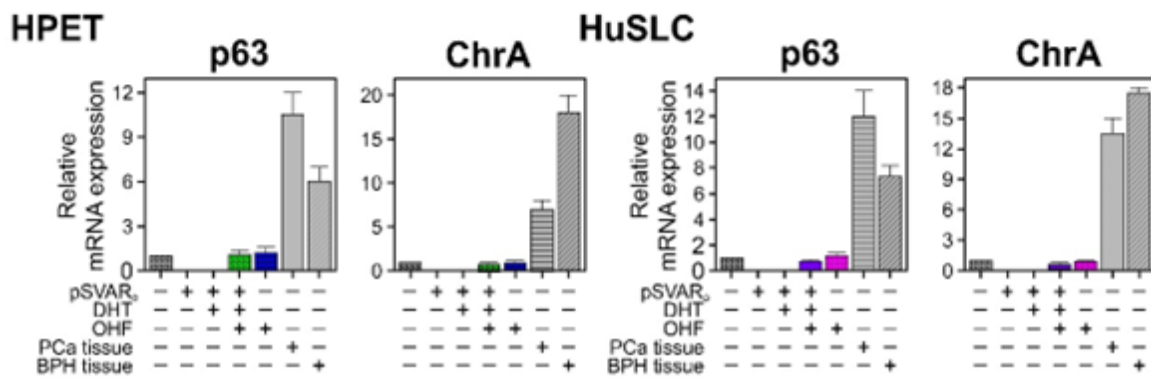


**Figure 5. Induction of exogenous AR down-regulates expression of stem cell-associated markers and promotes luminal epithelial cell fate.**

(A) HPET cells and HuSLCs were transfected with 30  $\mu$ g and 40  $\mu$ g of pSVAR<sub>0</sub> respectively and treated without/with DHT without/with OHF as indicated. Expression of the stem cell factors Oct4, Nanog,

Sox2, Nestin and CD44 were determined by RT-qPCR. **(B)** Cells were transfected and treated as in (A) and expression of prostate luminal epithelial cells factors PSA, PAP, Nkx3.1, TMPRSS2 and FGF5 were determined by RT-qPCR. **(C)** Cells were transfected and treated as in (A) and expression of p63 and ChrA were determined by RT-qPCR. Primer sets to characterize expression of all of these factors are listed in Supplementary Table S3. Data are expressed as mean  $\pm$  SEM; n=4. \*, p<0.01; \*\*, p<0.001; \*\*\*, p<0.0001.

These observations provide evidence that CSC-like cells lose stemness characteristics upon expression of AR. Since prostatic glandular epithelium consists of luminal secretory, basal, and neuroendocrine epithelial cells [2], we questioned whether loss of these factors would initiate epithelial cell specification. Indeed, androgen-regulated genes associated with luminal epithelial cell fate, including PSA and PAP (p<0.001) and Nkx3.1, TMPRSS2, and FGF5 (p<0.05) were induced upon activation of endogenous AR (Figure 4B) or pSVARo (Figure 5B) following treatment with DHT. Furthermore, expression of these luminal cell markers was inhibited by treatment with OHF. Similarly, the AR target genes HES1 and HEY1 were also induced following induction of AR expression (Supplementary Figure S5). In contrast, neither endogenous AR (Figure 4C) nor pSVARo (Figure 5C) induced expression of p63, a common basal epithelial cell marker, or Chromogranin A, typically expressed by prostate neuroendocrine cells, under any condition tested. Thus, AR appears to selectively promote luminal secretory cell fate.

#### **4.4.e. Poly-ubiquitination regulates the dynamic turnover of AR protein**

Several studies report that the UPS modulates transcription factor levels to regulate stem cell and CSC maintenance and differentiation [28-30]. To determine whether poly-ubiquitination regulates AR protein levels, HPET cells were transfected with 30  $\mu$ g pSVARo and increasing concentrations of the wild-type ubiquitin expression vector pRK5-HA-Ubiquitin-WT (HA-UbWt; Figure 6Ai). Exogenous AR was degraded in a dose-dependent manner with complete degradation occurring at 50  $\mu$ g HA-UbWt. In a similar manner, 20  $\mu$ g HA-UbWt was capable of degrading endogenous AR

protein induced with MG132 treatment (Figure 6Aii). Cells were then transfected with a mutant ubiquitin plasmid pRK5-HA-Ubiquitin-KO (HA-UbKO) that is incapable of adding ubiquitin molecules onto its target protein to determine if inhibition of AR poly-ubiquitination prevented AR degradation. Endogenous AR protein was strongly expressed following transfection with HA-UbKO (Figure 6Aiii). Collectively, these observations imply that the dynamic turnover of AR protein in prostate CSC-like cells is regulated by poly-ubiquitination.

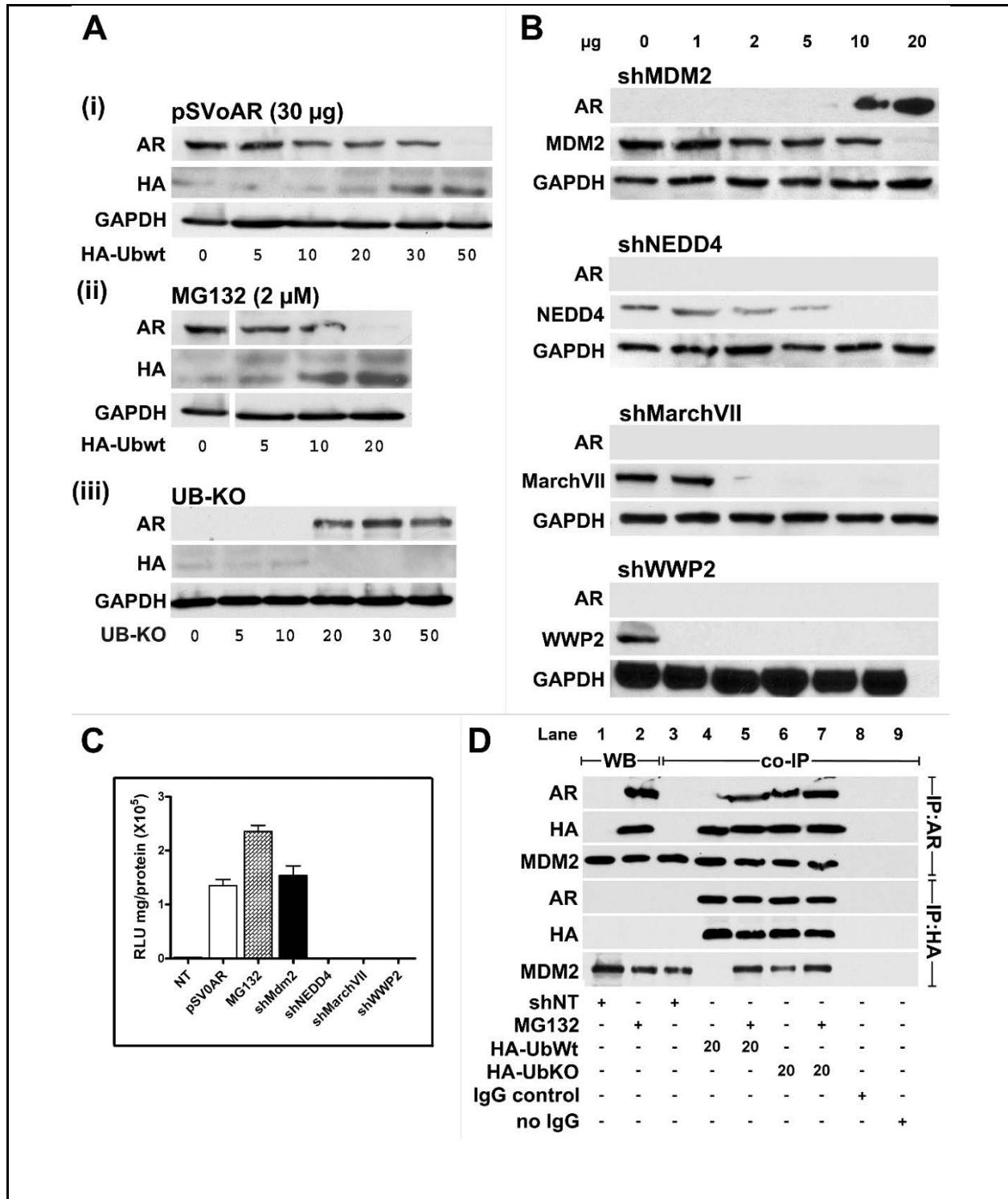


**Figure 6. The E3 ligase MDM2 selectively degrades AR in prostate CSCs.**

(A) HPET cells were transfected with either 30  $\mu$ g pSVAR<sub>o</sub> (i) or treated with 2  $\mu$ M MG132 (ii) and transfected with increasing concentrations of the wild-type ubiquitin expression vector pRK5-HA-Ubiquitin-WT (HA-UbWt) to determine whether poly-ubiquitination regulated AR protein levels. In addition, HPET cells were transfected with increasing concentrations of a mutant ubiquitin plasmid

pRK5-HA-Ubiquitin-KO (HA-UbKO, iii) which is incapable of adding ubiquitin molecules onto its target protein, to demonstrate that inhibiting AR poly-ubiquitination would prevent AR degradation. **(B)** HPET cells were transfected with increasing concentrations of shMDM2, shNEDD4, shMarchVII or shWWP2 plasmid and protein expression was analyzed by Western blot analysis. **(C)** Cells were co-transfected with 20  $\mu$ g of shMDM2, 10  $\mu$ g of shNEDD4, 2  $\mu$ g of shMarchVII or 1  $\mu$ g of shWWP2 plasmid and the ARR<sub>2</sub>PB-*luc* and *Renilla* luciferase reporter gene constructs. Luciferase activity was determined. Positive controls, cells transfected with 30  $\mu$ g pSVAR<sub>o</sub> or treated with 2  $\mu$ M MG132. NT, non-targeting shRNA control. **(D)** IP analysis was performed to determine whether MDM2 directly binds to AR. Cells were transfected with 20  $\mu$ g non-targeting shNT control plasmid, 20  $\mu$ g HA-UbWt, or 20  $\mu$ g HA-UbKO and treated with 2  $\mu$ M MG132 as indicated. Antibodies for Western blot analysis are listed in Supplementary Table S1. Data are expressed as mean  $\pm$  SEM; n=4.

#### 4.4.f. MDM2 E3 ligase selectively degrades AR in prostate CSCs

The final step in the ubiquitination cascade is carried out by E3 ligases [31]. Several E3 ligases, including MDM2 and NEDD4, are reported to regulate AR and/or AR-V protein levels in non-CSC, AR(+) PCa cells which comprise the bulk of prostate tumor cells and in AR(+) PCa cell lines derived from metastatic lesions. Whether MDM2 and/or NEDD4 degrade AR in prostate CSCs is unknown. Therefore, HPET cells were transfected with pSVAR<sub>o</sub> and increasing concentrations of shMDM2 plasmid to determine the level of MDM2 knock-down and whether AR protein would be induced. As shown in **Figure 6B**, MDM2 levels decreased in parallel with increasing concentrations of shMDM2; and AR expression was greatest when MDM2 protein was barely detectable. AR-mediated transcription was confirmed using the ARR<sub>2</sub>PB-*luc* assay (**Figure 6C**). In contrast, NEDD4 knockdown to undetectable levels did not induce AR protein, implying that it did not play a role in modulating AR levels in CSC-like cells.

Other E3 ligases not currently known to regulate AR protein include MarchVII, associated with adult stem cells [32], and WWP2, reported to regulate embryonic stem cell factors, e.g., Oct4 [33] and Sox2 [34]. Transfecting HPET cells with shMarchVII and shWWP2 in a dose-dependent manner determined that loss of MarchVII and WWP2 expression did not induce AR protein

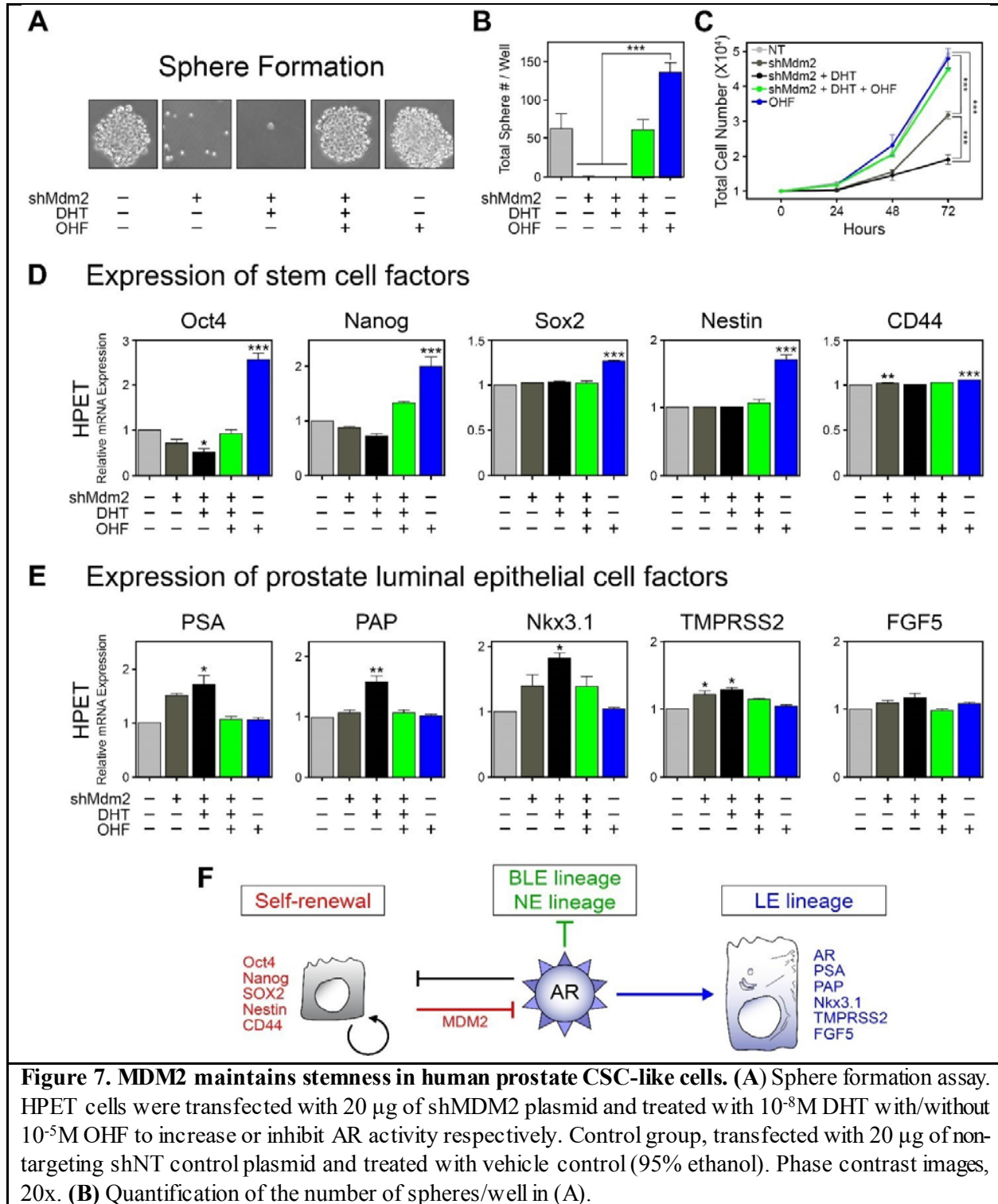
expression under any concentrations of shRNA tested (**Figure 6B**). Thus, MDM2 appears to selectively degrade AR in CSCs.

Immunoprecipitation (IP) analysis was performed to determine whether MDM2 directly binds AR (**Figure 6D**). When AR(-) HPET cells were transfected with HA-UbWt alone (lane 4), AR was not observed in the IP:AR fraction and MDM2 was absent in the IP:HA fraction, suggesting that AR expression was required for the formation of an AR/HA-UbWt/MDM2 binding complex. Once endogenous AR was expressed following MG132 treatment, both AR and MDM2 were observed following IP (lane 5), indicating that AR was necessary for AR/HA-UbWt/MDM2 complex formation. Similarly, an AR/HA-UbWt/MDM2 complex was observed in cells where expression of mutant HA-UbKO inhibited the degradation of endogenous AR (lane 6), confirming that AR could form a complex with ubiquitin and MDM2.

#### **4.4.g. MDM2 knockdown inhibits CSC self-renewal and cell proliferation and promotes luminal epithelial cell differentiation**

To determine the effects of MDM2 knockdown on CSC stemness, HPET cells were transfected with shMDM2 to prevent AR degradation. Knockdown of MDM2 alone was sufficient to abolish sphere formation and treatment with DHT did not alter these effects (**Figure 7A, 7B**). Again, sphere formation was rescued by addition of OHF. In addition, MDM2 knockdown alone decreased cell proliferation ( $p < 0.05$ ), addition of DHT inhibited cell proliferation even further, and proliferation was rescued with OHF treatment (**Figure 7C**). Furthermore, MDM2 knockdown decreased Oct-4 and potentially Nanog expression, and treatment with OHF alone increased their expression significantly (**Figure 7D**). In parallel, expression of luminal epithelial cell-specific genes, PSA, PAP, Nkx3.1, and TMPRSS2, increased with DHT treatment and decreased to basal

levels with addition of OHF, while FGF5 expression was regulated in a similar manner, it did not reach statistical significance (**Figure 7E**).



**(C)** Proliferation assay (19). HPET cells were transfected with 20  $\mu\text{g}$  of shMDM2 plasmid and treated with  $10^{-8}\text{M}$  DHT with/without  $10^{-5}\text{M}$  OHF treated as indicated. Total cell numbers/well were determined using the Trypan Blue Viability assay. **(D)** HPET cells were transfected with 20  $\mu\text{g}$  of shMDM2 and expression of the stem cell factors were determined by RT-qPCR. **(E)** HPET cells were transfected with 20  $\mu\text{g}$  of shMDM2 and expression of prostate luminal epithelial cells factors were determined by RT-qPCR. Data are expressed as mean  $\pm$  SEM;  $n = 4$ . **(F)** Schematic representation of MDM2-mediated regulation of AR expression in modulating self-renewal and epithelial cell specification. Details are provided in the main text.

These observations primarily recapitulated those observed in HPET and HuSLCs expressing AR following treatment with MG132 or transfection with pSVAR<sub>o</sub>. However, one difference was that not all of the stem cell factors decreased in response to DHT treatment (**Figure 7D**), suggesting that MDM2 may exert specificity in maintaining the steady-state expression of select stem/progenitor cell proteins. Whether MDM2-mediated degradation of AR involves p53 is unclear. HPET cells do not express p53 while HuSLCs express p53, suggesting that p53 activity is not essential for degrading AR (**Supplementary Figure S6**).

## 4.5 Discussion

Mechanisms that prevent AR expression in normal prostate stem cells and prostate CSCs remain largely unknown. Our study provides the first evidence that in stem-like AR(-) CSCs isolated from PCa biopsies, MDM2 promotes the constant degradation of AR protein, thereby maintaining prostate CSC pluripotency and inhibiting epithelial cell lineage specification (summarized in Figure 7F). The AR(-) signature also facilitates CSC proliferation and expansion, while induction of AR via MDM2 down-regulation selectively induces a luminal epithelial cell phenotype and loss of cell growth.

Most studies on prostate CSCs and AR have been performed in side-fractions of CSC-like cells isolated from LNCaP, LNCaP derivative, and LAPC9 cell lines [35,36]. Both AR mRNA and AR protein are down-regulated in LNCaP and LAPC9-derived PSA-/lo cells [6]. In the CAstration-Resistant Nkx3.1-expressing cells (CARNs) mouse model, CARNs expressed AR; however genetic deletion of AR did not alter their luminal progenitor/stem cell properties [37]. Only the rate of proliferation during prostate regeneration was reduced [37]. Taken together, these observations imply that AR is not required for prostate CSC or normal prostate progenitor/stem cell function.

Our study supports the role of MDM2 in blocking AR protein expression and proposes that MDM2 exerts fundamentally different functions in AR(-) prostate CSCs as compared to non-CSC, AR(+) PCa cells which comprise the bulk of prostate tumor cells (summarized in Supplementary Table S4). In AR(-) prostate CSCs, MDM2 continuously degrades AR to maintain an AR(-) phenotype, self-renewal, and proliferative potential. MDM2 is also reported to promote stemness properties in other tissue-derived stem cells, e.g., in generating induced pluripotent stem cells from

p53-deficient murine embryonic fibroblasts (MEFs) [38] and suppressing differentiation of human mesenchymal stem cells into osteoblasts; whereas MDM2 knockdown increases osteoblast differentiation [38]. In a similar manner, MDM2 knockdown in HPET and HuSLCs induced terminal differentiation to a luminal epithelial phenotype. However in non-CSC AR(+) PCa cells, it is well-documented that MDM2 temporally modulates AR protein levels to attenuate AR-mediated transcription during normal cellular function and to regulate cell cycle progression while retaining basal levels of AR expression [7]. Inhibition of MDM2 expression in LNCaP and androgen-resistant LNCaP (LNCaP-Res) cell lines down-regulates AR protein levels and decreases AR activity, however total AR expression is not lost during this process [39]. Thus, the mechanism regulating MDM2-mediated knockdown of HPET and HuSLC AR protein to undetectable levels remains to be elucidated.

Therapeutic resistance remains a persistent challenge in the treatment of PCa. Consequently, targeting the AR and androgens is still central to the management of advanced PCa (reviewed in [40]). The recent discovery that PCa cells synthesize steroids de novo has resulted in considerable interest in drugs that inhibit androgen synthesis [41]. Regrettably, since CSCs do not appear to require AR, none of the second-generation ADT and antagonist drugs, e.g., abiraterone and enzalutamide, would theoretically eliminate CSCs from the PCa cell pool. Moreover, our study suggests that antiandrogen treatment alone paradoxically increases CSC self-renewal and cell proliferation. If indeed induction of AR expression causes CSC differentiation into AR(+) luminal cells, then this could potentially re-sensitize CSCs to ADT and eliminate them along with the bulk of responsive AR(+) PCa cells. Induction of AR could also promote terminal differentiation and eliminate CSCs through this mechanism.

The emergence of therapeutic resistance is also attributed to production of AR-Vs (11,12,42). AR-Vs are expressed in clinical PCa biopsy specimens and PCa cell lines [13,26] and their expression is upregulated in metastatic and treatment-resistant disease [11,42]. One of the most commonly expressed variants is AR-V7. It is considered a valid therapeutic target in the treatment of CRPC; however the mechanisms by which AR-V7 drives CRPC progression remains to be elucidated [43]. Our study observed that biopsy-derived CSCs only expressed AR-fl, but not AR-V, in response to blocking MDM2 activity. Further studies are required to determine a putative role of AR-Vs in prostate CSCs. In addition, HPET cells do not express p53 while HuSLCs express p53, yet AR is continuously degraded and self-renewal and proliferation are maintained in both CSC-like cell lines, suggesting that p53 activity is not essential for these processes. Thus, therapeutic approaches that target MDM2-p53 interactions would likely be ineffective in inhibiting prostate CSC growth. Other reported p53-independent MDM2 activities include the promotion of cancer progression through EMT in AR(-) DU-145 cells which express a mutant/non-functional p53 [44], and clonogenic survival in MCF7, SJSA, and Panc1 cell lines (38). This is in contrast to AR(+)p53(+) cells where targeting MDM2/p53 interactions inhibit tumor cell growth. The small molecule inhibitor MI-219 selectively disrupts MDM2/p53 interactions, thereby activating p53 signaling and inducing apoptosis in LNCaP cells in vitro and inhibiting LNCaP xenograft growth in vivo [45]. Similarly, the MDM2 inhibitor Nutlin-3 activates p53 and inhibits the growth of SJSA-1 osteosarcoma xenografts by 90% [46]. In CRPC, lncRNA (AR-repressed long noncoding RNA) is up-regulated and binds AR protein to impair AR-MDM2 interactions. Consequently, AR is not ubiquitinated and degraded, resulting in the upregulation of AR transcriptional activity and increased CRPC cell growth [47].

Collectively, these studies infer that selectively targeting MDM2 activity, and not MDM2-p53 or AR-p53 interactions, could potentially eliminate CSCs more effectively than second generation ADT or antagonist drugs. Our study suggests that MDM2 conserves the AR(-) CSC signature and that this may be a critical step towards stimulating CSC expansion during the emergence of therapeutic resistance. Furthermore, treatments that promote antiandrogenic activities may signal CSCs to initiate proliferation and expansion [48]. Thus, selectively blocking MDM2 expression and/or MDM2-mediated activity in combination with AR/androgen-targeted treatments may offer a novel strategy for eliminating AR(-) CSCs and the bulk of AR(+) PCa cells to decrease tumor burden and metastasis, and/or inhibit the emergence of therapeutic resistant disease.

# Supplemental Tables

**Title: MDM2 Conserves Prostate Cancer Stem Cell Integrity through Constant Degradation of the Androgen Receptor**

**Authors: Premkumar Vummidi Giridhar *et al.***

**Corresponding Author: Susan Kasper**

## SUPPLEMENTARY TABLES

Supplementary information includes 4 tables.

### Supplementary Table S1. Primary antibody list (related to figures 1-5)

Antibody	Company	Product Code	IgG species	Conjugate	Dilution
AR (N20)	Santa Cruz	sc-816	IgG	none	1:200 (WB) 10 µg (IP)
GAPDH	Cell Signaling	2118	IgG	none	1:1000
HA	Santa Cruz	Sc-805	IgG	none	1:200 (WB) 5 µg (IP)
IgG	Cell Signaling	7074	Rabbit	HRP	1:5000 (WB)
MarchVII	Sigma	SAB2101435	Rabbit	none	1:1000 (WB)
MDM2	Genscript	Ab166	IgG	none	1:500 (WB)
NEDD4	Cell Signaling	3607	Rabbit	none	1:1000 (WB)
WWP2	Abcam	86544	Rabbit	none	1:1000 (WB)

**Supplementary Table S2. Primer sets used to characterize AR-V expression.**

<b>Primer Sets</b>	<b>Reverse Primer</b>	<b>Amplified Transcript Size (bp)</b>
<b>P1F/P1R</b>	Forward 5'- TGT CAC TAT GGA GCT CTC ACA TGT GG-3' Reverse 5'- CAC CTC TCA AAT ATGCTA GAC GAA TCT GT-3'	AR-V1: 842 AR-V2: 959 AR-V3: 1126 AR-V4: 1243
<b>P1F/P2R</b>	Forward 5'- TGT CAC TAT GGA GCT CTC ACA TGT GG-3' Reverse 5'- GTA CTC ATT CAA GTA TCA GAT ATG CCG TAT CAT-3'	AR-V5: 888 AR-V6: 968
<b>P1F/P3R</b>	Forward 5'- TGT CAC TAT GGA GCT CTC ACA TGT GG-3' Reverse 5'- CTG TGG ATCAGC TACTACCTT 5'- CAG CTC-3'	AR-V7: 834
<b>GAPDH</b>	Forward 5'- GAT CAT CAG CAA TGC CTC CT -3' Reverse 5'- TGT GGT CAT GAG TCC TTC CA -3'	NM_002046:97

\* Reference for AR-V primers: Hu R, et al., 2009. Ligand-independent Androgen Receptor Variants Derived from Splicing of Cryptic Exons Signify Hormone Refractory Prostate Cancer, Figure 1. Cancer Res. 69:16-22.

**Supplementary Table S3. Primers to characterize epithelial and stem cell marker expression.**

<b>Gene</b>	<b>Accession Number</b>	<b>Primer Sequence</b>
<b>PSA</b>	NM001648	Forward 5'- GTG CTT GTG GCC TCT CGT -3' Reverse 5'- AGC AAGATCACG CTT TTG TTC -3'
<b>PAP</b>	NM_001099.4	Forward 5'- AACCTC TTT GTG TCC CTT GGT CCT -3' Reverse 5'- ACG TGG TGC TCT CTT TCC TGA TGT -3'
<b>NKX3.1</b>	NM006167	Forward 5'- TTC TGC AACTCC ATCCTC CTG TGT -3' Reverse 5'- TGG TGA CAT CCT CAT CCT GGT TGT -3'
<b>TMPRSS2</b>	NM001135099	Forward 5'- TGC CAA AGC TTA CAG ACC AGG AGT -3' Reverse 5'- AACGAC GTC AAG GAC GAA GAC CAT -3'
<b>AR</b>	NM000044.4	Forward 5'- GCC CAG TGT CAA GTT GTG CTT GTT -3' Reverse 5'- AGC TCT CTA AACTTC CCG TGG CAT -3'
<b>Oct4</b>	NM002701	Forward 5'- ATG CAT TCA AACTGA GGT GCC TGC -3' Reverse 5'- AACTTC ACC TTC CCT CCA ACC AGT -3'
<b>Nanog</b>	NM024865	Forward 5'- CCC AAA GGC AAA CAA CCC ACT TCT -3' Reverse 5'- AGC TGG GTG GAA GAG AAC ACA GTT -3'
<b>Nestin</b>	NM006617	Forward 5'- TGG CAA AGG AGC CTA CTC CAA GAA -3' Reverse 5'- ATCGGG ATT CAGCTG ACT TAG CCT -3'
<b>SOX2</b>	NM003106	Forward 5'- CAC ATGAAGGAG CAC CCG GAT TAT -3' Reverse 5'- GTT CAT GTG CGC GTA ACT GTC CAT -3'
<b>CD133</b>	NM006017	Forward 5'- TACCAA GGA CAA GGC GTT CACAGA -3' Reverse 5'- GTG CAA GCT CTT CAA GGT GCT GTT -3'
<b>GAPDH</b>	Fermentas	Forward 5'- CAA GGT CAT CCA TGA CAA CTT TG -3' Reverse 5'- GTC CAC CAC CCT GTT GCT GTA G -3'
<b>p63</b>	NM001114978	Forward 5'- TTC GGA CAG TAC AAA GAA CGG -3' Reverse 5'- GCA TTT CAT AAGTCT CAC GGC -3'
<b>ChrA</b>	NM001275	Forward 5'- ATG TTT TGA GAC ACT CCG AGG -3' Reverse 5'- GAG TTC ATCTTC AAA ACCGCT G -3'
<b>p53</b>	NM000546	Forward 5'- GCC ATCTACAAGCAGTCA CAG -3' Reverse 5'- TCA TCC AAA TACTCCACA CGC -3'

**Supplementary Table S4. Summary comparing CSC-like AR(-) HPET and HuSLCs with a standard PCa cell line, AR(+) LNCaP cells.**

	<b>HPET and HuSLC</b>	<b>LNCaP</b>
AR status	- AR(-) - required for cell proliferation	- AR(+) (1) - required for cell proliferation (1)
Characteristics	stem-like	representative of the bulk of AR(+) PCa cells (2,3)
Culture conditions	- defined embryonic stem cell medium - no animal products	RPMI 1640 medium with 10% FBS (4)
Primary function of AR	- luminal cell specification - does not induce basal or neuroendocrine cell fate	transcription (1)
Androgens	not responsive	promotes cell growth (1)
Androgen deprivation	promotes growth	inhibits growth (1)
Xenografts <i>in vivo</i>	- forms prostatic tumors that show glandular structures# (5,6) - can be graded by Gleason Score (5) - glands contains AR(+) luminal cells, and AR(-) basal and neuroendocrine cells (5,6)	- forms solid AR(+) tumors (7) - no glandular structures (7)
MDM2 levels	high	low
MDM2 function	- continuously degrades total AR protein - maintains undetectable AR protein levels - appears p53-independent	- temporally modulates AR levels during transcription (8) - cells continue to express baseline AR protein levels throughout this process (9) - p53-dependent (10)
p53	- not expressed in HPET - expressed in HuSLC	expressed (10)

# HPE cells in (6) were subsequently renamed to “HuSLC” upon confirmation of cell line establishment.

Non-referenced information is based on data generated in this manuscript.

### Supplementary References for Table S4

1. Horoszewicz JS, Leong SS, Kawinski E, Karr JP, Rosenthal H, Chu TM, *et al.* LNCaP model of human prostatic carcinoma. *Cancer Res* **1983**;43:1809-18
2. Sobel RE, Sadar MD. Cell lines used in prostate cancer research: a compendium of old and new lines--part 1. *J Urol* **2005**;173:342-59
3. Sobel RE, Sadar MD. Cell lines used in prostate cancer research: a compendium of old and new lines--part 2. *J Urol* **2005**;173:360-72
4. Ghosh R, Gu G, Tillman E, Yuan J, Wang Y, Fazli L, *et al.* Increased expression and differential phosphorylation of stathmin may promote prostate cancer progression. *Prostate* **2007**;67:1038-52
5. Gu G, Yuan J, Wills M, Kasper S. Prostate cancer cells with stem cell characteristics reconstitute the original human tumor in vivo. *Cancer Res* **2007**;67:4807-15
6. Williams K, Ghosh R, Vummidi Giridhar P, Gu G, Case T, SM B, *et al.* Inhibition of Stathmin1 Accelerates the Metastatic Process *Cancer Res* **2012**;72:5407-17
7. Jin RJ, Wang Y, Masumori N, Ishii K, Tsukamoto T, Shappell SB, *et al.* NE-10 neuroendocrine cancer promotes the LNCaP xenograft growth in castrated mice. *Cancer Res* **2004**;64:5489-95
8. Lin HK, Wang L, Hu YC, Altuwajri S, Chang C. Phosphorylation-dependent ubiquitylation and degradation of androgen receptor by Akt require Mdm2 E3 ligase. *Embo J* **2002**;21:4037-48
9. Mu Z, Hachem P, Hensley H, Stoyanova R, Kwon HW, Hanlon AL, *et al.* Antisense MDM2 enhances the response of androgen insensitive human prostate cancer cells to androgen deprivation in vitro and in vivo. *Prostate* **2008**;68:599-609
10. Shangary S, Qin D, McEachern D, Liu M, Miller RS, Qiu S, *et al.* Temporal activation of p53 by a specific MDM2 inhibitor is selectively toxic to tumors and leads to complete tumor growth inhibition. *Proc Natl Acad Sci U S A* **2008**;105:3933-8

## **Supplemental Figures**

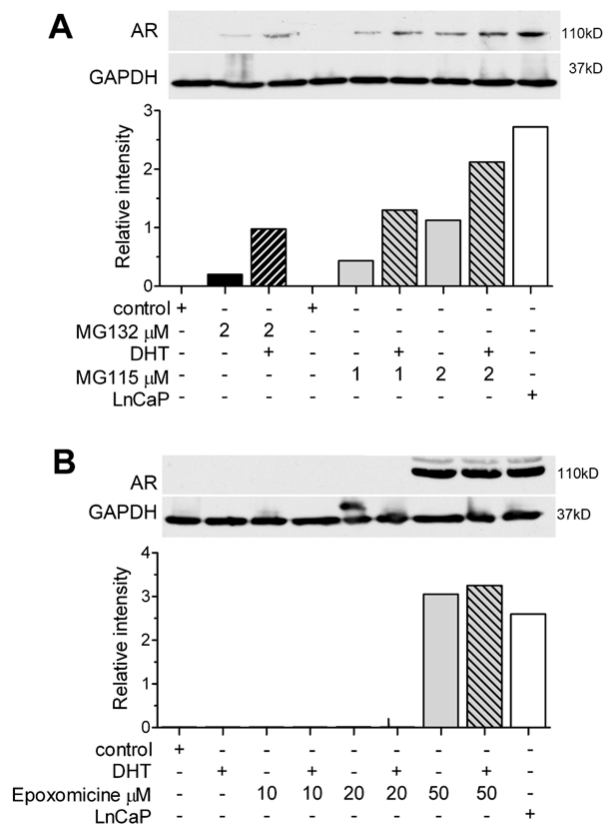
**Title: MDM2 Conserves Prostate Cancer Stem Cell Integrity through Constant Degradation of the Androgen Receptor**

**Authors: Premkumar Vummidi Giridhar *et al.***

**Corresponding Author: Susan Kasper**

### **SUPPLEMENTARY FIGURES**

Supplementary information includes 6 supplementary figures and legends.

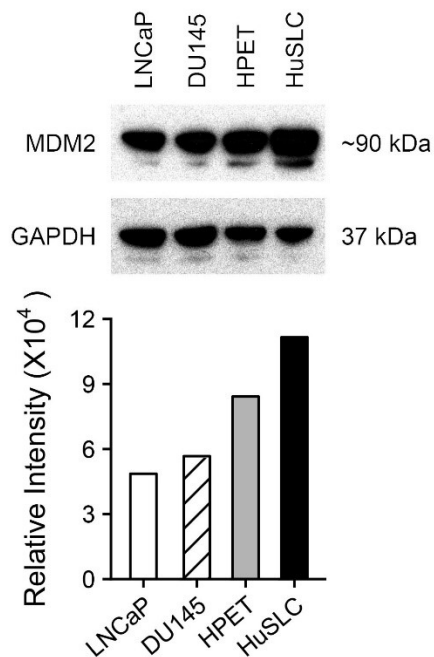


**Supplementary Figure S1. AR protein is induced following treatment with proteasomal inhibitors.**

**(A)** HPET cells were treated with MG115 (as indicated) with/without  $10^{-8}$  M DHT followed by Western blot analysis. Vehicle control, 0.1% ethanol; MG132, proteasome inhibitor control; LnCaP cell line, control for endogenous AR expression. AR protein was analyzed by Western blot analysis and semi-quantitated by densitometry.

**(B)** HPET cells were treated with Epoxomicine (as indicated) with/without  $10^{-8}$  M DHT and AR expression was analyzed as described in (A).

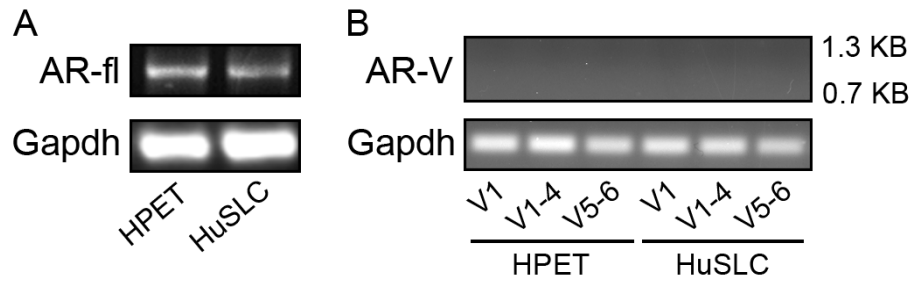
AR, androgen receptor; DHT, dihydrotestosterone,



**Supplementary Figure S2. CSC-like HuSLC and HPET cells express higher levels of the E3 ligase, MDM2, as compared to standard PCa cell lines.**

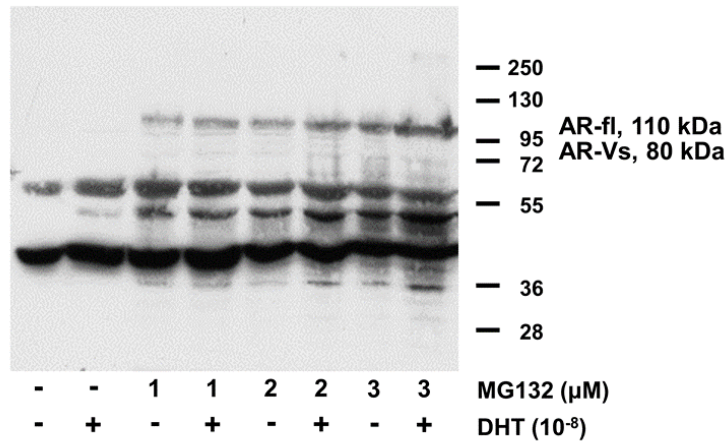
**Upper panel.** Western blot analysis to determine MDM2 levels in stem-like AR(-) HuSLC and HPET cells compared with AR(+) LNCaP and AR(-) DU-145 cells.

**Lower panel.** Densitometry analysis.

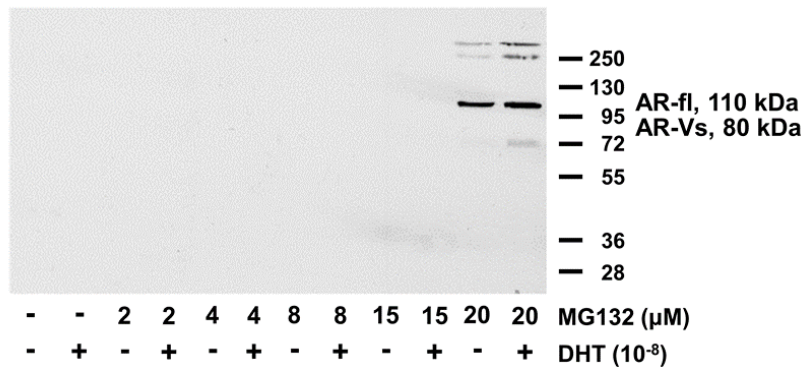


**Supplementary Figure S3. CSC-like HPET and HuSLCs express AR-fl, but not AR-Vs.** AR-V levels were analyzed using the primer sets outlined in Supplementary Table S2. Primer concentrations were 0.2  $\mu$ M per primer pair and cycling conditions (BioRad C1000 Thermal Cycler) were as follows: Stage 1: 180 seconds at 95  $^{\circ}$ C; Stage 2 (30x): 30 seconds at 95  $^{\circ}$ C, 30 seconds at 55  $^{\circ}$ C, and 60 seconds at 72  $^{\circ}$ C; and Stage 3: 300 seconds at 72  $^{\circ}$ C. AR variants and GAPDH were visualized by loading 10  $\mu$ l of the PCR reaction on a 2% agarose gel containing ethidium bromide at a concentration of 0.5  $\mu$ g/ml and approximate molecular weights were estimated using a 100 bp ladder (Promega, G695A).

**A. HPET cells**



**B. HuSLCs**

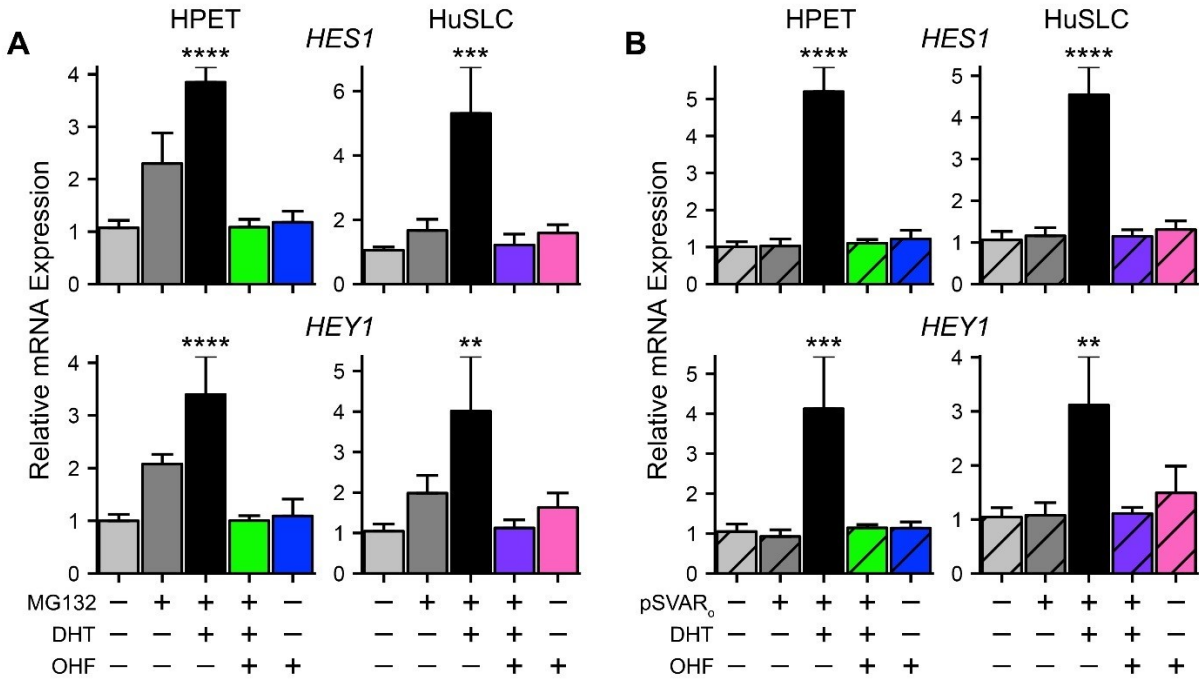


**Supplementary Figure S4. CSC-like HPET and HuSLCs express AR-fl, but not AR-Vs.**

**(A)** HPET cells were treated with increasing concentrations of MG132 (0 – 20  $\mu\text{M}$  as indicated) with/without addition of  $10^{-8}$  M DHT. Western blot analysis for AR-fl and AR-Vs was performed using anti AR (N20) antibody which binds at the N-terminal of AR and therefore recognizes both AR-fl and AR-Vs.

**(B)** HuSLCs were treated with increasing concentrations of MG132 with/without addition of  $10^{-8}$  M DHT and analyzed as in (A).

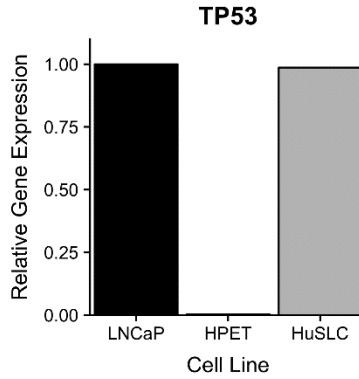
AR-fl, full-length androgen receptor; Vs, variants



**Supplementary Figure S5. Induction of AR promotes expression of AR target genes *HES1* and *HEY1*.**

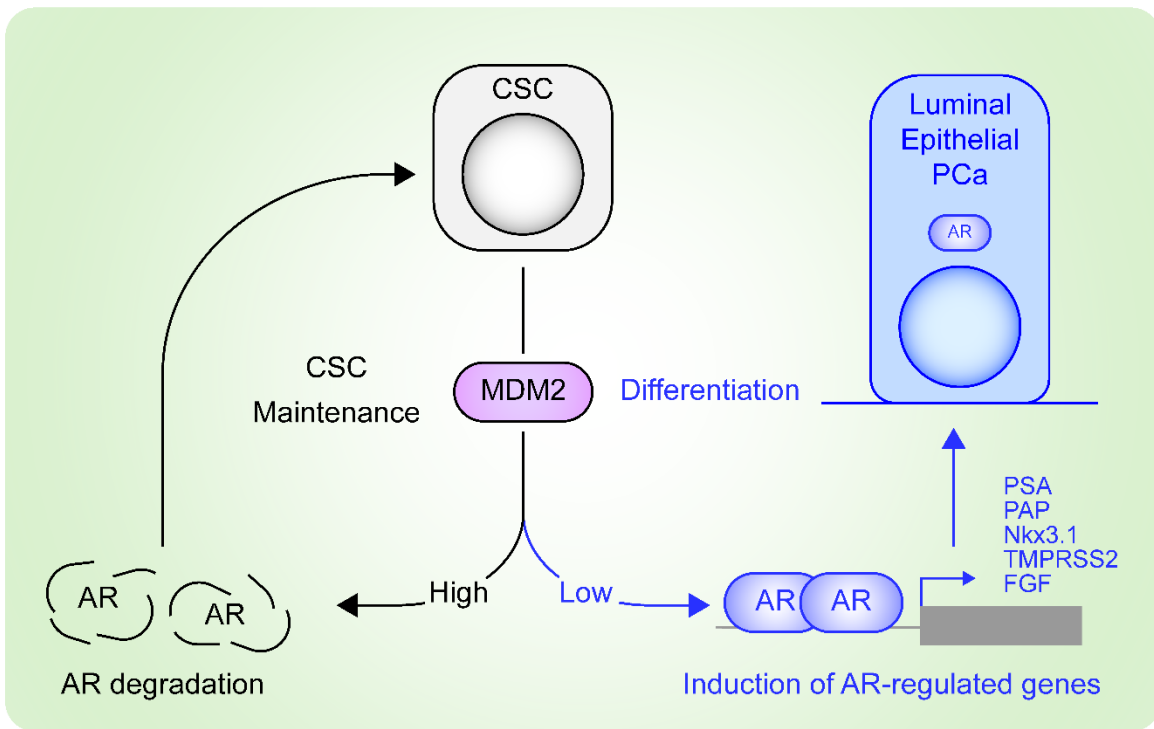
**(A)** HPET cells and HuSLCs were treated with 2  $\mu$ M and 20  $\mu$ M MG132 respectively and expression of the androgen-regulated genes *HES1* (upper panel) and *HEY1* (lower panel) were determined by RT-qPCR.

**(B)** HPET cells and HuSLCs were transfected with 30  $\mu$ g and 40  $\mu$ g of pSVAR<sub>0</sub> respectively and treated with/without 10<sup>-8</sup> M DHT with/without 10<sup>-3</sup> M OHF as indicated. Expression of *HES1* (upper panel) and *HEY1* (lower panel) were determined by RT-qPCR. Data are expressed as mean  $\pm$  SEM;  $n = 4$ . \*\*,  $p < 0.01$ ; \*\*\*,  $p < 0.001$ ; \*\*\*\*,  $p < 0.0001$ .



**Supplementary Figure S6. Expression of p53 is heterogeneous in prostate CSCs.** HPET cells do not express p53 while HuSLCs express p53 levels similar to that observed in LNCaP cells.

**Graphical Abstract**



# Chapter 5

## CRISPR/Cas9 - Advantages and Challenges

## 5.1. Abstract

Clustered Regularly Interspaced Short Palindromic Repeats (CRISPR)/Cas9 technology has provided researchers with a novel tool in genomic engineering to knock out genes via targeted nicks in the DNA sequence leading to non-homologous end joining (NHEJ) repair, however, it was hypothesized that the introduction of a double-stranded template DNA could allow for the damaged DNA to be repaired by homologous recombination (HDR). To create stable cell lines that expressed S-to-A and S-to-E substitution mutations in the four STMN1 regulatory serines, S16, S25, S38 and S63, we partnered with Invitrogen to design the guide RNAs (gRNAs) to target our sites of interest, and the double-stranded DNA templates that would be utilized in HDR to create our mutant cell lines. Regrettably, the strategy did not successfully generate stable cell lines expressing the mutant STMN1 proteins. Possible limitations in the execution included: 1) The technology to generate substitution mutations was in its infancy, and therefore the experimental strategy was not fully developed at the time. 2) Although it was discussed extensively, incorporating a tag or reporter gene was very difficult, and was therefore not included. A reporter would have helped identify cells that had been successfully mutated. CRISPR/Cas9 technology has improved considerably and generating substitution mutations can now be made with a much higher rate of efficiency.

## 5.2. Introduction

CRISPR technology is a bacterial defense strategy that was originally discovered and characterized by Francisco Mojica between 1999-2005 [1]. A series of repeats in bacteria align with specific viral DNA sequences, and when this specific virus invades a bacterium, the bacterium produces RNA that recognizes and binds to the viral DNA to break it down before it can destroy the bacterium. In addition to CRISPR, the Cas9 enzyme was discovered to be critically important in the destruction of foreign DNA by causing nicks and breaks in the DNA strands [2]. Upon discovery and further research into the biology behind this defense mechanism, CRISPR/Cas9 began to be engineered as a tool for locating specific genes or segments of DNA and targeting them for degradation. This allowed researchers to knock out specific genes-of-interest in a way that the cell would be less likely to repair it to full function. These knockouts did not involve introducing foreign plasmid DNA to generate silencing RNA to destroy mRNA of specific genes and was generally thought to be a more efficient method for creating knockout cell lines that would also carry the knockdown on to the next lineage.

As the use of CRISPR to create knockout cell lines was being established, some researchers began to turn CRISPR as a means of attempting to create substitution mutations [3]. In addition to the CRISPR scaffold, the guide RNA (gRNA), and the Cas9 enzyme needed to generate knockdown cells, double-stranded DNA fragments were designed and introduced along with the other three elements to create a complex that in theory was supposed to allow for the double stranded DNA to be incorporated at the site of DNA damage created by the Cas9 after it was brought to the correct site by the scaffold/gRNA.

Previously, our laboratory had published that knockdown of total STMN1 resulted in a decrease in cell proliferation following induction of EMT [4]. These findings, along with previously published work that inferred the activity of the STMN1 regulatory serines, led to the development of this project, which was to investigate the specific roles that S16, S25, S38, and S63 play in regulating cell proliferation and promoting EMT. To accomplish this, a key strategy of the project was to mutate the individual serine residues, and combinations of serine residues, and study their individual or combined impact on these cellular processes. While the generation of mutant protein could be toxic to the cells, there are a considerable number of publications that have utilized these specific mutations in transfection assays, demonstrating that these substitution mutations were not lethal to the cells [5-8]. Utilizing what we knew at the time of CRISPR/Cas9, we and Invitrogen then moved forward with plans to use the new tool to generate our substitution mutation cell lines.

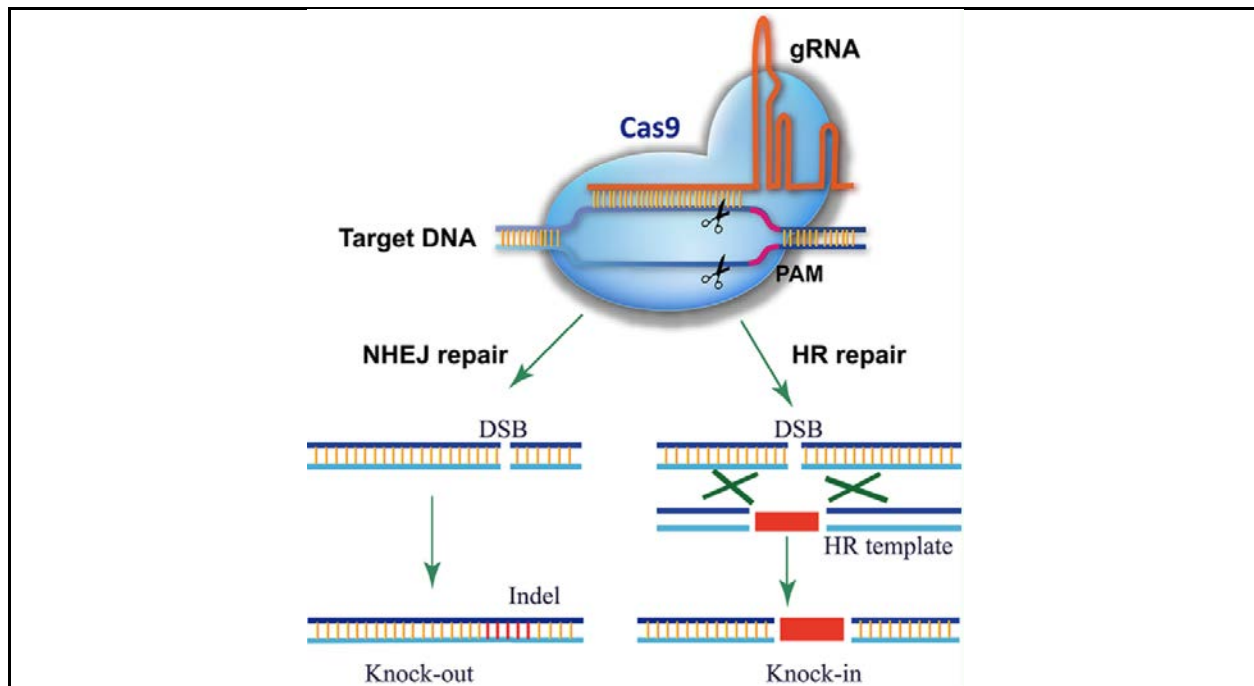


**Figure 1 taken from Ding et al 2016, to outline how CRISPR/Cas9 creates DNA damage, and the two primary processes of repair being NHEJ and HDR.**

## 5.3 Materials and Methods

### 5.3.a Sequencing the *STMN1* gene

To ensure an accurate design for gRNAs, genomic DNA was isolated from DU-145 cells and sequenced to confirm the sequence of the *STMN1* gene present in the DU-145 cell line. To isolate the genomic DNA for sequencing, cells were trypsinized, collected in medium, and centrifuged at 500 x g for 5 minutes. The cell pellet was resuspended in 2 mL Phosphate Buffered Saline (PBS) at room temperature, centrifuged, and the supernatant removed. Cells were resuspended in 100  $\mu$ L PBS before 90  $\mu$ L of 50 mM NaOH was added, and the cell solution was transferred to a PCR tube, where the sample was heated at 95° C for 10 minutes. Following this, 10  $\mu$ L of 1 M Tris HCl pH 7.8 was added to neutralize the reaction before the DNA was quantified via Nanodrop. Following quantification of the genomic DNA, the *STMN1* gene was sequenced by the Cincinnati Children's Hospital and Medical Center DNA Sequencing Core using primers towards *STMN1*.

The sequencing results of the *STMN1* gene above are annotated as follows: blue text is indicative of intronic sequence, while the black text indicates the exonic sequence of the *STMN1* gene. The bolded black region between the start and stop codons (in red font) represents the region of interest which codes for the functional *STMN1* protein. The underlined three sequence amino acids represent the four regulatory serines of interest. The lines separating the codons in the coding sequence indicate the cut sites that the Cas9 enzyme would be targeting that would create DNA damage that would be repaired via homology directed repair (HDR) to incorporate our mutant sequences.



AAGAGTATGTAGTGGCTTCTTTTGAAGTGTAGATGCTGAATATCTGTTCACTTTTCAATCCC  
AATTCTGTCCCAATCTTACCAGATGCTACTGGACTTGAATGGTTAATAAAAAGTGCACAGTGC  
TGTTGGTGGCAGTGACTTCTTTTGTAGTTAGGTTAATAAATCAAGCCATAGAGCCCTCCTGGT  
TGATACTTGTTCAGATGGGGCCTTTGGGGCTGGTAGAAATACCCAACGCACAAATGACCGC  
ACGTTCTCTGCCCGTTTCTTGCCCCAGTGTGGTTTGCATTGTCTCCTTCCACAATGACTGCTT  
TGTTTGGATGCCTCAGCCAGGTCAGCTGTTACTTTCTTTCAGATGTTTATTTGCAAACAACC  
ATTTTTTGTCTGTGTCCCTTTTAAAAGGCAGATTAAGCACAAGCGTGTCTAGAGAACA  
GTTGAGAGAGAATCTCAAGATTCTACTTGGTGGTTTGGCTTGTCTACGTTACAGGTGGGGCA  
TGTCCTCATCCTTTCCTGCCATAAAAAGCTATGACACGAGAATCAGAATATTAATAAAAAGTCTT  
ATGTAAGTGTGtagcaactcctgtgaaatgactaaaggaaccttaattattctaaagtagcatttgactcgggtggttaaggtggcagatacgtc  
atcattgatccagagctgtaatagtcctcctcaattcaggaacgccttggcagcttctgtctattgaga

Following sequencing, Invitrogen determined the appropriate cut site locations in the DNA for the Cas9 enzyme to create DNA damage.

### 5.3.b. Design of the CRISPR gRNA and dsDNA templates

After the sequencing of the STMN1 gene was completed and the cut sites were determined, next came the design of the gRNAs to target the specific underlined sequences representing the amino acids to mutate. Below are the sequences of the gRNAs that the Invitrogen scientists designed to target each serine site:

**Table 1: CRISPR gRNA design**

gRNA	CRISPR seq	Direction	PAM	Distance (bp) from SNP to cut	Length (bp)
S16A	gaactggagaagcgtgcctc	+	AGG	1	20
S25A	ttgagctgattctcagccct	+	CGG	0	20
S38A	ccttctctttggaggggaa	-	AGG	1	20
S63A	agacctcagcttcatgggac	-	TGG	1	20
S16E	gaactggagaagcgtgcctc	+	AGG	1	20
S25E	ttgagctgattctcagccct	+	CGG	0	20
S38E	ccttctctttggaggggaa	-	AGG	0	20
S63E	tttcagtcctgaagctg	+	AGG	8	20

In Table 2, the CRISPR gRNA sequence represents the complementary recognition sequence that is used to direct the CRISPR machinery to the precise region of the genomic DNA needed to make the nicks. The direction indicates the 3' to 5' annealing direction of the guide to the region of interest, while the PAM (protospacer adjacent motif) spacer sequence is the essential 3 base pair sequence that the Cas9 recognizes to make a cut. The cut is typically made 3-4 base pairs upstream of the PAM; therefore, it is typically beneficial for the PAM sequence to be within 0-3 base pairs from the desired damage site however some exceptions can be made (as was the case for S63E) [9]. Finally, the length of the gRNAs was recommended to be 20 bp in length, which was the reasoning for the standardized length seen in Table 2.

Following the design of the guides, the next experimental design aspect to be determined was the strategy to generate the combination of mutations. Generating the single amino acid substitution mutations was straightforward, simply introduce the CRISPR/Cas9 scaffold with the gRNA attached along with the double stranded template that was needed to incorporate the desired change. To generate the combination mutations (S[16,25,38,63]A, S[16,25,38,63]E, S16A[25,38,63]E, and S16E[25,38,63]A), Invitrogen advised to merely add the corresponding dsDNA templates and then screen the cells from the reaction to determine which combinations of mutants were achieved from the reaction itself. The sequences of the guides for each mutation are listed below.

**Table 2. CRISPR/Cas9 double-stranded template DNA sequences.**

<b>S1 6A</b>	TEETTTTCTGAATTATAAATATAATCAATTCTAGATATCCAGGTGAAAGAACTGGAG AAGCGTGCCGCAGGCCAGGCTTTTGAGCTGATTCTCAGCCOZC
<b>S1 6E</b>	TEETTTTCTGAATTATAAATATAATCAATTCTAGATATCCAGGTGAAAGAACTGGAG AAGCGTGCCGAAGGCCAGGCTTTTGAGCTGATTCTCAGCCOZC
<b>S2 5A</b>	TFEATATCCAGGTGAAAGAACTGGAGAAGCGTGCCTCAGGCCAGGCTTTTGAGCTGA TTCTCGCACCTCGGTCAAAGAATCTGTTCCAGAATTCCCOOT
<b>S2 5E</b>	TFEATATCCAGGTGAAAGAACTGGAGAAGCGTGCCTCAGGCCAGGCTTTTGAGCTGA TTCTCGAACCTCGGTCAAAGAATCTGTTCCAGAATTCCCOOT
<b>S3 8A</b>	TZZCTTCTGCAGCTTCTAATTTCTTCTGAATTTCTCCAGGGAAAGATCCTTCTTCTTT GGAGGGGCAAGGGGGAATTCTGGAACAGATTCTTTTGAOOG
<b>S3 8E</b>	TZZCTTCTGCAGCTTCTAATTTCTTCTGAATTTCTCCAGGGAAAGATCCTTCTTCTTT GGAGGTTCAAGGGGGAATTCTGGAACAGATTCTTTTGAOOG
<b>S6 3A</b>	TOZGAAGCACTTCTTTCTCGTGCTCTCGTTTCTCAGCCAGCTGCTTCAAGACCTCAGC TTCATGGGCCTGGAAAAAAAAGTTTAATAGGCTAGGCACZOT
<b>S6 3E</b>	AOFCCCAGCCTGAATACATTTTAGAGTGCCTAGCCTATTAACTTTTTTTTCCAGGAA CATGAAGCTGAGGTCTTGAAGCAGCTGGCTGAGAAACGAIEFG

### 5.3.c. Introduction of CRISPR/Cas9 to the cells

After design and production of the gRNAs, the final experimental design step was to determine the method of transfection. The two main delivery methods that had been utilized in literature were 1) lipid vesicles which would form around the CRISPR/Cas9 machinery and facilitate transportation through the cell membrane, and 2) electroporation, which utilizes an electric shock to briefly open the cell membranes to allow for the materials to flow in through osmosis before closing again with the materials inside the cell. 1mg of Cas9 enzyme, 5mg template DNA, 250ng/pmol gRNA, and 10 $\mu$ L of TrueGuide crRNA were added per each reaction tested. Once the materials enter, they translocate into the nucleus to find the region of interest in the genomic DNA via complementary binding to the gRNA, then the Cas9 enzyme creates the nicks in the genomic DNA, while the double stranded template DNA provides a template for the cell to use to repair the damaged piece via HDR [10,11].

The device used for electroporation was the Neon Electroporation System. Invitrogen scientists developed a protocol to provide optimal conditions for electroporation in a variety of cell lines. The parameters recommended for the DU-145 cell line were: 1,260 V for the pulse, a 20 ms pulse width, 2 pulses, with a cell density of  $5 \times 10^6$  cells/mL [12]. Once the recommended conditions were set, the electroporation took place, and the cells were pipetted into separate wells of a 24-well plate, and taken back to the incubator to recover from the transfection protocol.

## 5.4 Results

Throughout the next several months, the cells that survived the transfection process were cultured, with the experimental design dictating that single-cell sorting would take place as soon as the colony was established. Immediately after the electroporation took place, the cells were placed in 24-well plates to recover and grow until they could be grown in 6-well plates. The cells were then counted to establish concentration and diluted to a density of 10 cells/mL, such that pipetting them into a 96-well plate (100  $\mu$ L/well) should yield 1 cell/well on average. After the cells were given time to adhere, each plate was screened under the microscope to establish which cells contained 0, 1, or 2+ cells from the sorting. Each well that had 2 or more cells as a result of the sorting were immediately discounted, and wells that had 0 cells were monitored for further screening, as sometimes a single cell had been placed in the well but had adhered to the side of the well, and therefore it would eventually settle on the bottom of the well and would divide and establish its own colony. In order to correlate a particular phenotype with an identified mutation, each single cell derived colony was evaluated and documented for phenotypic changes other than the epithelial cobblestone phenotype.

As the single-cell derived colonies divided and grew, each colony was propagated from 96-well, to 24-well, and finally to 6-well, where it could be divided into continued culturing and into sequencing for incorporation of mutant sequences. One hundred and fourteen clones were isolated, sequenced, and evaluated for the incorporation of mutant sequences in the STMN1 gene, and none were found to have incorporated the mutant sequence in any of the various combinations that were attempted, however indels were seen in ~70% of the clones sequenced, indicative of NHEJ repair.

## 5.5. Discussion

Throughout the design and execution of this aspect of the project, there were three main weaknesses. The most critical weakness was that CRISPR/Cas9 technology was not yet fully developed for mutating single amino acids at the time we proposed the experiments. The first uses of CRISPR/Cas9 technology primarily involved the targeting of genes for silencing, via deletion of larger fragments of DNA sequence to generate truncated non-functional proteins. To achieve this, the gRNA would bring the CRISPR/Cas9 scaffold to the desired region and create nicks in the DNA that are known to cause DNA damage in the cells. When damage occurs, there are five primary methods of DNA repair based on the stage of the cell cycle: base excision repair (BER), nucleotide excision repair (NER), mismatch repair (MMR), HDR, NHEJ [13].

There are two main methods of DNA damage repair (DDR) associated with CRISPR/Cas9 experiments: HDR, and NHEJ. HDR is the process of repairing damaged DNA with a complementary template, such that the damaged piece is replaced with an intact replacement of the original sequence. This is useful in CRISPR/Cas9 experiments, when instead of knocking out a target gene, a mutation is desired [14,15]. To accomplish this, a fragment of double stranded DNA is generated with the desired mutated sequence that can be used as a template to replace the damaged fragment. For this project, the fragments above in **Table 3** were constructed with the four serine mutants and introduced into the cells via electroporation with the remainder of the CRISPR/Cas9 components.

After the break had been made by the Cas9 enzyme, template DNA was introduced to provide the mutation sequence that the HDR machinery would use to repair the break. In this way, a mutated protein would be produced, that could be inherited through multiple cell lineages,

without the need for other plasmids to be introduced into the cell. The main shortcoming of our CRISPR/Cas9 experiments is hypothesized to be the lack of inhibition of NHEJ.

When NHEJ occurs, there are many different types of proteins involved, such as DNA dependent protein kinases (DNA-PK), ligases, nucleases, and polymerases. These proteins work in combination to arrange the broken segments together, process, and ligate the pieces of broken DNA together, without regard for homology directed repair or the utilization of a template to replace/repair the corrupted segment of DNA [14,16,17]. Due to the threat that damaged DNA can cause in cells; the cell is incentivized to repair the damage promptly. When comparing the rates of NHEJ vs HDR, NHEJ can be completed in approximately 30 minutes, while the process of HDR can take up to 7 hours to complete. Because of this vast difference in time, NHEJ occurs at a much higher rate in the cells normally as compared with HDR. It was reported that NHEJ repaired 75% of DNA double strand breaks (DSBs), while HDR repaired 25%, which outlines an important disparity between the two DDR involved with CRISPR/Cas9 genomic editing [15]. This outlines a critical threat to the success of creating mutations in the native DNA with CRISPR/Cas9 technology. To address this, a few different strategies have been developed to lower the ratio of DSB repaired by NHEJ, to raise the rate of HDR, to increase mutation efficiency.

Rees et al. and Nambiar et al. have developed methods of raising the rate of HDR by introducing Rad variants such as hRad1 and Rad18, respectively to activate HDR [15,16]. The other strategy developed was the inhibition of NHEJ via tools such as CYREN, which inhibits cNHEJ (canonical NHEJ), in a cell cycle-dependent manner by “Ku70/80 heterodimer and preferentially inhibits cNHEJ at breaks with overhangs by protecting them”, or by inhibiting the proteins associated with NHEJ, such as the DNA-PKs via the kinase inhibitor M3814 [17-21]. The inhibition of NHEJ pharmacologically allows for a greater rate of HDR to rise from ~25% to as high as 87% [18]. This

results in a profound improvement in the experimental success of generating substitution mutations in desired genes to use as tools in research and would have been of great assistance for our project, had they been discovered when this work was being done.

Another weakness was that we did not incorporate a reporter gene which would have allowed sorting the labelled cells before plating and analysis. We discussed including a reporter gene with the Invitrogen representatives assisting with this project, and it was a joint decision not to include a reporter at the time as it could not be done in combination with the substitution mutations. Since a labeled DU-145 cell line was not available for purchase, we would have had to generate a DU-145 cell line stably transfected with a reporter gene first. A common disadvantage of adding a fluorescent protein such as ECFP is that they can exhibit low levels of toxicity. Transient transfections with a plasmid expressing the ECFP gene showed that the ECFP alone decreased DU-145 cell number compared to the untransfected controls. Future approaches would include testing a number of fluorescent proteins first to identify one with the least “side effects” and then using the gene to generate a stably labeled cell line.

A third weakness was that the DU-145 electroporation protocol developed by Invitrogen was not optimized for our DU-145 cell line. After electroporation, overall cell viability was very poor. Invitrogen reported that with their protocol, the expected cell death would be ~15%, however, we observed that cell death was ~30-40% and could be up to ~70% [12]. The higher rate of cell death also correlated with the surviving cells being weaker and more susceptible to apoptosis if trypsinized too early following electroporation. This necessitated culturing larger colonies before the cells were sorted and plated as single cells. While data to prove the following is not available, we hypothesize that if there were mutant cells in our cell populations, the growth rate of the wild

type population could have overwhelmed the mutant cells, causing their death before sorting could even take place.

In conclusion, while there were successful components to the execution of these CRISPR/Cas9 experiments, namely the isolation and sequencing of the DU-145 genomic DNA STMN1 sequence, the experiments as a whole failed primarily due to a lack of currently available strategies that limit the role NHEJ plays in the repair of DNA damage, and a lack of usage of a reporter gene that could have been used as a sorting tool in identifying successfully mutated cells. Recent updates have been made to the CRISPR/Cas9 protocol that did not exist when this experiment was designed and carried out in 2017-2018. This evolution of the methodology will have profound implications towards improving the mutation rate in CRISPR/Cas9 genome editing.

# Chapter 6

## Conclusions and Future Directions

## 6.1. Conclusions

### 6.1.a. The role of HGF in the phosphorylation of Stathmin on S16 in prostate cancer progression

#### 6.1.a.1 Therapeutic Relevance of HGF/MET signaling inhibitor in combination with ADT

Prostate cancer is an androgen-driven disease, with the upregulation of AR-regulated genes related to increased proliferation, migration and invasion often seen in cancer profiles [1]. Commonly, PCa is treated with a combination of ADT along with another traditional therapy, which could be either chemotherapy, radiation therapy, or other form of targeted therapy [2]. While these general therapies are used to treat a variety of cancers, PCa is uniquely suited for an approach that not only takes advantage of cancer cell characteristics, but also takes into account the mechanistic changes that result from treatment with ADT.

Verras and colleagues found that in early stages of PCa where AR activity dictates growth and development, levels of MET expression are low [3]. This is due to the inhibition of Sp1 activity by AR, thus repressing transcription of the *MET* gene [3]. However, after failure of ADT when AR is significantly downregulated, the *MET* gene is derepressed and expression is increased (along with *STMN1* expression), making PCa more responsive to HGF, and promoting increased expression of HGF by neighboring stromal cells and other associated tumor cells (such as the CAFs) [3,4]. Therefore, we propose a dual treatment strategy of ADT combined with an HGF/MET signaling inhibitor to potently inhibit and kill PCa cells in early and late-stage disease.

#### 6.1.a.2 Utilization of AMG337 to target HGF/MET signaling

A number of HGF/MET signaling inhibitors have been developed to target various processes related to the signaling axis [5,6]. In general, they can be broken up into three categories of function: targeting the HGF:MET binding pocket in the extracellular matrix, targeting the

intracellular domain of the MET receptor (c-MET), and finally targeting the downstream signaling effectors of the pathway [5]. AMG337 is a small molecule inhibitor that binds to c-MET and inhibits downstream signal transduction pathways [7]. Currently, AMG337 is in clinical trials for cancers with increased MET expression (e.g., gastric/esophageal adenocarcinoma and other advanced or metastatic solid tumors) [8,9].

The novel findings presented in this study demonstrate the efficacy of using AMG337 to target PCa in cells that do not express AR. In addition to being an AR<sup>-</sup> cell line, DU-145 cells express a non-functioning mutant p53. The ability of AMG337 to inhibit cell cycle progression, cell doubling, overall cell proliferation, and inducing cell death in an AR<sup>-</sup> cell line makes it an attractive candidate for future study to be used alongside ADT in the treatment of PCa.

#### **6.1.b. Implications on the tumor microenvironment**

The tumor microenvironment is a critical component to the overall survival and progression for any cancer. Prostate cancer is especially reliant upon its microenvironment, as it is strongly influenced by mitotic factors secreted by neighboring stromal cells, such as HGF [10-13]. While there are several components to the tumor microenvironment that include: immune cells, fibroblasts, dendrites, and stromal cells, the contribution of mitotic factors such as HGF create a large obstacle in treatment by promoting the progression of PCa. The production of HGF by cancer associated fibroblasts (CAFs) results in their significant role in furthering the development of metastatic PCa [14].

#### **6.1.c. Summary of the effect of HGF on cancer cell proliferation**

HGF/MET signaling increases cell proliferation in many cancers, including nasopharyngeal carcinoma, hepatocellular carcinoma, gastric cancers, esophageal carcinomas, and medulloblastomas [15-18]. In this study, we show that HGF treatment promotes cell proliferation,

shortens cell doubling time by decreasing the time required to progress through the cell cycle, and induces an earlier expression of cell cycle proteins. These observations reveal a novel role of HGF in PCa proliferation and highlight the importance in studying this mechanism.

#### **6.1.d. HGF phosphorylation results in increases in cell cycle progression and overall PCa cell proliferation without induction of metastasis**

HGF/MET signaling promotes cell proliferation primarily through phosphorylation/activation of Pak1 which has previously been shown to induce phosphorylation of STMN1 on S16 [19]. This study demonstrates for the first time that HGF/MET signaling regulates differential phosphorylation of STMN1 S16 which modulates cell cycle progression and proliferation in DU-145 cells without triggering metastasis.

While it has been established that increased levels of STMN1 and MET are indicative of an advanced disease state and poor prognosis, downregulation of total STMN1 is not a viable therapeutic strategy. In a previous study, we demonstrated that downregulation of total STMN1 induced EMT and metastasis, implying that STMN1 could function as a tumor suppressor [20]. Therefore, this study was designed to delineate the role of differential phosphorylation of STMN1 regulatory serines.

Cells transfected with different phosphor-mimetics of STMN1 demonstrated that S16 is the predominant serine that contributes to increased or decreased cell proliferation in DU-145 and NMuMG cells, representing mechanistic similarities between both cancerous and normal epithelial cells, respectively. This targeted phosphorylation also specifically affected cell doubling time in both cell types and cell cycle progression in the DU-145 cells.

To determine the impact of STMN1 S16 phosphorylation on metastatic processes, migration and invasion assays were conducted with treated and transfected DU-145 and NMuMG

cells. In comparison to knocking down STMN1 expression, none of the treatments resulted in a modulation of either metastatic process, confirming that S16 does not trigger metastasis in PCa and NMuMG cells known to undergo EMT [20].

#### **6.1.e. CAMKII phosphorylation of STMN1 on S16 is likely cell type specific**

Numerous studies reports that CAMKII phosphorylates STMN1 on S16 in a variety cell types such as anterior pituitary cells, breast cancer cells, and neuronal cells [21-25]. Activation of CAMKII occurs by upregulation of intracellular Ca<sup>2+</sup> which leads to autophosphorylation of CAMKII, which in turn, results in the phosphorylation of STMN1 S16 [21,22]. These observations and associations are what led to the initial investigation into the role of CAMKII in regulating DU-145 cell proliferation and whether STMN1 S16 phosphorylation regulated this process.

Our study outlined in Chapter 3 demonstrates that stimulation of CAMKII by Oleic Acid increased DU-145 cell proliferation in a dose-dependent manner, while inhibition of CAMKII by KN93 decreased proliferation and induced DU-145 cell death. These observations led to the experiments to determine whether CAMKII phosphorylated STMN1 S16. Unlike other studies, in DU-145 cells, S16 was not phosphorylated through CAMKII, indicating that CAMKII/STMN S16 activity is likely cell-type specific. This not only provides additional information regarding CAMKII signaling in AR- prostate cancer cells, but also contributes towards the overall development of therapeutic strategies that could target cancer cells based on their identifying characteristics.

#### **6.1.f. Discussion of the impact MDM2 has on maintaining PCa stem cell integrity through the degradation of the androgen receptor and the potential therapeutic implications**

The role of AR in PCa is a critical determinant to how it will respond to a variety of treatments, and the intracellular signaling mechanisms that occur [3]. The expression or degradation of the AR

plays a vital role in determining whether PCa stem cells can maintain their stemness or undergo terminal differentiation into luminal cells [26].

The regulation of the AR in PCa stem cells is dictated by the E-3 ubiquitin ligase MDM2. MDM2 constantly degrades the AR in PCa stem cells to inhibit the induction of AR-responsive genes such as: PSA, PAP, NKX3.1, TMPRSS2, and FGF5. Through the studies outlined in Chapter 4, we demonstrated in multiple stem-like cell lines that maintenance of MDM2 promoted the regulation of stem cell genes, including OCT4, NANOG, SOX2, and CD44, and NESTIN, but also self-renewal. Treatment with E-3 ubiquitin ligase inhibitors (e.g., MG132), inhibited MDM2 activity, causing the downregulation in expression of stem cell factors, loss of self-renewal, induction of AR and terminal differentiation into luminal epithelial cells and cell death. Similarly, transfection with a plasmid expressing AR (without or with the addition of androgens) resulted in a similar outcome. These data confirmed that the expression of AR is sufficient to induce differentiation of PCa stem cells, and that MDM2 is required to maintain the PCa stem cell population.

Current treatments primarily target AR<sup>+</sup> PCa cells. Our findings provide an important contribution towards the understanding of PCa stem cells and a possible mechanism for targeting AR<sup>-</sup> cancer stem cells. PCa stem cells can increase the risk of developing recurrent PCa, which arises through gain-of-function mutations that circumvent ADT and lead to the development of CRPC. Our study suggests that the E3 ligase inhibitor MG132 used in combination with ADT could eliminate both AR<sup>+</sup> bulk tumor cells and AR<sup>-</sup> PCa stem cells.

## **6.2. Future Directions**

The studies from this dissertation provide novel insights into the role of HGF/MET signaling in PCa progression, and the role of STMN1 S16 differential phosphorylation in the regulation of cell cycle progression. Additionally, evidence is provided suggesting that the role of CAMKII in phosphorylating STMN1 S16 is cell type specific. Finally, it discusses the published findings that outline the important role of MDM2 in constantly degrading the AR in order to promote cancer cell stemness. To that end, the future directions that would further these areas of research are listed below.

### **6.2.1.a. Determine the relationship between increased concentration of HGF and varied cellular processes.**

In the early attempts at studying the role of HGF on DU-145 cell proliferation, proliferation assays were conducted where an increasing dose of HGF was added to the treatment media, which contained 1% FBS. This resulted in no change in cell proliferation from 0-40 ng/mL of HGF. Upon further investigation in the literature, it was common protocol to carry out the proliferation assays in serum-free media, as the concentration of growth factors (including HGF) in even 1% FBS (and 0.1% FBS) were enough to interfere with the results [27,28]. Once the experiments were conducted in serum-free media + HGF, morphological changes were observed after 72 hours of treatment.

We observed that 25 ng/mL HGF in serum-free media resulted in no change in cell morphology after 72 hrs, while 40 ng/mL resulted in cells exhibiting a change from cobblestone-epithelial phenotype to spindle-like mesenchymal phenotype. These cells divided at a reduced rate compared

to the control cells and those treated with a lower concentration of HGF, indicating a change in cellular processes from one that works towards cell proliferation, towards one that favors cell motility. The first experiment to better understand the role of HGF concentrations on PCa development would be to treat PCa cell lines with increasing doses of HGF for 72 hours, collect RNA from the cells each day and then a microarray could be designed and executed to highlight epithelial cell-specific genes and genes likely to be induced by HGF treatment. If the findings suggested that a small number of pathways were activated by HGF at moderate concentrations, the inhibition of those pathways prior to HGF treatment by small molecule inhibitors or siRNA could provide further information towards understanding differential signaling mechanisms as a result of HGF stimulation of the MET signaling pathway.

#### **6.2.1.b. Determine the role of differential phosphorylation of STMN1 S16 *in vivo*.**

The experiments conducted in this dissertation outline the impact of HGF/MET-mediated phosphorylation of STMN1 S16 *in vitro*. In order to make substantial claims as to the efficacy of the proposed therapeutic strategy to use AMG337 in combination with ADT, *in vivo* data that considers not only the cell-environment interactions of the PCa cells + treatment, but also the interactions occurring in the tumor microenvironment will provide further validity to the treatment strategy. Based on our findings, I would hypothesize that AMG337 would inhibit tumor growth and induce death in cells grafted into the host animal through inhibition of the MET signaling pathway.

### **6.2.2. Examine the efficacy of dual treatment of a MDM2 inhibitor and ADT *in vivo*.**

The data presented in Chapter 4 discusses the mechanistic regulation of PCa stem cell maintenance, and the role of MDM2 in constantly degrading the AR to maintain stemness. While these experiments were conducted *in vitro* along with spheres grown in Matrigel, these experiments do not completely represent the entire environment of cancer therapeutics. Therefore, an *in vivo* study of PCa xenograft in humanized mice that would mimic the human tumor microenvironment would be a helpful background from which to treat the tumors with ADT + MG132, or a different E-3 ubiquitin ligase to inhibit MDM2 activity. This would provide novel and important insights into the effects of ADT on PCa stem cell populations, and potential therapeutic strategies that could result in total elimination of both PCa stem cells and bulk tumor cells.

# Bibliography

## Chapter 1 Bibliography

1. HUGGINS, C. “Androgen and anaplasia.” *The Yale journal of biology and medicine* vol. 19,3 (1947): 319-30.
2. J. Thomas Sanderson, The Steroid Hormone Biosynthesis Pathway as a Target for Endocrine-Disrupting Chemicals, *Toxicological Sciences*, Volume 94, Issue 1, November 2006, Pages 3–21, <https://doi.org/10.1093/toxsci/kfl051>
3. Mahadik, Namita, et al. “Targeting Steroid Hormone Receptors for Anti-Cancer Therapy—a Review on Small Molecules and Nanotherapeutic Approaches.” *WIREs Nanomedicine and Nanobiotechnology*, vol. 14, no. 2, 2021, <https://doi.org/10.1002/wnan.1755>.
4. Skowron, Kornelia J et al. “Steroid receptor/coactivator binding inhibitors: An update.” *Molecular and cellular endocrinology* vol. 493 (2019): 110471. doi:10.1016/j.mce.2019.110471
5. Anderson NM, Simon MC. The tumor microenvironment. *Curr Biol*. 2020 Aug 17;30(16):R921-R925. doi: 10.1016/j.cub.2020.06.081. PMID: 32810447; PMCID: PMC8194051.
6. Francis, Jeffrey C, and Amanda Swain. “Prostate Organogenesis.” *Cold Spring Harbor perspectives in medicine* vol. 8,7 a030353. 2 Jul. 2018, doi:10.1101/cshperspect.a030353
7. Henry, Gervaise H et al. “A Cellular Anatomy of the Normal Adult Human Prostate and Prostatic Urethra.” *Cell reports* vol. 25,12 (2018): 3530-3542.e5. doi:10.1016/j.celrep.2018.11.086
8. Cunha, G.R., and L.W.K. Chung. “Stromal-Epithelial Interactions—I. Induction of Prostatic Phenotype in Urothelium of Testicular Feminized (TFM/Y) Mice.” *Journal of Steroid Biochemistry*, vol. 14, no. 12, 1981, pp. 1317–1324., [https://doi.org/10.1016/0022-4731\(81\)90338-1](https://doi.org/10.1016/0022-4731(81)90338-1).
9. “NCI Dictionary of Cancer Terms.” *National Cancer Institute*, <https://www.cancer.gov/publications/dictionaries/cancer-terms/def/gleason-score>.
10. Lahtonen, Riitta, et al. “Nuclear Androgen Receptors in the Epithelium and Stroma of Human Benign Prostatic Hypertrophic Glands.” *The Prostate*, vol. 4, no. 2, 1983, pp. 129–139., <https://doi.org/10.1002/pros.2990040204>.
11. Li, Yirong, et al. “Decrease in Stromal Androgen Receptor Associates with Androgen-Independent Disease and Promotes Prostate Cancer Cell Proliferation and Invasion.” *Journal of Cellular and Molecular Medicine*, vol. 12, no. 6b, 2008, pp. 2790–2798., <https://doi.org/10.1111/j.1582-4934.2008.00279.x>.
12. Singh M, Jha R, Melamed J, Shapiro E, Hayward SW, Lee P. Stromal androgen receptor in prostate development and cancer. *Am J Pathol*. 2014 Oct;184(10):2598-607. doi:

- 10.1016/j.ajpath.2014.06.022. Epub 2014 Aug 1. PMID: 25088980; PMCID: PMC4188859.
13. Fujita, Kazutoshi, and Norio Nonomura. "Role of Androgen Receptor in Prostate Cancer: A Review." *The world journal of men's health* vol. 37,3 (2019): 288-295. doi:10.5534/wjmh.180040
  14. Bahmad, Hisham F., et al. "Tumor Microenvironment in Prostate Cancer: Toward Identification of Novel Molecular Biomarkers for Diagnosis, Prognosis, and Therapy Development." *Frontiers in Genetics*, vol. 12, 2021, <https://doi.org/10.3389/fgene.2021.652747>.
  15. Hayward SW, Wang Y, Cao M, Hom YK, Zhang B, Grossfeld GD, Sudilovsky D, Cunha GR. Malignant transformation in a nontumorigenic human prostatic epithelial cell line. *Cancer Res.* 2001 Nov 15;61(22):8135-42. PMID: 11719442.
  16. San Francisco IF, DeWolf WC, Peehl DM, Olumi AF. Expression of transforming growth factor-beta 1 and growth in soft agar differentiate prostate carcinoma-associated fibroblasts from normal prostate fibroblasts. *Int J Cancer.* 2004 Nov 1;112(2):213-8. doi: 10.1002/ijc.20388. PMID: 15352032.
  17. Ao M, Franco OE, Park D, Raman D, Williams K, Hayward SW. Cross-talk between paracrine-acting cytokine and chemokine pathways promotes malignancy in benign human prostatic epithelium. *Cancer Res.* 2007 May 1;67(9):4244-53. doi: 10.1158/0008-5472.CAN-06-3946. PMID: 17483336.
  18. Mao, Xiaoqi et al. "Crosstalk between cancer-associated fibroblasts and immune cells in the tumor microenvironment: new findings and future perspectives." *Molecular cancer* vol. 20,1 131. 11 Oct. 2021, doi:10.1186/s12943-021-01428-1
  19. Feig, Christine, et al. "Targeting CXCL12 from FAP-Expressing Carcinoma-Associated Fibroblasts Synergizes with Anti-Pd-L1 Immunotherapy in Pancreatic Cancer." *Proceedings of the National Academy of Sciences*, vol. 110, no. 50, 2013, pp. 20212–20217., <https://doi.org/10.1073/pnas.1320318110>.
  20. Montico F, Kido LA, San Martin R, Rowley DR, Cagnon VH. Reactive stroma in the prostate during late life: The role of microvasculature and antiangiogenic therapy influences. *Prostate.* 2015 Oct;75(14):1643-61. doi: 10.1002/pros.23045. Epub 2015 Jul 17. PMID: 26184673.
  21. Giannoni, Elisa, et al. "Reciprocal Activation of Prostate Cancer Cells and Cancer-Associated Fibroblasts Stimulates Epithelial-Mesenchymal Transition and Cancer Stemness." *Cancer Research*, vol. 70, no. 17, 2010, pp. 6945–6956., <https://doi.org/10.1158/0008-5472.can-10-0785>.
  22. Shiao, Stephen L., et al. "Regulation of Prostate Cancer Progression by the Tumor Microenvironment." *Cancer Letters*, vol. 380, no. 1, 2016, pp. 340–348., <https://doi.org/10.1016/j.canlet.2015.12.022>.
  23. Matsumoto K, Umitsu M, De Silva DM, Roy A, Bottaro DP. Hepatocyte growth factor/MET in cancer progression and biomarker discovery. *Cancer Sci.* 2017 Mar;108(3):296-307. doi: 10.1111/cas.13156. PMID: 28064454; PMCID: PMC5378267.

24. Organ, Shawna Leslie, and Ming-Sound Tsao. "An overview of the c-MET signaling pathway." *Therapeutic advances in medical oncology* vol. 3,1 Suppl (2011): S7-S19. doi:10.1177/1758834011422556
25. Mo, Hong-Nan, and Peng Liu. "Targeting MET in cancer therapy." *Chronic diseases and translational medicine* vol. 3,3 148-153. 19 Jul. 2017, doi:10.1016/j.cdtm.2017.06.002
26. Qin H, Yang Y, Jiang B, Pan C, Chen W, Diao W, Ding M, Cao W, Zhang Z, Chen M, Gao J, Zhao X, Qiu X, Guo H. SOX9 in prostate cancer is upregulated by cancer-associated fibroblasts to promote tumor progression through HGF/c-Met-FRA1 signaling. *FEBS J.* 2021 Sep;288(18):5406-5429. doi: 10.1111/febs.15816. Epub 2021 Apr 2. PMID: 33705609.
27. Vancauwenberghe E, Noyer L, Derouiche S, Lemonnier L, Gosset P, Sadofsky LR, Mariot P, Warnier M, Bokhobza A, Slomianny C, Mauroy B, Bonnal JL, Dewailly E, Delcourt P, Allart L, Desruelles E, Prevarskaya N, Roudbaraki M. Activation of mutated TRPA1 ion channel by resveratrol in human prostate cancer associated fibroblasts (CAF). *Mol Carcinog.* 2017 Aug;56(8):1851-1867. doi: 10.1002/mc.22642. Epub 2017 May 22. PMID: 28277613.
28. Ziaee, Shabnam, and Leland WK Chung. "Induction of Integrin  $\alpha 2$  in a Highly Bone Metastatic Human Prostate Cancer Cell Line: Roles of Rankl and AR under Three-Dimensional Suspension Culture." *Molecular Cancer*, vol. 13, no. 1, 2014, p. 208., <https://doi.org/10.1186/1476-4598-13-208>.
29. Bonollo, Francesco et al. "The Role of Cancer-Associated Fibroblasts in Prostate Cancer Tumorigenesis." *Cancers* vol. 12,7 1887. 13 Jul. 2020, doi:10.3390/cancers12071887
30. Erdogan, Begum, and Donna J Webb. "Cancer-associated fibroblasts modulate growth factor signaling and extracellular matrix remodeling to regulate tumor metastasis." *Biochemical Society transactions* vol. 45,1 (2017): 229-236. doi:10.1042/BST20160387
31. Linares, Jenniffer, et al. "Determinants and Functions of CAFs Secretome during Cancer Progression and Therapy." *Frontiers in Cell and Developmental Biology*, vol. 8, 2021, <https://doi.org/10.3389/fcell.2020.621070>.
32. Varkaris, Andreas et al. "The role of HGF/c-Met signaling in prostate cancer progression and c-Met inhibitors in clinical trials." *Expert opinion on investigational drugs* vol. 20,12 (2011): 1677-84. doi:10.1517/13543784.2011.631523
33. Karantanos, T et al. "Prostate cancer progression after androgen deprivation therapy: mechanisms of castrate resistance and novel therapeutic approaches." *Oncogene* vol. 32,49 (2013): 5501-11. doi:10.1038/onc.2013.206
34. Han, J., Zhang, J., Zhang, W. *et al.* Abiraterone and MDV3100 inhibits the proliferation and promotes the apoptosis of prostate cancer cells through mitophagy. *Cancer Cell Int* **19**, 332 (2019). <https://doi.org/10.1186/s12935-019-1021-9>
35. Alcaraz, Antonio. "Re: Enzalutamide with Standard First-Line Therapy in Metastatic Prostate Cancer." *European Urology*, vol. 77, no. 2, 2020, pp. 286–287., <https://doi.org/10.1016/j.eururo.2019.08.033>.
36. Verras M, Lee J, Xue H, Li TH, Wang Y, Sun Z. The androgen receptor negatively regulates the expression of c-Met: implications for a novel mechanism of prostate cancer

- progression. *Cancer Res.* 2007 Feb 1;67(3):967-75. doi: 10.1158/0008-5472.CAN-06-3552. PMID: 17283128.
37. Liao, Chun-Peng et al. "Androgen receptor in cancer-associated fibroblasts influences stemness in cancer cells." *Endocrine-related cancer* vol. 24,4 (2017): 157-170. doi:10.1530/ERC-16-0138
  38. Hughes, Veronica S, and Dietmar W Siemann. "Have Clinical Trials Properly Assessed c-Met Inhibitors?." *Trends in cancer* vol. 4,2 (2018): 94-97. doi:10.1016/j.trecan.2017.11.009
  39. De Mello, Ramon Andrade et al. "The Role of MET Inhibitor Therapies in the Treatment of Advanced Non-Small Cell Lung Cancer." *Journal of clinical medicine* vol. 9,6 1918. 19 Jun. 2020, doi:10.3390/jcm9061918
  40. Lennerz JK, Kwak EL, Ackerman A, Michael M, Fox SB, Bergethon K, Lauwers GY, Christensen JG, Wilner KD, Haber DA, Salgia R, Bang YJ, Clark JW, Solomon BJ, Iafrate AJ. MET amplification identifies a small and aggressive subgroup of esophagogastric adenocarcinoma with evidence of responsiveness to crizotinib. *J Clin Oncol.* 2011 Dec 20;29(36):4803-10. doi: 10.1200/JCO.2011.35.4928. Epub 2011 Oct 31. PMID: 22042947; PMCID: PMC3255989.
  41. Robinson, Kyle W, and Alan B Sandler. "The role of MET receptor tyrosine kinase in non-small cell lung cancer and clinical development of targeted anti-MET agents." *The oncologist* vol. 18,2 (2013): 115-22. doi:10.1634/theoncologist.2012-0262
  42. "Types of Cancer Treatment." *National Cancer Institute*, <https://www.cancer.gov/about-cancer/treatment/types>.
  43. Crosswell, H.E., Dasgupta, A., Alvarado, C.S. *et al.* PHA665752, a small-molecule inhibitor of c-Met, inhibits hepatocyte growth factor-stimulated migration and proliferation of c-Met-positive neuroblastoma cells. *BMC Cancer* **9**, 411 (2009). <https://doi.org/10.1186/1471-2407-9-411>
  44. Choi, MH., Kim, J., Ha, J.H. *et al.* A selective small-molecule inhibitor of c-Met suppresses keloid fibroblast growth in vitro and in a mouse model. *Sci Rep* **11**, 5468 (2021). <https://doi.org/10.1038/s41598-021-84982-4>
  45. Zhao, Shankun, et al. "Selective Inhibitor of the C-Met Receptor Tyrosine Kinase in Advanced Hepatocellular Carcinoma: No Beneficial Effect with the Use of Tivantinib?" *Frontiers in Immunology*, vol. 12, 2021, <https://doi.org/10.3389/fimmu.2021.731527>.
  46. Chi, M., Evans, H., Gilchrist, J. et al. Phosphorylation of calcium/calmodulin-stimulated protein kinase II at T286 enhances invasion and migration of human breast cancer cells. *Sci Rep* **6**, 33132 (2016). <https://doi.org/10.1038/srep33132>
  47. Alesi, G. N., Jin, L., Li, D., Magliocca, K. R., Kang, Y., Chen, Z. G., Shin, D. M., Khuri, F. R., & Kang, S. (2016). RSK2 signals through stathmin to promote microtubule dynamics and tumor metastasis. *Oncogene*, *35*(41), 5412–5421. <https://doi.org/10.1038/onc.2016.79>
  48. Banerjee M, Worth D, Prowse DM, Nikolic M. Pak1 phosphorylation on t212 affects microtubules in cells undergoing mitosis. *Curr Biol.* 2002 Jul 23;12(14):1233-9. doi: 10.1016/s0960-9822(02)00956-9. PMID: 12176334

49. Gadea BB, Ruderman JV. Aurora B is required for mitotic chromatin-induced phosphorylation of Op18/Stathmin. *Proc Natl Acad Sci U S A*. 2006 Mar 21;103(12):4493-8. doi: 10.1073/pnas.0600702103. Epub 2006 Mar 14. PMID: 16537398; PMCID: PMC1401233.
50. Karst, A. M., Levanon, K., Duraisamy, S., Liu, J. F., Hirsch, M. S., Hecht, J. L., & Drapkin, R. (2011). Stathmin 1, a marker of PI3K pathway activation and regulator of microtubule dynamics, is expressed in early pelvic serous carcinomas. *Gynecologic oncology*, 123(1), 5–12. <https://doi.org/10.1016/j.ygyno.2011.05.021>
51. Kuang, X. Y., Chen, L., Zhang, Z. J., Liu, Y. R., Zheng, Y. Z., Ling, H., Qiao, F., Li, S., Hu, X., & Shao, Z. M. (2015). Stathmin and phospho-stathmin protein signature is associated with survival outcomes of breast cancer patients. *Oncotarget*, 6(26), 22227–22238. <https://doi.org/10.18632/oncotarget.4276>
52. Marklund U, Brattsand G, Shingler V, Gullberg M. Serine 25 of oncoprotein 18 is a major cytosolic target for the mitogen-activated protein kinase. *The Journal of biological chemistry*. 1993;268:15039–15047.
53. Hayashi K, Pan Y, Shu H, Ohshima T, Kansy JW, White CL 3rd, Tamminga CA, Sobel A, Curmi PA, Mikoshiba K, Bibb JA. Phosphorylation of the tubulin-binding protein, stathmin, by Cdk5 and MAP kinases in the brain. *J Neurochem*. 2006 Oct;99(1):237-50. doi: 10.1111/j.1471-4159.2006.04113.x. Epub 2006 Aug 21. PMID: 16925597.
54. Beretta, L, et al. "Multiple Phosphorylation of Stathmin. Identification of Four Sites Phosphorylated in Intact Cells and in Vitro by Cyclic AMP-Dependent Protein Kinase and P34CDC2." *Journal of Biological Chemistry*, vol. 268, no. 27, 1993, pp. 20076–20084., [https://doi.org/10.1016/s0021-9258\(20\)80696-6](https://doi.org/10.1016/s0021-9258(20)80696-6).
55. K. Hayashi, Y. Pan, H. Shu, T. Ohshima, J. W. Kansy, C. L. White, 3rd, et al., "Phosphorylation of the tubulin-binding protein, stathmin, by Cdk5 and MAP kinases in the brain," *J Neurochem*, vol. 99, pp. 237-50, Oct 2006.
56. L. Beretta, M. F. Dubois, A. Sobel, and O. Bensaude, "Stathmin is a major substrate for mitogen-activated protein kinase during heat shock and chemical stress in HeLa cells," *Eur J Biochem*, vol. 227, pp. 388-95, Jan 15 1995.
57. Marklund U, Osterman O, Melander H, Bergh A, Gullberg M. The phenotype of a "Cdc2 kinase target site-deficient" mutant of oncoprotein 18 reveals a role of this protein in cell cycle control. *J Biol Chem*. 1994 Dec 2;269(48):30626-35. PMID: 7982983.
58. Ng, D. C., Zhao, T. T., Yeap, Y. Y., Ngoei, K. R., & Bogoyevitch, M. A. (2010). c-Jun N-terminal kinase phosphorylation of stathmin confers protection against cellular stress. *The Journal of biological chemistry*, 285(37), 29001–29013. <https://doi.org/10.1074/jbc.M110.128454>
59. Küntziger, Thomas, et al. "Differential Effect of Two Stathmin/OP18 Phosphorylation Mutants on Xenopus Embryo Development." *Journal of Biological Chemistry*, vol. 276, no. 25, 2001, pp. 22979–22984., <https://doi.org/10.1074/jbc.m101466200>.
60. Rubin, Camelia Iancu, and George F. Atweh. "The Role of Stathmin in the Regulation of the Cell Cycle." *Journal of Cellular Biochemistry*, vol. 93, no. 2, 2004, pp. 242–250., <https://doi.org/10.1002/jcb.20187>.

61. Filbert, Erin L et al. "Stathmin regulates microtubule dynamics and microtubule organizing center polarization in activated T cells." *Journal of immunology (Baltimore, Md. : 1950)* vol. 188,11 (2012): 5421-7. doi:10.4049/jimmunol.1200242
62. Tian X, Tian Y, Moldobaeva N, Sarich N, Birukova AA. Microtubule dynamics control HGF-induced lung endothelial barrier enhancement. *PLoS One*. 2014 Sep 8;9(9):e105912. doi: 10.1371/journal.pone.0105912. PMID: 25198505; PMCID: PMC4157766.
63. Schmitt, Sabrina, et al. "Stathmin Regulates Keratinocyte Proliferation and Migration during Cutaneous Regeneration." *PLoS ONE*, vol. 8, no. 9, 2013, <https://doi.org/10.1371/journal.pone.0075075>.
64. Zhang, Rui et al. "STMN1 upregulation mediates hepatocellular carcinoma and hepatic stellate cell crosstalk to aggravate cancer by triggering the MET pathway." *Cancer science* vol. 111,2 (2020): 406-417. doi:10.1111/cas.14262
65. Xie L, Law BK, Aakre ME, Edgerton M, Shyr Y, Bhowmick NA, Moses HL. Transforming growth factor beta-regulated gene expression in a mouse mammary gland epithelial cell line. *Breast Cancer Res*. 2003;5(6):R187-98. doi: 10.1186/bcr640. Epub 2003 Aug 20. PMID: 14580254; PMCID: PMC314403.

## Chapter 2 Bibliography

1. Dai, Charles et al. "Androgen Signaling in Prostate Cancer." *Cold Spring Harbor perspectives in medicine* vol. 7,9 a030452. 1 Sep. 2017, doi:10.1101/cshperspect.a030452
2. Nacusi, Lucas P, and Donald J Tindall. "Androgen receptor abnormalities in castration-recurrent prostate cancer." *Expert review of endocrinology & metabolism* vol. 4,5 (2009): 417-422. doi:10.1586/eem.09.34
3. Anderson NM, Simon MC. The tumor microenvironment. *Curr Biol*. 2020 Aug 17;30(16):R921-R925. doi: 10.1016/j.cub.2020.06.081. PMID: 32810447; PMCID: PMC8194051.
4. Sahai, E., Astsaturov, I., Cukierman, E. *et al.* A framework for advancing our understanding of cancer-associated fibroblasts. *Nat Rev Cancer* **20**, 174–186 (2020). <https://doi.org/10.1038/s41568-019-0238-1>
5. Bahmad, Hisham F., et al. "Tumor Microenvironment in Prostate Cancer: Toward Identification of Novel Molecular Biomarkers for Diagnosis, Prognosis, and Therapy Development." *Frontiers in Genetics*, vol. 12, 2021, <https://doi.org/10.3389/fgene.2021.652747>.
6. Sun, Rui et al. "HGF stimulates proliferation through the HGF/c-Met pathway in nasopharyngeal carcinoma cells." *Oncology letters* vol. 3,5 (2012): 1124-1128. doi:10.3892/ol.2012.613
7. Wang, Haiyu, et al. "The Function of the HGF/c-Met Axis in Hepatocellular Carcinoma." *Frontiers in Cell and Developmental Biology*, vol. 8, 2020, <https://doi.org/10.3389/fcell.2020.00055>.

8. Organ, Shawna Leslie, and Ming-Sound Tsao. "An overview of the c-MET signaling pathway." *Therapeutic advances in medical oncology* vol. 3,1 Suppl (2011): S7-S19. doi:10.1177/1758834011422556
9. Mo, Hong-Nan, and Peng Liu. "Targeting MET in cancer therapy." *Chronic diseases and translational medicine* vol. 3,3 148-153. 19 Jul. 2017, doi:10.1016/j.cdtm.2017.06.002
10. Verras M, Lee J, Xue H, Li TH, Wang Y, Sun Z. The androgen receptor negatively regulates the expression of c-Met: implications for a novel mechanism of prostate cancer progression. *Cancer Res.* 2007 Feb 1;67(3):967-75. doi: 10.1158/0008-5472.CAN-06-3552. PMID: 17283128.
11. Williams, Karin et al. "Inhibition of stathmin1 accelerates the metastatic process." *Cancer research* vol. 72,20 (2012): 5407-17. doi:10.1158/0008-5472.CAN-12-1158
12. Zhang, Rui et al. "STMN1 upregulation mediates hepatocellular carcinoma and hepatic stellate cell crosstalk to aggravate cancer by triggering the MET pathway." *Cancer science* vol. 111,2 (2020): 406-417. doi:10.1111/cas.14262
13. "Search of: Met+Inhibitor - List Results." Home - ClinicalTrials.gov, <https://www.clinicaltrials.gov/ct2/results?cond=&term=MET%2Binhibitor&cntry=&state=&city=&dist=>.
14. Varkaris, Andreas et al. "The role of HGF/c-Met signaling in prostate cancer progression and c-Met inhibitors in clinical trials." *Expert opinion on investigational drugs* vol. 20,12 (2011): 1677-84. doi:10.1517/13543784.2011.631523
15. Huang, Xing, et al. "Targeting the HGF/Met Axis in Cancer Therapy: Challenges in Resistance and Opportunities for Improvement." *Frontiers in Cell and Developmental Biology*, vol. 8, 2020, <https://doi.org/10.3389/fcell.2020.00152>.
16. "Types of Cancer Treatment." *National Cancer Institute*, <https://www.cancer.gov/about-cancer/treatment/types>.
17. Robinson, Kyle W, and Alan B Sandler. "The role of MET receptor tyrosine kinase in non-small cell lung cancer and clinical development of targeted anti-MET agents." *The oncologist* vol. 18,2 (2013): 115-22. doi:10.1634/theoncologist.2012-0262
18. Hughes PE, Rex K, Caenepeel S, Yang Y, Zhang Y, Broome MA, Kha HT, Burgess TL, Amore B, Kaplan-Lefko PJ, Moriguchi J, Werner J, Damore MA, Baker D, Choquette DM, Harmange JC, Radinsky R, Kendall R, Dussault I, Coxon A. In Vitro and In Vivo Activity of AMG 337, a Potent and Selective MET Kinase Inhibitor, in MET-Dependent Cancer Models. *Mol Cancer Ther.* 2016 Jul;15(7):1568-79. doi: 10.1158/1535-7163.MCT-15-0871. Epub 2016 Apr 19. PMID: 27196782.
19. Kuželová K, Grebeňová D, Holoubek A, Röselová P, Obr A (2014) Group I PAK Inhibitor IPA-3 Induces Cell Death and Affects Cell Adhesivity to Fibronectin in Human Hematopoietic Cells. *PLoS ONE* 9(3): e92560. <https://doi.org/10.1371/journal.pone.0092560>
20. Whang, Young Mi et al. "Targeting the Hepatocyte Growth Factor and c-Met Signaling Axis in Bone Metastases." *International journal of molecular sciences* vol. 20,2 384. 17 Jan. 2019, doi:10.3390/ijms20020384
21. Choudhury, A. D., Gray, K. P., Supko, J. G., Harshman, L. C., Taplin, M. E., Pace, A. F., Farina, M., Zukotynski, K. A., Bernard, B., Kantoff, P. W., Pomerantz, M., & Sweeney,

- C. (2018). A dose finding clinical trial of cabozantinib (XL184) administered in combination with abiraterone acetate in metastatic castration-resistant prostate cancer. *The Prostate*, 10.1002/pros.23662. Advance online publication. <https://doi.org/10.1002/pros.23662>
22. Kumar, Akash et al. "Substantial interindividual and limited intraindividual genomic diversity among tumors from men with metastatic prostate cancer." *Nature medicine* vol. 22,4 (2016): 369-78. doi:10.1038/nm.4053
  23. Chen HC. Boyden chamber assay. *Methods Mol Biol* 2005;294:15–22.
  24. Kleinman HK, Jacob K. Invasion assays. *Curr Protoc Cell Biol* 2001; Chapter 12:Unit 12.12.
  25. Harper, J W et al. "Inhibition of cyclin-dependent kinases by p21." *Molecular biology of the cell* vol. 6,4 (1995): 387-400. doi:10.1091/mbc.6.4.387
  26. Magron, Audrey, et al. "The Fanconi Anemia C Protein Binds to and Regulates Stathmin-1 Phosphorylation." *PLOS ONE*, vol. 10, no. 10, 2015, <https://doi.org/10.1371/journal.pone.0140612>.
  27. Bosco EE, Mulloy JC, Zheng Y. Rac1 GTPase: a "Rac" of all trades. *Cell Mol Life Sci*. 2009 Feb;66(3):370-4. doi: 10.1007/s00018-008-8552-x. PMID: 19151919; PMCID: PMC6669905.
  28. Tian X, Tian Y, Moldobaeva N, Sarich N, Birukova AA. Microtubule dynamics control HGF-induced lung endothelial barrier enhancement. *PLoS One*. 2014 Sep 8;9(9):e105912. doi: 10.1371/journal.pone.0105912. PMID: 25198505; PMCID: PMC4157766.
  29. Schmitt, Sabrina, et al. "Stathmin Regulates Keratinocyte Proliferation and Migration during Cutaneous Regeneration." *PLoS ONE*, vol. 8, no. 9, 2013, <https://doi.org/10.1371/journal.pone.0075075>.
  30. Bonollo, Francesco et al. "The Role of Cancer-Associated Fibroblasts in Prostate Cancer Tumorigenesis." *Cancers* vol. 12,7 1887. 13 Jul. 2020, doi:10.3390/cancers12071887
  31. Hayward SW, Wang Y, Cao M, Hom YK, Zhang B, Grossfeld GD, Sudilovsky D, Cunha GR. Malignant transformation in a nontumorigenic human prostatic epithelial cell line. *Cancer Res*. 2001 Nov 15;61(22):8135-42. PMID: 11719442.
  32. Hughes, Veronica S, and Dietmar W Siemann. "Have Clinical Trials Properly Assessed c-Met Inhibitors?." *Trends in cancer* vol. 4,2 (2018): 94-97. doi:10.1016/j.trecan.2017.11.009
  33. De Mello, Ramon Andrade et al. "The Role of MET Inhibitor Therapies in the Treatment of Advanced Non-Small Cell Lung Cancer." *Journal of clinical medicine* vol. 9,6 1918. 19 Jun. 2020, doi:10.3390/jcm9061918
  34. Lennerz JK, Kwak EL, Ackerman A, Michael M, Fox SB, Bergethon K, Lauwers GY, Christensen JG, Wilner KD, Haber DA, Salgia R, Bang YJ, Clark JW, Solomon BJ, Iafrate AJ. MET amplification identifies a small and aggressive subgroup of esophagogastric adenocarcinoma with evidence of responsiveness to crizotinib. *J Clin Oncol*. 2011 Dec 20;29(36):4803-10. doi: 10.1200/JCO.2011.35.4928. Epub 2011 Oct 31. PMID: 22042947; PMCID: PMC3255989.

35. Erdogan, Begum, and Donna J Webb. "Cancer-associated fibroblasts modulate growth factor signaling and extracellular matrix remodeling to regulate tumor metastasis." *Biochemical Society transactions* vol. 45,1 (2017): 229-236. doi:10.1042/BST20160387
36. Kwak, Eunice Lee, et al. "Clinical Activity of AMG 337, an Oral Met Kinase Inhibitor, in Adult Patients (PTS) with Met-Amplified Gastroesophageal Junction (GEJ), Gastric (g), or Esophageal (e) Cancer." *Journal of Clinical Oncology*, vol. 33, no. 3\_suppl, 2015, pp. 1-1., [https://doi.org/10.1200/jco.2015.33.3\\_suppl.1](https://doi.org/10.1200/jco.2015.33.3_suppl.1).
37. "Quilt-3.036: AMG 337 in Subjects with Advanced or Metastatic Solid Tumors - Full Text View." *Full Text View - ClinicalTrials.gov*, <https://clinicaltrials.gov/ct2/show/NCT03147976>.

### Chapter 3 Bibliography

1. Bao P, Yokobori T, Altan B, Iijima M, Azuma Y, Onozato R, Yajima T, Watanabe A, Mogi A, Shimizu K, Nagashima T, Ohtaki Y, Obayashi K, Nakazawa S, Bai T, Kawabata-Iwakawa R, Asao T, Kaira K, Nishiyama M, Kuwano H. High STMN1 Expression is Associated with Cancer Progression and Chemo-Resistance in Lung Squamous Cell Carcinoma. *Ann Surg Oncol*. 2017 Dec;24(13):4017-4024. doi: 10.1245/s10434-017-6083-0. Epub 2017 Sep 20. PMID: 28933054.
2. Williams, Karin et al. "Inhibition of stathmin1 accelerates the metastatic process." *Cancer research* vol. 72,20 (2012): 5407-17. doi:10.1158/0008-5472.CAN-12-1158
3. Chakravarthi, B., Chandrashekar, D. S., Agarwal, S., Balasubramanya, S., Pathi, S. S., Goswami, M. T., Jing, X., Wang, R., Mehra, R., Asangani, I. A., Chinnaiyan, A. M., Manne, U., Sonpavde, G., Netto, G. J., Gordetsky, J., & Varambally, S. (2018). miR-34a Regulates Expression of the Stathmin-1 Oncoprotein and Prostate Cancer Progression. *Molecular cancer research : MCR*, 16(7), 1125–1137. <https://doi.org/10.1158/1541-7786.MCR-17-0230>
4. Anderson, Mark E. "Pathways for CaMKII activation in disease." *Heart rhythm* vol. 8,9 (2011): 1501-3. doi:10.1016/j.hrthm.2011.04.027
5. Chi, Mengna, et al. "Phosphorylation of Calcium/Calmodulin-Stimulated Protein Kinase II at T286 Enhances Invasion and Migration of Human Breast Cancer Cells." *Scientific Reports*, vol. 6, no. 1, 2016, <https://doi.org/10.1038/srep33132>.
6. He, Q., Li, Z. The dysregulated expression and functional effect of CaMK2 in cancer. *Cancer Cell Int* 21, 326 (2021). <https://doi.org/10.1186/s12935-021-02030-7>
7. Britschgi A, et al. Calcium-activated chloride channel ANO1 promotes breast cancer progression by activating EGFR and CAMK signaling. *Proc Natl Acad Sci USA*. 2013;110(11):E1026–34.
8. Swulius, M T, and M N Waxham. "Ca(2+)/calmodulin-dependent protein kinases." *Cellular and molecular life sciences : CMLS* vol. 65,17 (2008): 2637-57. doi:10.1007/s00018-008-8086-2
9. Curmi PA, Noguès C, Lachkar S, Carelle N, Gonthier MP, Sobel A, Lidereau R, Bièche I. Overexpression of stathmin in breast carcinomas points out to highly proliferative

- tumours. *Br J Cancer*. 2000 Jan;82(1):142-50. doi: 10.1054/bjoc.1999.0891. PMID: 10638981; PMCID: PMC2363189.
10. Yoshie, Mikihiro et al. "Stathmin dynamics modulate the activity of eribulin in breast cancer cells." *Pharmacology research & perspectives* vol. 9,4 (2021): e00786. doi:10.1002/prp2.786
  11. Miceli, C., Tejada, A., Castaneda, A. et al. Cell cycle inhibition therapy that targets stathmin in in vitro and in vivo models of breast cancer. *Cancer Gene Ther* 20, 298–307 (2013). <https://doi.org/10.1038/cgt.2013.21>
  12. Wang, Yan-yang, et al. "The Emerging Role of CaMKII in Cancer." *Oncotarget*, vol. 6, no. 14, 2015, pp. 11725–11734., <https://doi.org/10.18632/oncotarget.3955>.
  13. Ohkawa N, Fujitani K, Tokunaga E, Furuya S, Inokuchi K. The microtubule destabilizer stathmin mediates the development of dendritic arbors in neuronal cells. *J Cell Sci*. 2007 Apr 15;120(Pt 8):1447-56. doi: 10.1242/jcs.001461. Epub 2007 Mar 27. PMID: 17389683.
  14. Poulain, F. E., et al. "SCLIP Is Crucial for the Formation and Development of the Purkinje Cell Dendritic Arbor." *Journal of Neuroscience*, vol. 28, no. 29, 2008, pp. 7387–7398., <https://doi.org/10.1523/jneurosci.1942-08.2008>.
  15. Biaoxue, Rong et al. "Stathmin-dependent molecular targeting therapy for malignant tumor: the latest 5 years' discoveries and developments." *Journal of translational medicine* vol. 14,1 279. 27 Sep. 2016, doi:10.1186/s12967-016-1000-z
  16. Tseng, YH., Huang, YH., Lin, TK. *et al.* Thyroid hormone suppresses expression of stathmin and associated tumor growth in hepatocellular carcinoma. *Sci Rep* 6, 38756 (2016). <https://doi.org/10.1038/srep38756>
  17. Hep G2 [hepg2] | ATCC. <https://www.atcc.org/products/hb-8065>.
  18. Li, Chao et al. "PIWIL1 destabilizes microtubule by suppressing phosphorylation at Ser16 and RLIM-mediated degradation of Stathmin1." *Oncotarget* vol. 6,29 (2015): 27794-804. doi:10.18632/oncotarget.4533
  19. Chen X, Shen J, Li X, Wang X, Long M, Lin F, Wei J, Yang L, Yang C, Dong K, Zhang H. Rlim, an E3 ubiquitin ligase, influences the stability of Stathmin protein in human osteosarcoma cells. *Cell Signal*. 2014 Jul;26(7):1532-8. doi: 10.1016/j.cellsig.2014.03.018. Epub 2014 Mar 29. PMID: 24686088.
  20. Marklund U, Larsson N, Brattsand G, Osterman O, Chatila TA, Gullberg M. Serine 16 of oncoprotein 18 is a major cytosolic target for the Ca<sup>2+</sup>/calmodulin-dependent kinase-Gr. *Eur J Biochem*. 1994 Oct 1;225(1):53-60. doi: 10.1111/j.1432-1033.1994.00053.x. PMID: 7925472.
  21. le Gouvello S, Manceau V, Sobel A. Serine 16 of stathmin as a cytosolic target for Ca<sup>2+</sup>/calmodulin-dependent kinase II after CD2 triggering of human T lymphocytes. *J Immunol*. 1998 Aug 1;161(3):1113-22. PMID: 9686569.
  22. Beretta L, Dobránsky T, Sobel A. Multiple phosphorylation of stathmin. Identification of four sites phosphorylated in intact cells and in vitro by cyclic AMP-dependent protein kinase and p34cdc2. *J Biol Chem*. 1993 Sep 25;268(27):20076-84. PMID: 8376365.
  23. LIU, ZHAOLONG, et al. "Calcium/Calmodulin-Dependent Protein Kinase II Enhances Metastasis of Human Gastric Cancer by Upregulating Nuclear Factor-KB and Akt-

- Mediated Matrix Metalloproteinase-9 Production.” *Molecular Medicine Reports*, vol. 10, no. 5, 2014, pp. 2459–2464., <https://doi.org/10.3892/mmr.2014.2525>.
24. Chi, M., Evans, H., Gilchrist, J. et al. Phosphorylation of calcium/calmodulin-stimulated protein kinase II at T286 enhances invasion and migration of human breast cancer cells. *Sci Rep* 6, 33132 (2016). <https://doi.org/10.1038/srep33132>
  25. Wang YY, Zhao R, Zhe H. The emerging role of CaMKII in cancer. *Oncotarget*. 2015 May 20;6(14):11725-34. doi: 10.18632/oncotarget.3955. PMID: 25961153; PMCID: PMC4494900.
  26. Hayashi, Kanehiro, et al. “Phosphorylation of the Tubulin-Binding Protein, Stathmin, by Cdk5 and MAP Kinases in the Brain.” *Journal of Neurochemistry*, vol. 99, no. 1, 2006, pp. 237–250., <https://doi.org/10.1111/j.1471-4159.2006.04113.x>.
  27. Taylor SL, Kinchington PR, Brooks A, Moffat JF. Roscovitine, a cyclin-dependent kinase inhibitor, prevents replication of varicella-zoster virus. *J Virol*. 2004 Mar;78(6):2853-62. doi: 10.1128/jvi.78.6.2853-2862.2004. PMID: 14990704; PMCID: PMC353735.
  28. Guo B, Qi M, Huang S, Zhuo R, Zhang W, Zhang Y, Xu M, Liu M, Guan T, Liu Y. Cadherin-12 Regulates Neurite Outgrowth Through the PKA/Rac1/Cdc42 Pathway in Cortical Neurons. *Front Cell Dev Biol*. 2021 Nov 8;9:768970. doi: 10.3389/fcell.2021.768970. PMID: 34820384; PMCID: PMC8606577.

## Chapter 4 Bibliography

1. Zhang K, Zhou S, Wang L, Wang J, Zou Q, Zhao W, et al. Current Stem Cell Biomarkers and Their Functional Mechanisms in Prostate Cancer. *Int J Mol Sci* 2016;17 [PMC free article] [PubMed] [Google Scholar]
2. Gu G, Yuan J, Wills M, Kasper S. Prostate cancer cells with stem cell characteristics reconstitute the original human tumor in vivo. *Cancer Res* 2007;67:4807–15 [PubMed] [Google Scholar]
3. Hu WY, Hu DP, Xie L, Li Y, Majumdar S, Nonn L, et al. Isolation and functional interrogation of adult human prostate epithelial stem cells at single cell resolution. *Stem Cell Res* 2017;23:1–12 [PMC free article] [PubMed] [Google Scholar]
4. Aumuller G, Groos S, Renneberg H, Konrad L, Aumueller M. Embryological and Postnatal Development of the Prostate Foster C, Bostwick D, editors. Philadelphia, Pennsylvania: 19106: W.B. Saunders Company; 1998. [Google Scholar]
5. Cooke PS, Young P, Cunha GR. Androgen receptor expression in developing male reproductive organs. *Endocrinology* 1991;128:2867–73 [PubMed] [Google Scholar]
6. Qin J, Liu X, Laffin B, Chen X, Choy G, Jeter CR, et al. The PSA(-/lo) prostate cancer cell population harbors self-renewing long-term tumor-propagating cells that resist castration. *Cell Stem Cell* 2012;10:556–69 [PMC free article] [PubMed] [Google Scholar]

7. Lin HK, Wang L, Hu YC, Altuwajiri S, Chang C. Phosphorylation-dependent ubiquitylation and degradation of androgen receptor by Akt require Mdm2 E3 ligase. *Embo J* 2002;21:4037–48 [PMC free article] [PubMed] [Google Scholar]
8. Burska UL, Harle VJ, Coffey K, Darby S, Ramsey H, O'Neill D, et al. Deubiquitinating enzyme Usp12 is a novel co-activator of the androgen receptor. *J Biol Chem* 2013;288:32641–50 [PMC free article] [PubMed] [Google Scholar]
9. Cardozo CP, Michaud C, Ost MC, Fliss AE, Yang E, Patterson C, et al. C-terminal Hsp-interacting protein slows androgen receptor synthesis and reduces its rate of degradation. *Archives of biochemistry and biophysics* 2003;410:134–40 [PubMed] [Google Scholar]
10. Li B, Lu W, Yang Q, Yu X, Matusik RJ, Chen Z. Skp2 regulates androgen receptor through ubiquitin-mediated degradation independent of Akt/mTOR pathways in prostate cancer. *Prostate* 2014;74:421–32 [PMC free article] [PubMed] [Google Scholar]
11. Antonarakis ES, Armstrong AJ, Dehm SM, Luo J. Androgen receptor variant-driven prostate cancer: clinical implications and therapeutic targeting. *Prostate Cancer Prostatic Dis* 2016;19:231–41 [PMC free article] [PubMed] [Google Scholar]
12. Ho Y, Dehm SM. Androgen Receptor Rearrangement and Splicing Variants in Resistance to Endocrine Therapies in Prostate Cancer. *Endocrinology* 2017;158:1533–42 [PMC free article] [PubMed] [Google Scholar]
13. Kong D, Sethi S, Li Y, Chen W, Sakr WA, Heath E, et al. Androgen receptor splice variants contribute to prostate cancer aggressiveness through induction of EMT and expression of stem cell marker genes. *Prostate* 2015;75:161–74 [PMC free article] [PubMed] [Google Scholar]
14. Li Y, Xie N, Gleave ME, Rennie PS, Dong X. AR-v7 protein expression is regulated by protein kinase and phosphatase. *Oncotarget* 2015;6:33743–54 [PMC free article] [PubMed] [Google Scholar]
15. Singh S, Chitkara D, Mehrazin R, Behrman SW, Wake RW, Mahato RI. Chemoresistance in prostate cancer cells is regulated by miRNAs and Hedgehog pathway. *PLoS ONE* 2012;7:e40021. [PMC free article] [PubMed] [Google Scholar]
16. Mathew G, Timm EA Jr., Sotomayor P, Godoy A, Montecinos VP, Smith GJ, et al. ABCG2-mediated DyeCycle Violet efflux defined side population in benign and malignant prostate. *Cell Cycle* 2009;8:1053–61 [PMC free article] [PubMed] [Google Scholar]
17. Bisson I, Prowse DM. WNT signaling regulates self-renewal and differentiation of prostate cancer cells with stem cell characteristics. *Cell Res* 2009;19:683–97 [PubMed] [Google Scholar]
18. Zhang D, Lin K, Lu Y, Rycaj K, Zhong Y, Chao HP, et al. Developing a Novel Two-Dimensional Culture System to Enrich Human Prostate Luminal Progenitors that Can Function as a Cell of Origin for Prostate Cancer. *Stem cells translational medicine* 2017;6:748–60 [PMC free article] [PubMed] [Google Scholar]

19. Williams K, Ghosh R, Vummidi Giridhar P, Gu G, Case T, SM B, et al. Inhibition of Stathmin1 Accelerates the Metastatic Process *Cancer Res* 2012;72:5407–17 [PMC free article] [PubMed] [Google Scholar]
20. Zhang J, Gao N, Kasper S, Reid K, Nelson C, Matusik RJ. An androgen-dependent upstream enhancer is essential for high levels of probasin gene expression. *Endocrinology* 2004;145:134–48 [PubMed] [Google Scholar]
21. Pitkanen-Arsiola T, Tillman JE, Gu G, Yuan J, Roberts RL, Wantroba M, et al. Androgen and anti-androgen treatment modulates androgen receptor activity and DJ-1 stability. *Prostate* 2006;66:1177–93 [PubMed] [Google Scholar]
22. Winer J, Jung CK, Shackel I, Williams PM. Development and validation of real-time quantitative reverse transcriptase-polymerase chain reaction for monitoring gene expression in cardiac myocytes in vitro. *Anal Biochem* 1999;270:41–9 [PubMed] [Google Scholar]
23. Mulholland DJ, Cheng H, Reid K, Rennie PS, Nelson CC. The androgen receptor can promote beta-catenin nuclear translocation independently of adenomatous polyposis coli. *J Biol Chem* 2002;277:17933–43 [PubMed] [Google Scholar]
24. Tillman JE, Yuan J, Gu G, Fazli L, Ghosh R, Flynt AS, et al. DJ-1 binds androgen receptor directly and mediates its activity in hormonally treated prostate cancer cells. *Cancer Res* 2007;67:4630–7 [PubMed] [Google Scholar]
25. Hu R, Dunn TA, Wei S, Isharwal S, Veltri RW, Humphreys E, et al. Ligand-independent androgen receptor variants derived from splicing of cryptic exons signify hormone-refractory prostate cancer. *Cancer Res* 2009;69:16–22 [PMC free article] [PubMed] [Google Scholar]
26. Watson PA, Chen YF, Balbas MD, Wongvipat J, Socci ND, Viale A, et al. Constitutively active androgen receptor splice variants expressed in castration-resistant prostate cancer require full-length androgen receptor. *Proc Natl Acad Sci U S A* 2010;107:16759–65 [PMC free article] [PubMed] [Google Scholar]
27. Hornberg E, Ylitalo EB, Crnalic S, Antti H, Stattin P, Widmark A, et al. Expression of androgen receptor splice variants in prostate cancer bone metastases is associated with castration-resistance and short survival. *PLoS ONE* 2011;6:e19059. [PMC free article] [PubMed] [Google Scholar]
28. Szutorisz H, Georgiou A, Tora L, Dillon N. The proteasome restricts permissive transcription at tissue-specific gene loci in embryonic stem cells. *Cell* 2006;127:1375–88 [PubMed] [Google Scholar]
29. Sakurai M, Ayukawa K, Setsuie R, Nishikawa K, Hara Y, Ohashi H, et al. Ubiquitin C-terminal hydrolase L1 regulates the morphology of neural progenitor cells and modulates their differentiation. *J Cell Sci* 2006;119:162–71 [PubMed] [Google Scholar]

30. Jian R, Cheng X, Jiang J, Deng S, Hu F, Zhang J. A cDNA-based random RNA interference library for functional genetic screens in embryonic stem cells. *Stem Cells* 2007;25:1904–12 [PubMed] [Google Scholar]
31. Lee JH, Lee MJ. Emerging roles of the ubiquitin-proteasome system in the steroid receptor signaling. *Archives of pharmacal research* 2012;35:397–407 [PubMed] [Google Scholar]
32. Szigyarto CA, Sibbons P, Williams G, Uhlen M, Metcalfe SM. The E3 ligase axotrophin/MARCH-7: protein expression profiling of human tissues reveals links to adult stem cells. *J Histochem Cytochem* 2010;58:301–8 [PMC free article] [PubMed] [Google Scholar]
33. Xu H, Wang W, Li C, Yu H, Yang A, Wang B, et al. WWP2 promotes degradation of transcription factor OCT4 in human embryonic stem cells. *Cell Res* 2009;19:561–73 [PubMed] [Google Scholar]
34. Fang L, Zhang L, Wei W, Jin X, Wang P, Tong Y, et al. A methylation-phosphorylation switch determines Sox2 stability and function in ESC maintenance or differentiation. *Mol Cell* 2014;55:537–51 [PubMed] [Google Scholar]
35. Collins AT, Berry PA, Hyde C, Stower MJ, Maitland NJ. Prospective identification of tumorigenic prostate cancer stem cells. *Cancer Res* 2005;65:10946–51 [PubMed] [Google Scholar]
36. Tang DG, Patrawala L, Calhoun T, Bhatia B, Choy G, Schneider-Broussard R, et al. Prostate cancer stem/progenitor cells: identification, characterization, and implications. *Mol Carcinog* 2007;46:1–14 [PubMed] [Google Scholar]
37. Chua CW, Epsi NJ, Leung EY, Xuan S, Lei M, Li BI, et al. Differential requirements of androgen receptor in luminal progenitors during prostate regeneration and tumor initiation. *eLife* 2018;7 [PMC free article] [PubMed] [Google Scholar]
38. Wienken M, Dickmanns A, Nemajero A, Kramer D, Najafova Z, Weiss M, et al. MDM2 Associates with Polycomb Repressor Complex 2 and Enhances Stemness-Promoting Chromatin Modifications Independent of p53. *Mol Cell* 2016;61:68–83 [PMC free article] [PubMed] [Google Scholar]
39. Mu Z, Hachem P, Hensley H, Stoyanova R, Kwon HW, Hanlon AL, et al. Antisense MDM2 enhances the response of androgen insensitive human prostate cancer cells to androgen deprivation in vitro and in vivo. *Prostate* 2008;68:599–609 [PMC free article] [PubMed] [Google Scholar]
40. Graham L, Schweizer MT. Targeting persistent androgen receptor signaling in castration-resistant prostate cancer. *Medical oncology* 2016;33:44. [PubMed] [Google Scholar]
41. Attard G, Reid AH, A'Hern R, Parker C, Oommen NB, Folkard E, et al. Selective inhibition of CYP17 with abiraterone acetate is highly active in the treatment of castration-resistant prostate cancer. *J Clin Oncol* 2009;27:3742–8 [PMC free article] [PubMed] [Google Scholar]

42. Uo T, Plymate SR, Sprenger CC. The potential of AR-V7 as a therapeutic target. *Expert Opin Ther Targets* 2018;22:201–16 [PubMed] [Google Scholar]
43. Dehm SM, Schmidt LJ, Heemers HV, Vessella RL, Tindall DJ. Splicing of a novel androgen receptor exon generates a constitutively active androgen receptor that mediates prostate cancer therapy resistance. *Cancer Res* 2008;68:5469–77 [PMC free article] [PubMed] [Google Scholar]
44. Slabakova E, Kharraishvili G, Smejova M, Pernicova Z, Suchankova T, Remsik J, et al. Opposite regulation of MDM2 and MDMX expression in acquisition of mesenchymal phenotype in benign and cancer cells. *Oncotarget* 2015;6:36156–71 [PMC free article] [PubMed] [Google Scholar]
45. Shangary S, Qin D, McEachern D, Liu M, Miller RS, Qiu S, et al. Temporal activation of p53 by a specific MDM2 inhibitor is selectively toxic to tumors and leads to complete tumor growth inhibition. *Proc Natl Acad Sci U S A* 2008;105:3933–8 [PMC free article] [PubMed] [Google Scholar]
46. Vassilev LT, Vu BT, Graves B, Carvajal D, Podlaski F, Filipovic Z, et al. In vivo activation of the p53 pathway by small-molecule antagonists of MDM2. *Science* 2004;303:844–8 [PubMed] [Google Scholar]
47. Zhang A, Zhao JC, Kim J, Fong KW, Yang YA, Chakravarti D, et al. LncRNA HOTAIR Enhances the Androgen-Receptor-Mediated Transcriptional Program and Drives Castration-Resistant Prostate Cancer. *Cell reports* 2015;13:209–21 [PMC free article] [PubMed] [Google Scholar]
48. Lee SO, Ma Z, Yeh CR, Luo J, Lin TH, Lai KP, et al. New therapy targeting differential androgen receptor signaling in prostate cancer stem/progenitor vs. non-stem/progenitor cells. *Journal of molecular cell biology* 2013;5:14–26 [PMC free article] [PubMed] [Google Scholar]
49. Zhang J, Thomas TZ, Kasper S, Matusik RJ. A small composite probasin promoter confers high levels of prostate-specific gene expression through regulation by androgens and glucocorticoids in vitro and in vivo. *Endocrinology* 2000;141:4698–710 [PubMed] [Google Scholar]

## Chapter 5 Bibliography

1. “CRISPR Timeline.” *Broad Institute*, 7 Dec. 2018, <https://www.broadinstitute.org/what-broad/areas-focus/project-spotlight/crispr-timeline>.
2. Shabbir, M.A.B., Shabbir, M.Z., Wu, Q. *et al.* CRISPR-cas system: biological function in microbes and its use to treat antimicrobial resistant pathogens. *Ann Clin Microbiol Antimicrob* **18**, 21 (2019). <https://doi.org/10.1186/s12941-019-0317-x>
3. Neggers, Jasper Edgar et al. “Heterozygous mutation of cysteine528 in XPO1 is sufficient for resistance to selective inhibitors of nuclear export.” *Oncotarget* vol. 7,42 (2016): 68842-68850. doi:10.18632/oncotarget.11995

4. Williams, Karin et al. "Inhibition of stathmin1 accelerates the metastatic process." *Cancer research* vol. 72,20 (2012): 5407-17. doi:10.1158/0008-5472.CAN-12-1158
5. Amayed, Phedra, et al. "The Effect of Stathmin Phosphorylation on Microtubule Assembly Depends on Tubulin Critical Concentration." *Journal of Biological Chemistry*, vol. 277, no. 25, 2002, pp. 22718–22724., <https://doi.org/10.1074/jbc.m111605200>.
6. Larsson, Niklas, et al. "Mutations of Oncoprotein 18/Stathmin Identify Tubulin-Directed Regulatory Activities Distinct from Tubulin Association." *Molecular and Cellular Biology*, vol. 19, no. 3, 1999, pp. 2242–2250., <https://doi.org/10.1128/mcb.19.3.2242>.
7. Alesi, Gina, et al. "Abstract B15: RSK2 Signals through Stathmin to Promote Microtubule Dynamics and Tumor Metastasis." *Genetics and Evolution of Metastatic Tumors*, 2016, <https://doi.org/10.1158/1538-7445.tummet15-b15>.
8. Wittmann, Torsten, et al. "Regulation of Microtubule Destabilizing Activity of OP18/Stathmin Downstream of RAC1." *Journal of Biological Chemistry*, vol. 279, no. 7, 2004, pp. 6196–6203., <https://doi.org/10.1074/jbc.m307261200>.
9. "Full Stack Genome Engineering." *Synthego*, <https://www.synthego.com/guide/how-to-use-crispr/transfection-protocols>.
10. Chatterjee, Nimrat, and Graham C Walker. "Mechanisms of DNA damage, repair, and mutagenesis." *Environmental and molecular mutagenesis* vol. 58,5 (2017): 235-263. doi:10.1002/em.22087
11. Cortez, Chari. "CRISPR 101: Homology Directed Repair." Addgene Blog, <https://blog.addgene.org/crispr-101-homology-directed-repair>.
12. "Neon Electroporation Transfection: Thermo Fisher Scientific - US." *Neon Electroporation Transfection | Thermo Fisher Scientific - US*, <https://www.thermofisher.com/us/en/home/life-science/cell-culture/transfection/neon-transfection-system.html>.
13. Mao, Zhiyong et al. "Comparison of nonhomologous end joining and homologous recombination in human cells." *DNA repair* vol. 7,10 (2008): 1765-71. doi:10.1016/j.dnarep.2008.06.018
14. Chiruvella, Kishore K et al. "Repair of double-strand breaks by end joining." *Cold Spring Harbor perspectives in biology* vol. 5,5 a012757. 1 May. 2013, doi:10.1101/cshperspect.a012757
15. Rees HA, Yeh WH, Liu DR. Development of hRad51-Cas9 nickase fusions that mediate HDR without double-stranded breaks. *Nat Commun.* 2019 May 17;10(1):2212. doi: 10.1038/s41467-019-09983-4. PMID: 31101808; PMCID: PMC6525190.
16. Nambiar TS, Billon P, Diedenhofen G, Hayward SB, Taglialatela A, Cai K, Huang JW, Leuzzi G, Cuella-Martin R, Palacios A, Gupta A, Egli D, Ciccia A. Stimulation of CRISPR-mediated homology-directed repair by an engineered RAD18 variant. *Nat Commun.* 2019 Jul 30;10(1):3395. doi: 10.1038/s41467-019-11105-z. PMID: 31363085; PMCID: PMC6667477.
17. Arnoult, N., Correia, A., Ma, J. *et al.* Regulation of DNA repair pathway choice in S and G2 phases by the NHEJ inhibitor CYREN. *Nature* **549**, 548–552 (2017). <https://doi.org/10.1038/nature24023>

18. Riesenberger S, Chintalapati M, Macak D, Kanis P, Maricic T, Pääbo S. Simultaneous precise editing of multiple genes in human cells. *Nucleic Acids Res.* 2019 Nov 4;47(19):e116. doi: 10.1093/nar/gkz669. PMID: 31392986; PMCID: PMC6821318.
19. Fu, J., Fu, YW., Zhao, JJ. et al. Improved and Flexible HDR Editing by Targeting Introns in iPSCs. *Stem Cell Rev and Rep* (2022). <https://doi.org/10.1007/s12015-022-10331-1>
20. Shrivastav, M., De Haro, L. & Nickoloff, J. Regulation of DNA double-strand break repair pathway choice. *Cell Res* 18, 134–147 (2008). <https://doi.org/10.1038/cr.2007.111>
21. Bosch, Nuria. “Enhancing CRISPR Deletion via Pharmacological Delay of DNA-PK.” 2020, <https://doi.org/10.26226/morressier.5ebd45acffea6f735881b0f7>.

## Chapter 6 Bibliography

1. Cui F, Ning S, Xu Z, Hu J. Spindle pole body component 25 in the androgen-induced regression of castration-resistant prostate cancer. *Transl Androl Urol.* 2022 Apr;11(4):519-527. doi: 10.21037/tau-22-214. PMID: 35558271; PMCID: PMC9085928.
2. “Prostate Cancer Treatment (PDQ®)—Patient Version.” National Cancer Institute, <https://www.cancer.gov/types/prostate/patient/prostate-treatment-pdq#:~:text=External%20radiation%20therapy%2C%20internal%20radiation,bladder%20and%20for%20gastrointestinal%20cancer.>
3. Verras M, Lee J, Xue H, Li TH, Wang Y, Sun Z. The androgen receptor negatively regulates the expression of c-Met: implications for a novel mechanism of prostate cancer progression. *Cancer Res.* 2007 Feb 1;67(3):967-75. doi: 10.1158/0008-5472.CAN-06-3552. PMID: 17283128.
4. Zhang, Rui et al. “STMN1 upregulation mediates hepatocellular carcinoma and hepatic stellate cell crosstalk to aggravate cancer by triggering the MET pathway.” *Cancer science* vol. 111,2 (2020): 406-417. doi:10.1111/cas.14262
5. Mo, Hong-Nan, and Peng Liu. “Targeting MET in cancer therapy.” *Chronic diseases and translational medicine* vol. 3,3 148-153. 19 Jul. 2017, doi:10.1016/j.cdtm.2017.06.002
6. Hughes, Veronica S, and Dietmar W Siemann. “Have Clinical Trials Properly Assessed c-Met Inhibitors?.” *Trends in cancer* vol. 4,2 (2018): 94-97. doi:10.1016/j.trecan.2017.11.009
7. Hughes PE, Rex K, Caenepeel S, Yang Y, Zhang Y, Broome MA, Kha HT, Burgess TL, Amore B, Kaplan-Lefko PJ, Moriguchi J, Werner J, Damore MA, Baker D, Choquette DM, Harmange JC, Radinsky R, Kendall R, Dussault I, Coxon A. In Vitro and In Vivo Activity of AMG 337, a Potent and Selective MET Kinase Inhibitor, in MET-Dependent Cancer Models. *Mol Cancer Ther.* 2016 Jul;15(7):1568-79. doi: 10.1158/1535-7163.MCT-15-0871. Epub 2016 Apr 19. PMID: 27196782.
8. “Phase 2 Study of AMG 337 in Met Amplified Gastric/Esophageal Adenocarcinoma or Other Solid Tumors - Full Text View.” *Full Text View - ClinicalTrials.gov*, <https://clinicaltrials.gov/ct2/show/NCT02016534>.
9. “Quilt-3.036: AMG 337 in Subjects with Advanced or Metastatic Solid Tumors - Full Text View.” *Full Text View - ClinicalTrials.gov*, <https://clinicaltrials.gov/ct2/show/NCT03147976>.

10. Bahmad, Hisham F., et al. "Tumor Microenvironment in Prostate Cancer: Toward Identification of Novel Molecular Biomarkers for Diagnosis, Prognosis, and Therapy Development." *Frontiers in Genetics*, vol. 12, 2021, <https://doi.org/10.3389/fgene.2021.652747>.
11. Thienger, P., Rubin, M.A. Prostate cancer hijacks the microenvironment. *Nat Cell Biol* **23**, 3–5 (2021). <https://doi.org/10.1038/s41556-020-00616-3>
12. Ge, R., Wang, Z. & Cheng, L. Tumor microenvironment heterogeneity an important mediator of prostate cancer progression and therapeutic resistance. *npj Precis. Onc.* **6**, 31 (2022). <https://doi.org/10.1038/s41698-022-00272-w>
13. Kwon, J T W et al. "The tumor microenvironment and immune responses in prostate cancer patients." *Endocrine-related cancer* vol. 28,8 T95-T107. 15 Jul. 2021, doi:10.1530/ERC-21-0149
14. Sahai, E., Astsaturov, I., Cukierman, E. *et al.* A framework for advancing our understanding of cancer-associated fibroblasts. *Nat Rev Cancer* **20**, 174–186 (2020). <https://doi.org/10.1038/s41568-019-0238-1>
15. Sun, Rui et al. "HGF stimulates proliferation through the HGF/c-Met pathway in nasopharyngeal carcinoma cells." *Oncology letters* vol. 3,5 (2012): 1124-1128. doi:10.3892/ol.2012.613
16. Wang, Haiyu, et al. "The Function of the HGF/c-Met Axis in Hepatocellular Carcinoma." *Frontiers in Cell and Developmental Biology*, vol. 8, 2020, <https://doi.org/10.3389/fcell.2020.00055>.
17. Organ, Shawna Leslie, and Ming-Sound Tsao. "An overview of the c-MET signaling pathway." *Therapeutic advances in medical oncology* vol. 3,1 Suppl (2011): S7-S19. doi:10.1177/1758834011422556
18. Lee, K.H., Kim, JR. Regulation of HGF-mediated cell proliferation and invasion through NF- $\kappa$ B, JunB, and MMP-9 cascades in stomach cancer cells. *Clin Exp Metastasis* **29**, 263–272 (2012). <https://doi.org/10.1007/s10585-011-9449-x>
19. Takahashi K, Suzuki K. Membrane transport of WAVE2 and lamellipodia formation require Pak1 that mediates phosphorylation and recruitment of stathmin/Op18 to Pak1-WAVE2-kinesin complex. *Cell Signal.* 2009 May;21(5):695-703. doi: 10.1016/j.cellsig.2009.01.007. Epub 2009 Jan 7. PMID: 19162178.
20. Williams, Karin et al. "Inhibition of stathmin1 accelerates the metastatic process." *Cancer research* vol. 72,20 (2012): 5407-17. doi:10.1158/0008-5472.CAN-12-1158
21. Anderson, Mark E. "Pathways for CaMKII activation in disease." *Heart rhythm* vol. 8,9 (2011): 1501-3. doi:10.1016/j.hrthm.2011.04.027
22. Chi, Mengna, et al. "Phosphorylation of Calcium/Calmodulin-Stimulated Protein Kinase II at T286 Enhances Invasion and Migration of Human Breast Cancer Cells." *Scientific Reports*, vol. 6, no. 1, 2016, <https://doi.org/10.1038/srep33132>.
23. He, Q., Li, Z. The dysregulated expression and functional effect of CaMK2 in cancer. *Cancer Cell Int* **21**, 326 (2021). <https://doi.org/10.1186/s12935-021-02030-7>
24. Britschgi A, et al. Calcium-activated chloride channel ANO1 promotes breast cancer progression by activating EGFR and CAMK signaling. *Proc Natl Acad Sci USA.* 2013;110(11):E1026–34.

25. Swulius, M T, and M N Waxham. "Ca(2+)/calmodulin-dependent protein kinases." *Cellular and molecular life sciences : CMLS* vol. 65,17 (2008): 2637-57. doi:10.1007/s00018-008-8086-2
26. Vummidi Giridhar P, Williams K, VonHandorf AP, Deford PL, Kasper S. Constant Degradation of the Androgen Receptor by MDM2 Conserves Prostate Cancer Stem Cell Integrity. *Cancer Res.* 2019 Mar 15;79(6):1124-1137. doi: 10.1158/0008-5472.CAN-18-1753. Epub 2019 Jan 9. PMID: 30626627; PMCID: PMC6428062.
27. Sun, Rui et al. "HGF stimulates proliferation through the HGF/c-Met pathway in nasopharyngeal carcinoma cells." *Oncology letters* vol. 3,5 (2012): 1124-1128. doi:10.3892/ol.2012.613
28. Sugawara, Junichi, et al. "Hepatocyte Growth Factor Stimulates Proliferation, Migration, and Lumen Formation of Human Endometrial Epithelial Cells in Vitro." *Biology of Reproduction*, vol. 57, no. 4, 1997, pp. 936–942., <https://doi.org/10.1095/biolreprod57.4.936>.